12-2012

PROSTATE CANCER STEM CELLS: DRUG TOLERANCE, EXPERIMENTAL RECONSTITUTION AND CASTRATION RESISTANCE

Xin Chen

PROSTATE CANCER STEM CELLS: DRUG TOLERANCE, EXPERIMENTAL RECONSTITUTION AND CASTRATION RESISTANCE

by

Xin Chen, M.S.

APPROVED:

_____
Supervisory Professor: Dean G. Tang, M.D., Ph.D.

_____
Ellen R. Richie, Ph.D.

_____
Donna F. Kusewitt, D.V.M, Ph.D.

_____
Feng Wang-Johanning, M.D., Ph.D.

_____
Taiping Chen, Ph.D.

APPROVED:

_____
Dean, The University of Texas
Graduate School of Biomedical Sciences at Houston

PROSTATE CANCER STEM CELLS: DRUG TOLERANCE, EXPERIMENTAL RECONSTITUTION AND CASTRATION RESISTANCE

A

DISSERTATION

Presented to the Faculty of
The University of Texas
Health Science Center at Houston
and
The University of Texas
M. D. Anderson Cancer Center
Graduate School of Biomedical Sciences
in Partial Fulfillment

of the Requirements

for the Degree of

DOCTOR OF PHILOSOPHY

by

Xin Chen, M.S.

Houston, Texas

December, 2012

DEDICATION

To my dearest parents, Dr. Weimin Chen and Ms. Guimei Peng,

who made all this possible,

and for their eternal love and endless support;

To my beloved wife, Ms. Qiuhui Li,

for her patience, encouragement and company,

and for her incomparable love

ACKNOWLEDGMENTS

I have been in Science Park for more than 7 years, during which I have experienced both great joys and great disappointments. I vividly remember the excitement that filled my heart when my first paper was published. But then there was the crushing heartbreak of losing nearly two years worth of samples due to the 2011 Bastrop Wildfire. Given the good and bad I have experienced during my time here, I still consider myself a lucky person. That luck has been largely ascribed to the people I have been honored to know and work with, and I would like to take this opportunity to express my gratitude for their contributions.

First and foremost, I would like to thank my advisor, Dr. Dean G. Tang. I have known Dean since I was a child, for he is my father's best friend. He was a great support to me before I even came to the US. However, when I did arrive in the US, I was then lucky enough to enter GSBS and join his lab, starting as a Master's student. Dean is a great scientist and a wonderful individual as well. During the past 7 years, his dedication, intelligence, persistence, passion, enthusiasm, vigorousness and remarkable memory have impressed me and significantly influenced me to purse my dream. His guidance, patience, support and strictness have made it possible for me to take this journey and reach this point. There are no words to adequately express my appreciation and gratitude, but I would like to say, sincerely, 'Thank you very much, Dean".

Moreover, I would like to thank my advisory, candidacy and supervisory committee members, Dr. Susan Fischer, Dr. Ellen Richie, Dr. Donna Kusewitt, Dr. Feng Wang-Johanning, Dr. Mark Bedford, Dr. Taiping Chen, Dr. David Mitchell, Dr. Gary Johanning,

and Dr. Robin Fuchs-Young. They are always supportive and their insights, expertise and wisdom have helped me a great deal to accomplish this work.

Furthermore, I would like to thank all past and present Tang Lab members for their years of friendship: Ms. Tammy Davis, Dr. Collene Jeter, Mr. Bigang Liu, Dr. Can Liu, Dr. Kiera Rycaj, Dr. Mahipal Suraneni, Dr. Dingxiao Zhang, Mr. Xin Liu, Ms. Qu Deng, Mr. John Moore, Dr. Mark Badeaux, Dr. Hangwen Li, Dr. Jichao Qin, Dr. Hong Yan, Ms. Shuai Gong, Ms. Min Jin, and Ms. Yang Shi. A special thank-you goes to Ms. Tammy Davis and Mr. Bigang Liu for being true friends, and Dr. Kiera Rycaj for proof-reading my draft dissertation.

I am also grateful to all my other friends and colleagues at Science Park for their help, encouragement, and support. Especially, I am thankful to Dr. Jianjun Shen, Ms. Pam Whitney, Mr. Kevin Lin, and Ms. Rebecca Deen for their unselfish assistance in my research. In addition, I would like to thank a few wonderful individuals at GSBS who are always generous with their time and expertise, helping me to clear the roadblocks I came across during this journey: Dr. Vicki Knutson, Ms. Bunny Perez, and Ms. Becky Brooks.

Additionally, I would like to express my sincere gratitude to a few people for their moral support and constant encouragement, without which this work would have been much more difficult: Mr. Alex Zacharek, Ms. Grace Zacharek, and Dr. Kim Cardenas.

Last but not the least, I am eternally grateful for the love, patience and support from my parents and my wife.

PROSTATE CANCER STEM CELLS: DRUG TOLERANCE, EXPERIMENTAL RECONSTITUTION AND CASTRATION RESISTANCE

Publication No._____

Xin Chen, M.S.

Supervisory Professor: Dean G. Tang, M.D., Ph.D.

Prostate cancer (PCa) is one of the leading malignancies affecting men in the Western world. Although tremendous effort has been made towards understanding PCa development and developing clinical treatments in the past decades, the exact mechanisms of PCa are still not clearly understood. Emerging evidence has postulated that a population of stem cell-like cells inside a tumor, termed 'cancer stem cells (CSCs)', may be the cells responsible for tumor initiation, progression, recurrence, metastasis and therapy resistance. Like CSC studies in other cancer types, it has been reported that PCa also contains CSCs. However, there remain several unresolved questions that need to be clarified. *First*, the relationship between prostate CSCs (PCSCs) and therapy resistance (chemo- and radio-) is not known. Herein, we have found that not all CSCs are drug-tolerant, and not all drug-tolerant cells are CSCs. *Second,* whether primary human PCa (HPCa) actually contain PCSCs remains unclear, due to the well-known fact that we have yet to establish a reliable assay system that can reproducibly and faithfully reconstitute tumor regeneration from single HPCa cells. Herein, after utilizing more than 114 HPCa samples we have provided evidence that immortalized bone marrow-derived stromal cells (Hs5) can help dissociated HPCa cells generate undifferentiated tumors in immunodeficient NOD/SCID-IL2R$\gamma^{-/-}$ mice,

and the undifferentiated PCa cells seem to have a survival advantage to generate tumors. *Third,* the evolution of PCa from androgen dependent to the lethally castration resistant (CRPC) stage remains enigmatic, and the cells responsible for CRPC development have not been identified. Herein, we have found a putative cell population, $ALDH^{+}CD44^{+}\alpha2\beta1^{+}$ PCa cells that may represent a cell-of-origin for CRPC. Taken together, our work has improved our understanding of PCSC properties, possibly highlighting a potential therapeutic target for CRPC.

TABLE OF CONTENTS

APPROVAL PAGE……..i

TITLE PAGE…….…...ii

DEDICATION…….……...iii

ACKNOWLEDGEMENTS…….……iv

ABSTRACT……..…….……..vi

TABLE OF CONTENTS…….…..…viii

LIST OF ILLUSTRATIONS…….……..……xi

LIST OF TABLES…….……..……...xv

ABBREVIATIONS…….…….xvii

Chapter 1: Introduction…….……...……1

1.1 Anatomy of human and mouse prostate……...2

1.2 Histology of normal prostate……4

1.3 Stem cells: definition, identification and characterization……...4

1.4 Normal prostate stem cells (PSCs): identification and characterization……..7

1.4.1 Normal PSCs in mice: basal origin……..8

1.4.2 Normal PSCs in mice: luminal origin……..9

1.4.3 Normal PSCs in human…….....10

1.5 Natural history of PCa development……...11

1.6 CSCs: definition, identification and characterization…….....14

1.7 Studies of human PCSCs……....21

1.8 Studies of mouse PCSCs……....23

1.9 Outline of Ph.D. projects: a brief overview……....24

Chapter 2: Drug-tolerant cancer cells show reduced tumor-initiating capacity: depletion of CD44^{+} cells and evidence of epigenetic mechanisms….....25

2.1 Introduction……...26

2.2 Materials and Methods…….....29

2.3 Results……....33

2.4 Discussion……..57

2.5 Future Studies…….....62

Chapter 3: Dissociated Primary Human Prostate Cancer Cells Coinjected with the Immortalized Hs5 Bone Marrow Stromal Cells Generate Undifferentiated Tumors in NOD/SCID-IL2Rγ$^{-/-}$ Mice……...64

3.1 Introduction……..……...……65

3.2 Materials and Methods……...67

3.3 Results……74

3.4 Discussion…….....107

3.5 Future Studies……...113

Chapter 4: Studies on the cell-of-origin for castration-resistant prostate cancer (CRPC) ……...115

4.1 Introduction……...116

4.1.1. Natural process of androgen action...…….... 116

4.1.2. Mechanisms of CRPC development……..119

4.1.3. Current studies of castration-resistant prostate cancer stem cells (CaRP-CSCs)……120

4.2 Materials and Methods…….122

4.3 Preliminary Results……...125

4.4 Future Studies……...133

Chapter 5: Conclusion and Perspective……...137

BIBLIOGRAPHY……...140

VITA……170

LIST OF ILLUSTRATIONS

CHAPTER 1

Figure 1-1. Schematic illustration of the anatomy of the human and mouse prostate……..3

Figure 1-2. Self-renewal and differentiation of stem cells……...6

Figure 1-3. Progression pathway for human prostate cancer…….13

Figure 1-4. Schemata of the clonal evolution and cancer stem cell models……...17

Figure 1-5. Xenograft assays to measure human CSCs……..20

CHATPER 2

Figure 2-1. Drug-tolerant Du145 cells were more resistant to the selection drugs……34

Figure 2-2. Drug-tolerant Du145 cells were cross-resistant to non-selecting drugs……..36

Figure 2-3. Drug-tolerant DLD1 cells were resistant to selecting and non-selecting drugs.....37

Figure 2-4. Orthotopically implanted drug-tolerant Du145 cells showed reduced tumorigenic and metastatic potential……..40

Figure 2-5. Drug-tolerant Du145 cells were less proliferative and showed low cloning efficiency……44

Figure 2-6. Western blotting of different molecules in drug-tolerant Du145 cells cultures……46

Figure 2-7. Representative images of immunofluorescent staining of CD44 in drug-tolerant Du145 cells cultures……...47

Figure 2-8. Quantification of $CD44^+$ cells in drug-tolerant Du145 cells cultures……..48

Figure 2-9. CD44 knockdown in Du145 cells and *in vitro* characterizations……50

Figure 2-10. CD44 knockdown in Du145 cells and *in vivo* characterizations……...51

Figure 2-11. CD44 overexpression in Du145 cells and *in vitro* characterizations…….52

Figure 2-12. Paclitaxel inhibits PC3 orthotopic tumor growth and metastasis……..53

Figure 2-13. 'Stemness' gene expression profiles in Du145-VP16 cells……...55

Figure 2-14. Epigenetic mechanisms in Du145-VP16 cells……...56

CHATPER 3

Figure 3-1. Experimental scheme in using HPCa samples…….75

Figure 3-2. IHC analysis of HPCa57 patient sample (GS7) and its xenograft tumor……87

Figure 3-3. Testing antibody specificity in mouse prostate tumors……88

Figure 3-4. IHC analysis of HPCa58 patient sample (GS7) and its xenograft tumor……89

Figure 3-5. RT-PCR characterization of HPCa/Hs5 xenograft tumors……..90

Figure 3-6. Western blotting characterizations of HPCa/Hs5 xenograft tumors……91

Figure 3-7. Cytogenetic analysis of HPCa/Hs5 xenograft tumors…….95

Figure 3-8. Histological analysis of Hs5 tumors……96

Figure 3-9. Functional characterizations of $EpCAM^+$ cells in HPCa/Hs5 tumors…….98

Figure 3-10. Histological and cellular heterogeneity in HPCa57 (GS7) prostate tumors…….101

Figure 3-11. Histological and cellular heterogeneity in HPCa58 (GS7) prostate tumors……..102

Figure 3-12. Histological and cellular heterogeneity in HPCa70 (GS7) prostate tumors……103

Figure 3-13. Histological and cellular heterogeneity in HPCa101 (GS9) prostate tumors…….104

Figure 3-14. Histological analysis of HPCa70 (GS7) patient sample and its piece implant-derived xenograft tumor……...105

Figure 3-15. Histological analysis of HPCa101 (GS9) patient sample and its piece implant-derived xenograft tumor……..106

CHATPER 4

Figure 4-1. Androgen action…….118

Figure 4-2. Experimental scheme for establishing AD and AI xenograft tumor lines…….124

Figure 4-3. Abundance of $ALDH^{+}CD44^{+}\alpha2\beta1^{+}$ cells in LAPC9 AD and AI tumors……..128

Figure 4-4. $ALDH^{+}CD44^{+}\alpha2\beta1^{+}$ LAPC9 AI cells were significantly more tumorigenic than the isogenic $ALDH^{-}CD44^{-}\alpha2\beta1^{-}$ cells……...129

Figure 4-5. TM^{+} LAPC9 AI cells were significantly more tumorigenic than the isogenic TM^{+}-depleted cells……130

Figure 4-6. Characterization of clonogenicity of both TM^{+} and TM^{-} LAPC9 AI cells using sphere formation assays……131

LIST OF TABLES

CHAPTER 2

Table 2-1. Drug-tolerant Du145 cells possess much reduced tumorigenic potential…….38

Table 2-2. Reduced tumorigenic potential of orthotopically implanted drug-tolerant Du145 cells……39

Table 2-3. Reduced tumorigenic potential in drug-tolerant DLD1 cells……42

Table 2-4. Drug-tolerant UC14 cells demonstrate drug-dependent changes in tumorigenicity……43

CHAPTER 3

Table 3-1. Primary antibodies used in Chapter 3……...73

Table 3-2. HPCa xenotransplantation using tumor pieces in immunodeficient mice……76

Table 3-3. Unsorted or marker-sorted HPCa cells mixed with CAFs fail to initiate transplantable tumors in NOD/SCID mice…….79

Table 3-4. Unsorted or marker-sorted HPCa cells mixed with Hs5 cells fail to initiate transplantable tumors in NOD/SCID mice…….80

Table 3-5. Freshly purified and unsorted HPCa cells injected in NSG mice…….83

Table 3-6. HPCa cells mixed with Hs5 cells initiate serially transplantable tumors in NSG mice…….84

Table 3-7. Reconstituted 'prostate' tumors are independent of Hs5 cells, host, and injection site……..85

Table 3-8. Cultured Hs5 cells initiate tumor development in NSG mice……...97

CHAPTER 4

Table 4-1. Triple marker analysis in purified primary prostate cancer cells……132

ABBREVIATIONS

μg	microgram
kg	kilogram
mg	milligram
μM	micromolar
nM	nanomolar
ml	milliliter
ABC	ATP-binding cassette
ACD	asymmetric cell division
ADT	androgen-deprivation therapy
ADPC	androgen-dependent prostate cancer
AIPC	androgen-independent prostate cancer
ALDH	aldehyde dehydrogenase
AML	acute myeloid leukemia
AP	anterior prostate
AR	androgen receptor
ATCC	American Type Culture Collection
Aza	5'-aza-deoxycytidine
BrdU	5-bromo-2'-deoxyuridine
CAFs	carcinoma-associated fibroblasts
CARNs	castration-resistant Nkx3.1- expressing cells
CaRP-CSCs	castration-resistant prostate cancer stem cells
ChIP	chromatin immunoprecipitation

ChIP-Seq	chromatin immunoprecipitation sequencing
CML	chronic myelogenous leukemia
CK	cytokeratin
CRPC	castration resistant prostate cancer
CSC	cancer stem cell
DF	drug free medium
DHT	dihydrotestosterone
DMEM	Dulbecco's Modified Eagle Medium
Dox	doxorubicin
DP	dorsal prostate
DTCs	drug-tolerant cancer cells
EpCAM	epithelial cell adhesion molecule
FBS	fetal bovine serum
FACS	Fluorescence-Activated Cell Sorting
GO	Gene Ontology
GS	Gleason Score
HE	hematoxylin and eosin staining
HSP	heat-shock protein
HPCa	human prostate cancer
IF	immunofluorescent staining
IHC	immunohistochemistry
i.p	intra-peritoneal injection
KC	kidney capsule

LDA	limiting dilution assay
LP	lateral prostate
LRCs	label-retaining cells
LSC	$Lin^{-}Sca\text{-}1^{+}CD49^{+}$ cells
mAb	monoclonal antibody
MOI	multiplicity of infection
MSC	bone marrow derived mesenchymal stromal (or stem) cells
NOD/SCID	Nonobese diabetic/severe combined immunodeficiency mice
NS	NOD/SCID mice
NSG	NOD/SCID interleukin-2 receptor gamma chain null mice (NOD/SCID-IL2R$\gamma^{-/-}$)
pAb	polyclonal antibody
PAP	prostatic acid phosphatase
PBS	phosphate buffered saline
PCa	prostate cancer
PCSCs	prostate cancer stem cells
PIN	prostatic intraepithelial neoplasia
PSA	prostate-specific antigen
PSCs	prostate stem cells
PCSCs	prostate cancer stem cells
ROS	reactive oxygen species
RPMI	Roswell Park Memorial Institute (medium)
RT-PCR	reverse transcription polymerase chain reaction

qPCR	quantitative real time polymerase chain reaction
rUGM	rat urogenital mesenchyme
SCs	stem cells
s.c	subcutaneous(ly)
SCD	symmetric cell division
SP	side population
STS	staurosporine
Taxol	paclitaxel
TIF	tumor-initiating frequency
TM^+	$ALDH^+CD44^+\alpha2\beta1^+$ or triple marker-positive
TM^-	$ALDH^-CD44^-\alpha2\beta1^-$ or triple marker-negative
TMZ	temozolomide
TP	testosterone pellets
TSA	trichostatin A
USG	urogenital sinus
VP	ventral prostate
VP16	etoposide
15-LOX2	15-lipoxygenase-2

Chapter 1

Introduction

Prostate cancer (PCa) is one of the most common malignancies, and the second leading cause for cancer-related mortality following lung cancer in American males (1). According to the Cancer Statistics 2012, it was estimated that there will be ~241,740 new cases and ~28,170 related deaths in the USA this year (1). Although much progress has been made in the past decades, the exact mechanisms underlying PCa development remain unclear (2). Emerging evidence has shown that many human malignancies, including PCa, contain a subset of stem cell-like cancer cells, termed 'cancer stem cells (CSCs)', which are proposed to be responsible to drive tumor formation and progression, mediate therapy resistance and recurrence, and facilitate metastasis (3-8). The CSC model has provided new insights into the mechanistic studies of human cancers, which could potentially lead to drug development and clinical treatments.

1.1. Anatomy of human and mouse prostate

The prostate is a sex hormone regulated organ, which is located at the base of bladder surrounds the urethra, and contributes to semen production. Based on the seminal work from McNeal, human prostate glands are classified into three zonal structures, i.e., peripheral, central, and transition zones (9-11), and it is widely believed that most human PCa arise in the peripheral zone, due to the fact that it makes up ~ 70% volume of the prostate gland (Figure 1-1). In contrast, a mouse prostate is composed of four lobes, i.e., dorsal (DP), ventral (VP), lateral (LP) and anterior (AP) lobes (Figure 1-1). It has been suggested that the mouse dorsolateral prostate and the human peripheral zone are functionally identical, based on gene profiling (12).

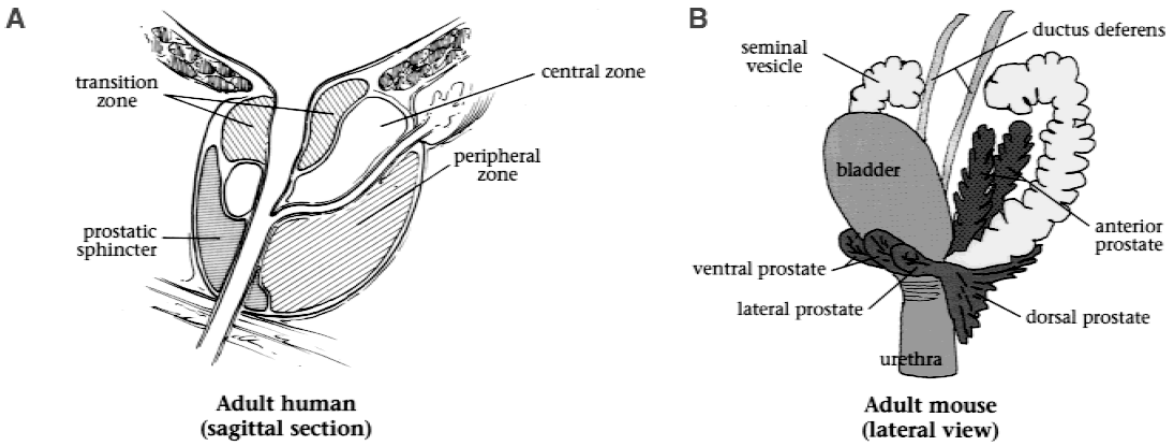

Figure 1-1. Schematic illustration of the anatomy of the human and mouse prostate. Taken from (13) with permission from Cold Spring Harbor Laboratory (CSHL) Press.

1.2. Histology of normal prostate

Histologically, prostate glands (human and mouse) are composed of three different epithelial cell types: basal, luminal and neuroendocrine cells (2, 14, 15). Basal cells reside in the basal layer that sits above the basement membrane, and these cells express cytokeratin 5 (CK5), CK14, p63 (16), CD44 (17), CD133, Bcl-2, telomerase, GST-π, and low or undetectable levels of androgen receptor (AR) protein. In contrast, luminal cells constitute the luminal layer that situates above the basal layer, generate secretory proteins into the lumen, and express prostate-specific antigen (PSA), CK8, CK18, CK19, prostatic acid phosphatase (PAP), 15-lipoxygenase-2 (15-LOX2) (18), CD57 (17), and high levels of AR. Neuroendocrine cells are localized throughout the basal layer, and express synaptophaysin and chromogranin A. These cells are rare and their functions are not clearly understood (2, 14, 15).

1.3. Stem cells: definition and identification

In general, normal stem cells (SCs) are defined as cells that are endowed with self-renewal abilities and differentiation capacities (6, 7, 19). SCs possess several fundamental characteristics. *First*, they are generally rare (6). *Second*, they exist in a specific microenvironment, termed 'niche', where they are maintained in an undifferentiated state and self-renew if needed (19). *Third*, recent evidence suggests that adult SCs can be either quiescent or proliferating (20), whereas most primitive SCs are generally quiescent in the niche. However, SCs possess high proliferative potential, which can be manifested in response to stimulation (e.g., injury). *Fourth*, SCs maintain themselves via self-renewal, which can be achieved through either asymmetric cell division (ACD), or symmetric cell

division (SCD). In SCD, a SC replenish itself by generating two identical daughter cells, while in ACD, a SC can give rise to two distinct daughter cells (an identical SC, and a committed progenitor cell) (Figure 1-2). The committed progenitor cells generated by SCs will eventually differentiate into mature cells composing a specific tissue, a process called differentiation (Figure 1-2).

SCs are typically functionally characterized by tissue reconstitution assays or lineage tracing (7, 21). In a tissue reconstitution assay, a candidate SC population is isolated by cell surface marker(s) via florescence-activated cell sorting (FACS), and tested for SC properties in xeno-, syngeneic, or allogeneic transplantation, to determine if these cells have the ability to regenerate the tissue from which they are derived. However, the main limitation of this process is the uncertainty of whether it represents the natural process of regeneration in the target tissue. Alternatively, the lineage-tracing strategy is designed to circumvent such confusions, by utilizing a reporter system of 'stem cell-specific' inducible Cre mice to characterize SC properties in their orthotopic sites. However, it is frequently unclear how relevant the data is to human samples and it is not known how specific Cre recombination is within the cells (or tissue) of interest.

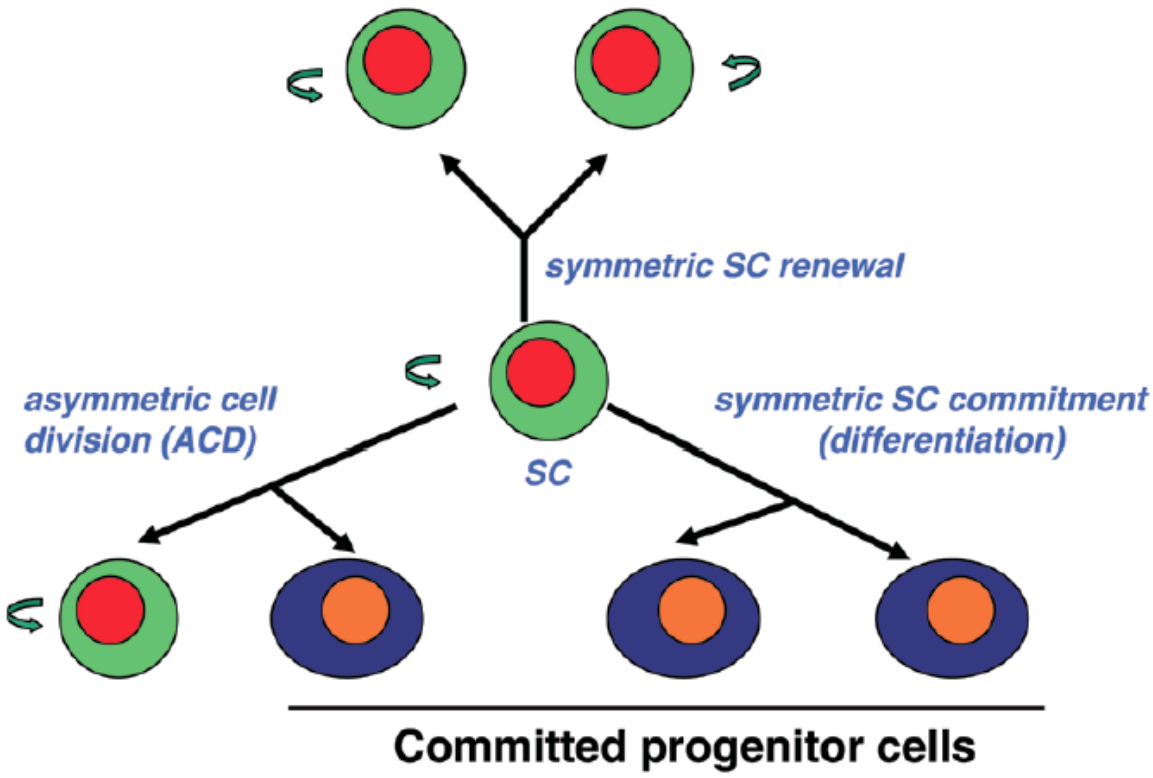

Figure 1-2. Self-renewal and differentiation of stem cells. The stem cell self-renewal is indicated by curved arrows. Only a uni-potent progenitor cell is depicted. Take from (7) with permission from Nature Publishing Group.

Additionally, SCs can be enriched by other ways. For example, a label-retaining strategy (i.e., BrdU) is commonly used, based on the observations that SCs are quiescent (22). These label-retaining cells (or LRCs) can then be sorted out by FACS to further characterize their SCs properties *in vivo* and *in vitro* with combined strategies. Furthermore, SCs can be purified via functional methods, including side population (SP), or the ALDEFLUOR assay, based on the fact that SCs highly express detoxification molecules, e.g., ABC transporter ABCG2 in SP, and aldehyde dehydrogenase 1 A1 (ALDH1A1) in the ALDEFLUOR analysis (23-26). Moreover, *in vitro* characterization of SC properties involves two-dimensional clonal cultures and three-dimensional serial sphere-formation assays, to mainly examine proliferative/clonal potentials and self-renewal abilities, respectively, of a candidate cell (or a cell population) (27). In reality, none of the above-mentioned methods can demonstrate on their own that the candidate cell population is truly enriched in SCs, and several methods often need to be combined.

1.4. Normal prostate stem cells (PSCs): identification and characterization

Previous studies have shown that the adult rodent prostate regresses after castration, but will return to normal size after androgen restoration. Such regression-restoration events can be repeated for multiple cycles (28, 29), which strongly suggests the presence of PSCs. Using the BrdU label-retaining strategy, $BrdU^+$ basal and luminal cells in the proximal region of the prostate have been identified after 39 weeks (16 cycles) of prostate regression-restoration. Importantly, such slow-cycling cells have a high proliferative potential and can regenerate glandular structures *in vitro* that are positive for both CK8 and CK14 (30). In the past decade, many studies in animal models have reported the presence of putative PSCs in

both basal and luminal layers, but the interpretations of these data are highly dependent on the methodology utilized.

1.4.1. Normal PSCs in mice: basal origin

During prostate regression, ~90% of luminal cells and a small subset of basal cells undergo apoptosis after androgen deprivation, indicating that the castration-resistant PSCs are likely to be localized in the basal cell layer. Indeed, most recent evidence supports the hypothesis that basal cells are enriched in PSCs, many of which have been evinced using the aforementioned tissue reconstitution assay (31). For example, the Sca-1^+ basal cells isolated from the proximal prostatic glands have been shown to be slow cycling and highly capable of regenerating prostate-like tissues in the renal grafts compared to the corresponding Sca-1^- cells (32, 33). In addition, most Sca-1^+ cells (~60%) are also positive for α6 integrin and anti-apoptotic molecules Bcl-2 (32). Later studies have shown that Lin^-Sca-1^+CD49^+ (LSC) prostate cells reside in the basal layer of the proximal region, and are highly enriched for colony- and sphere-forming cells *in vitro* and tissue-regenerative cells *in vivo* (34). Similarly, the same group has reported that $Trop2^{hi}$ LSC mouse prostate cells, localized in the basal layer, are further enriched for PSCs using the same experimental strategies (35). Recently, CD117 (c-kit) expression has been shown to be mainly localized in the proximal region of mouse prostate glands and is enhanced after castration, suggesting that CD117 is likely a new marker to enrich mouse PSCs (36). Interestingly, a single Lin^-Sca-$1^+CD133^+CD44^+CD117^+$ murine prostatic cell is able to reconstitute a prostate in the renal grafts (~10%), and the regenerated prostate glands contain cells positive for basal-, luminal- and neuroendocrine cell-markers (36). In addition, this report has also shown that $CD117^+$

cells are preferentially enriched in the basal-cell layer in mouse prostate epithelium (36). Taken together, these results suggest that some mouse PSCs with regenerative capacity, identified via the FACS-based tissue reconstitution assays, reside in the basal-cell layer.

1.4.2. Normal PSCs in mice: luminal origin

The possibility that luminal prostatic cells harbor PSCs originated from the early observations that grafting of urogenital sinus (UGS) from $p63^{-/-}$ mouse embryos can lead to prostatic tissues under the kidney capsule, which contain luminal and neuroendocrine cells but lack basal cells (37). In addition, such $p63^{-/-}$ prostate grafts can undergo several cycles of androgen deprivation and restoration (37). Recently, using a genetic lineage tracing strategy, a small population of luminal Nkx3.1 - expressing cells, termed 'CARNs', have been reported in castrated mouse prostates, and these cells possess long-term self-renewal potentials *in vivo* (38). CARNs are capable of reconstituting a prostate at the single-cell level when used in tissue reconstitution assays (38). Dr. Li Xin's group used lineage tracing approach in double transgenic mouse model (K14-$CreER^{Tg/Tg}$; $mTmG^{Tg/Tg}$) to show that, in adult mouse prostate, the GFP-labeled prostate basal cells can only give rise to basal cells positive for CK5 after prostate gland regression-restoration experiments (39). When they employed a similar strategy in another double transgenic mouse model (K8-$CreERT2^{Tg/Tg}$; $mTmG^{Tg/Tg}$), they observed that the GFP-labeled prostate luminal cells can only give rise to luminal cells positive for CK8 after the regression-restoration experiments (39). These results seem to suggest that in adult mouse prostates, there exist lineage-restricted progenitor cells that can regenerate cells in the same lineage. Interestingly, the same study (39) provided evidence that prostate luminal cells are more sensitive to malignant transformation

in a *PTEN*-null model whereas prostate basal cells, seemingly, need to first differentiate into transformation-competent luminal cells before they can be oncogenically transformed by *PTEN* loss (39). These data suggest that although both prostate basal and luminal layers harbor cells that can self sustain *in vivo*, the prostate luminal cells are more susceptible to direct oncogenic transformation than basal cells (39). Another group recently has combined the lineage tracing and prostate regression-restoration assays in their double transgenic mouse model (PSA-CreER^{T2}/R26-lacZ and PSA-CreER^{T2}/Rosa26R mT/mG) and reported that the preexisting luminal cells harbor castration-resistant cells, which can generate new luminal cells *in vivo* (40). Collectively, these results all suggest that luminal cells may also contain a subset of PSCs or progenitor cells.

The relationship between each reported PSC population whether basal or luminal is presently unclear.

1.4.3. Normal PSCs in human

The studies of PSCs in human cells are not feasible due to technical and ethical issues that will arise if the lineage-tracing strategy is applied. Therefore, the possible presence of putative PSCs in the human prostate gland have to be inferred from several pieces of evidence, but mostly from the reports using FACS-based *in vivo* and *in vitro* assays (21). The results from these assays generally suggest that human PSCs are of basal origin. For instance, ~1% of basal cells from benign human prostate tissues are found to express high levels of α2β1-integrin, and possess SC properties, based on the observations that they have more clonogenic and prostate duct-regenerative capacities than other cell populations (41). In addition, it was later reported that putative human PSCs may be

enriched in ~1% of human prostate basal cells positive for CD133 and restricted to α2β1-integrin$^{hi/+}$ cell populations, which possess higher proliferative and prostate duct-regenerative capacities than the isogenic CD133^{-} cells (42). Similarly, human PSCs can also be enriched in ~1% of ABCG2 $^{+}$(BCRP^{+}) cells, which are located in the basal-cell layer (43). In support, small subsets of human prostate cells are able to form prostaspheres that display a basal phenotype, i.e., CD44^{+}CD49f^{+}CK5^{+}p63^{+}Trop2^{+}CK8^{-}AR^{-}PSA^{-}, and these sphere-forming cells can generate prostate-like ducts in renal grafts using the tissue reconstitution assay (44). However, whether human prostate luminal cells also contain PSCs is not clear and this possibility cannot be completely excluded.

1.5. Natural history of PCa development

PCa takes time to develop, from normal prostate, to prostatic intraepithelial neoplasia (PIN), then to early and late stage carcinoma, and finally to metastatic and castration resistant disease (2). Early-stage PCa patients are commonly treated by radical prostatectomy with good prognosis, whereas late-stage PCa patients are mainly treated by androgen-deprivation therapy (ADT) with the majority of patients eventually developing an incurable and lethal stage termed ‘castration resistant prostate cancer (CRPC)’ (or androgen independent prostate cancer/AIPC) (45, 46). CRPC has a high propensity to metastasize to bone, lung, liver and other sites, which creates a barrier for effective clinical treatments (Figure 1-3).

Histopathologically, the majority (>95%) of PCa are adenocarcinoma, manifested by the expansion of luminal-like cells expressing high levels of luminal markers, such as AR, CK18, PSA, and the rarity of basal-like cells expressing low levels of basal markers, such as

CK5, CK14 and p63. At the molecular level, as shown in Figure 1-3, many key regulators become dysregulated as PCa develops, such as down-regulation of *NKX3.1*, up-regulation of *MYC*, inactivation of *PTEN* and *TP53*, and overexpression of *EZH2* and *ERK/MAPK*, etc (2). In addition, at the genomic level, the oncogenic gene fusions of *TMPRESS2* and *ERG* are the most frequent genomic rearrangement in PCa (>50%) (47, 48). However, our understanding of the etiology for PCa is still superficial, and a great deal of work is still needed.

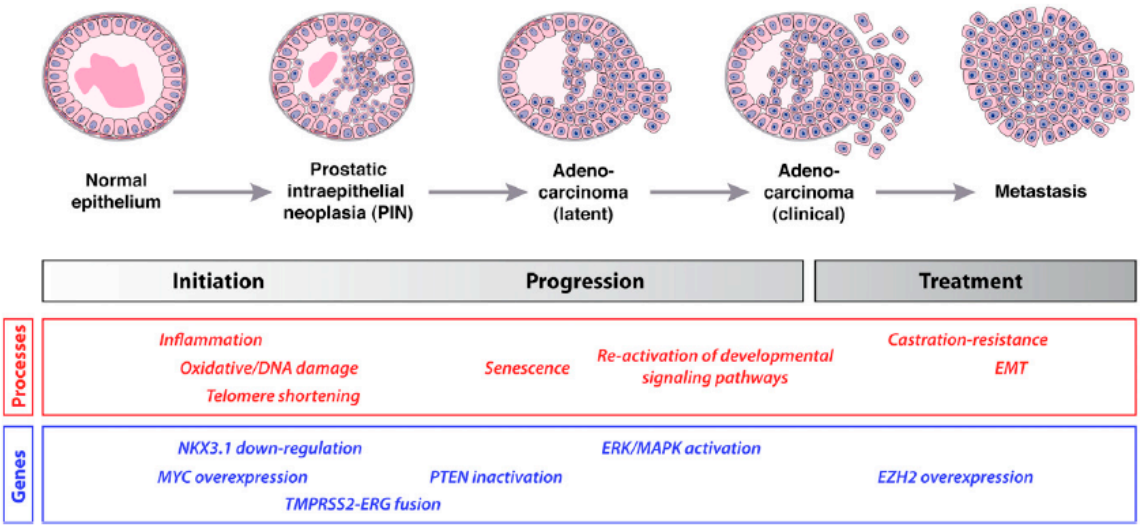

Figure 1-3. Progression pathway for human prostate cancer. Stages of progression are shown, together with molecular processes and genes/pathways that are likely to be significant at each stage. Taken from (2) with permission from Cold Spring Harbor Laboratory (CSHL) Press.

1.6. CSCs: definition, identification and characterization

Cellular heterogeneity exists in both normal and cancerous tissues. Tumor cell heterogeneity can be explained by two models: the clonal evolution (stochastic) model and the cancer stem cell (hierarchical) model (3-8, 21, 49-51). The well-established clonal evolution model has long been established (52), in which genetic mutations (52) and epigenetic alterations (53) in the tumor bestow a selective growth advantage, leading to a dominant clone. In this model, most tumor cells are believed to possess similar tumorigenicity after clonal selection. In contrast, emerging evidence has shown that in hematopoietic malignancies and solid tumors, there exists a subset of stem cell-like cancer cells, namely 'CSCs', which stands at the apex of a hierarchy of cancer cells, and are cells responsible for sustaining tumor development (Figure 1-4). By comparison, non-CSCs or CSC progeny have much more limited tumorigenicity. Recent evidence suggests that these two models may not necessarily be mutually exclusive (4, 5, 8, 50).

The CSC model was proposed decades ago. It was reported in 1937 that a single murine leukemic cell possessed the ability to regenerate tumors in a mouse, providing evidence for the existence of leukemia-initiating cells (54). In the 1960s and 1970s, several pieces of evidence from different tumor systems demonstrated the presence of stem-like cancer cells, which are highly tumorigenic *in vivo* and could give rise to the bulk of non-tumorigenic cells (55-59). Nevertheless, the first definitive evidence for true CSCs came from John Dick's lab in the 1990s. They showed that small subsets of leukemic cells from most of their human AML samples share the same phenotypic markers ($CD34^+CD38^-$) as normal hematopoietic stem cells, and these $CD34^+CD38^-$ stem cell-like leukemic cells have the capacity to serially reinitiate AML in immunodeficient mice (i.e., NOD/SCID) (60, 61).

In 2003, a report showed that $CD44^{+}CD24^{-/lo}$ human breast cancer cells could regenerate serially transplantable tumors with as few as 100 cells whereas cells from other populations were much less tumorigenic, providing the first evidence that CSCs exist in solid tumors (62). From then on, the CSC model has been widely studied in a variety of human tumors, including leukemia (63-66), cancers of breast (67-69), brain (70-73), colon(74-77) , prostate (15, 43, 78-105), lung (106-108), liver (109-111), pancreas (112, 113), kidney (114, 115), bladder (116, 117), ovary (118, 119), head and neck (120), and melanoma (121-123).

How should a CSC be defined? In theory, a CSC is the cell in a tumor that has the potential to self-renew and gives rise to all other types of cancer cells. Experimentally, the CSC hypothesis will be examined in functional studies, in which a population of cancer cells will be defined as stem-like cancer cells, or 'CSCs', by their virtue of reconstituting serially transplantable tumors that histopathologically resemble, at least partially, the parental tumor. Therefore, the 'gold' standard to test CSC properties of certain cells is to examine their capacity to reinitiate tumor development and self renew in immunodeficient mice (3) (Figure 1-5). The reported CSC populations are mainly identified via the approaches similar to those used to enrich for normal SCs, including FACS-based cell surface markers (60-62) and functional assays (68, 86), followed by functional validation via injection of such CSC-enriched cells into immunodeficient mice at various cell numbers (i.e., limiting dilution assay/LDA), or plating the sorted cells *in vitro* to test their serial sphere formation capacities. The majority of aforementioned studies of CSCs utilized this FACS-based cell surface marker approach. In addition, recent studies in animal models have provided solid evidence that CSCs can be tracked using a lineage-tracing strategy in their natural

microenvironment, i.e., glioma, epidermal squamous cell carcinoma, and intestinal adenoma (124-126). For example, it has been shown that a subpopulation of glioma tumor cells can be labeled by a *nestin-ΔTK-GFP* transgene in the subventricular zone of the brain, where the adult neural stem cells are localized. After administration of the drug temozolomide (TMZ), the quiescent GFP^+ glioma cells can self-renew and generate GFP^- glioma cells, which comprise the majority of the tumor, suggesting that these quiescent GFP^+ glioma cells are the cells responsible for sustaining long-term glioma growth, are resistant to the drug treatment, and contain CSCs properties (126). Collectively, current evidence has implied the existence of CSCs in some, if not all, human and mouse tumors.

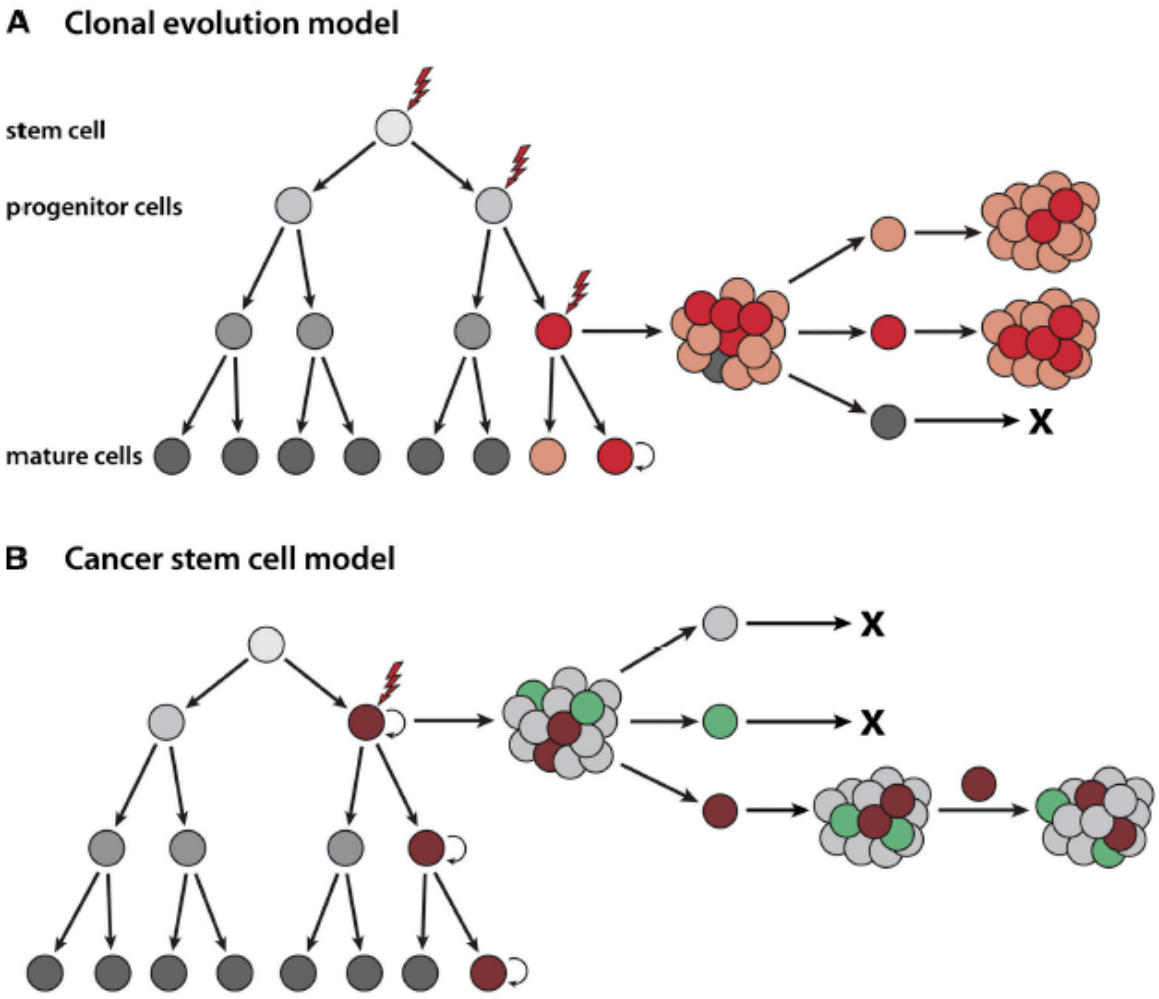

Figure 1-4. Schemata of the clonal evolution and cancer stem cell models. (A) The clonal evolution model is a nonhierarchical model where mutations arising in tumor cells confer a selective growth advantage. Depicted here is a cell (red) that has acquired a series of mutations and produced a dominant clone. Tumor cells (red and orange) arising from this clone have similar tumorigenic capacity. Other derivatives (grey) may lack tumorigenicity due to stochastic events. Tumor heterogeneity results from the diversity of cells present within the tumor. (B) The cancer stem cell model is predicated on a hierarchical organization of cells, where a small subset of cells has the ability to sustain tumorigenesis and generate heterogeneity through differentiation. In the example shown, a mutation(s) in a progenitor cell (depicted as the brown cell) has endowed the tumor cell with stem cell-like properties. These cells have self-renewing capability and give rise to a range of tumor cells (depicted as gray and green cells), thereby accounting for tumor heterogeneity. Taken from (8) with permission from Elsevier.

However, there is some confusion and misunderstanding about CSCs. *First*, the frequency of CSCs is variable and highly dependent on the system studied. For example, a small subset of melanoma cells (1 in 10^6) expressing ABCB5 has been shown to have long-term tumor-initiating properties, self-renewal ability *in vivo* and the ability to differentiate into $ABCB5^-$ bulk cells (121). However, a later study showed that as high as 1 in 4 melanoma cells were CSCs if more immunodeficient mice were utilized (122), suggesting that the relative abundance of putative CSCs may vary with different strains of immunodeficient mice, experimental methodologies, and primary samples utilized. *Second*, there may be no universal CSC markers for all tumors. It has been reported that CSCs can be enriched by phenotypic cell surface markers and functional assays, such as CD44 (85), SSEA-1 (127), ALDH (68), etc. For instance, CD133 has been used to enrich for CSCs in brain tumors (70). However, in some reports, $CD133^+$ colon cancer cells seem to be equally tumorigenic to $CD133^-$ colon cancer cells (77), indicating that this marker may not discern CSCs in all types of cancer. *Third*, CSCs may not necessarily originate from normal stem cells. It has been postulated that CSCs are derived from their corresponding normal counterpart, in that CSCs are commonly purified by the markers used for enriching normal SCs (60, 61). However, recent evidence has shown that CSCs can also originate from progenitors or differentiated cells. For instance, a study of transformation targets in human basal-like breast cancer has provided strong evidence that luminal progenitors ($CD49f^+EpCAM^+$) rather than basal stem/progenitor ($CD49f^{hi}EpCAM^-$) are likely the targets for malignant transformation (128). Similarly, it has been shown that restricted progenitors in medulloblastoma, the most malignant brain tumor in children, can be malignant targets via activation of the Sonic hedgehog (Shh) pathway (129). *Fourth*, CSCs are heterogeneous.

For example, putative prostate cancer stem cells (PCSCs) can be phenotypically enriched in different populations, such as $CD44^+$ (85), $ALDH1A1^+$ (91), $TRA\text{-}1\text{-}60^+CD151^+CD166^+$ (94), PSA^- (98), etc, via distinct methodologies. In most cases, it remains generally unclear which CSC population represents the most primitive CSCs. Also, the interrelationship among all CSC-enriched populations is largely unknown. *Fifth*, CSCs may not necessarily be all resistant to chemo- and radio- therapy, which I will discuss further in Chapter 2.

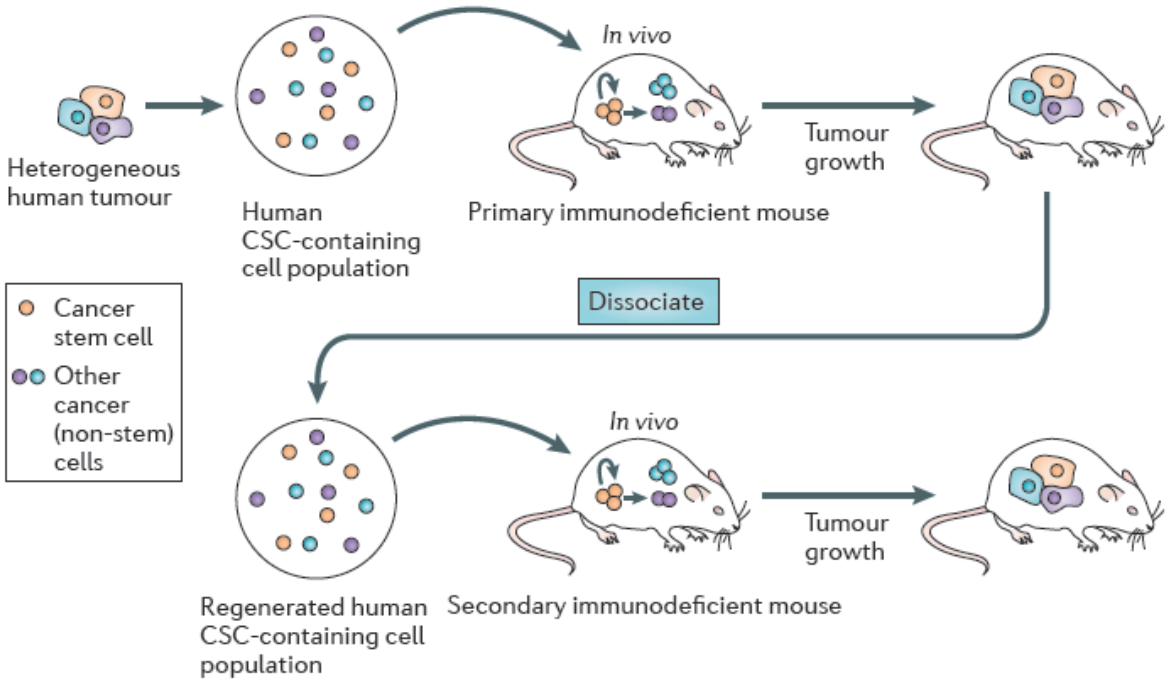

Figure 1-5. Xenograft assays to measure human CSCs. Cancer stem cells (CSCs) are most rigorously and specifically defined by their demonstrated ability to produce a progressively growing tumour consisting of cells that resemble those in the original tumour. For this reason, CSCs are also frequently referred to operationally as tumour-initiating cells. Limiting-dilution transplants or other clonal tracking strategies are typically used to determine the frequency of CSCs in the initial tumour-derived cell suspension. Ideally, the tumours that form in primary hosts are again tested for their content of cells with CSC activity (demonstrable in injected secondary hosts) to formally confirm that the initial CSCs had self-replicating ability. These principles apply both to measurements of the CSC frequency and the total CSC content, either in the bulk population or in isolated subpopulations of dissociated tumour cells. The most sensitive assays are those in which there is no immunological difference between the host and the tumour. When this is not possible (such as for human tumours), xenografts into highly immunodeficient mice are used. Taken from (50) with permission from Nature Publishing Group.

1.7. Studies of human PCSCs

Like CSCs reported in other cancer types, PCSCs have been identified mainly based on studies via FACS-based cell surface markers and functional assays followed by LDA in xenotransplatation models or *in vitro* sphere formation assays. Using cell surface markers, we revealed that $CD44^+$ PCa cells in the xenograft tumors (e.g., Du145, LAPC9 and LAPC4) are more clonal, clonogenic, tumorigenic and metastatic than the corresponding $CD44^-$ PCa cells (85). More importantly, $CD44^+$ PCa cells are quiescent, express SC-related molecules (e.g., Oct-3/4, Bmi, β-catenin, and SMO), and can give rise to $CD44^-$ PCa cells. These results suggest that $CD44^+$ PCa cells are enriched in tumorigenic and metastatic stem/progenitor cells (85). Due to the fact that CSCs are heterogeneous, we reported in subsequent studies that $CD44^+\alpha2\beta1^+$ combinatorial markers can further enrich for PCSCs in the LAPC9 model (87). Similar work has been shown in other PCa cell lines and xenograft models (84, 88, 94, 102, 130). The identification of PCSC in patient samples is extraordinarily challenging, due to the well-known fact that it is extremely difficult to re-initiate PCa development in immunodeficient mice using single primary HPCa cells (131), which I will discuss in Chapter 3. Notably, a report has shown that a small subset of primary HPCa cells expressing the phenotypic markers $CD44^+\alpha2\beta1^{hi}CD133^+$, are highly clonogenic and proliferative, suggesting the presence of stem-like cancer cells in the patient samples (78). However, whether these cells harbor tumorigenic and metastatic CSCs is still not clear as in vivo tumor experiments were not done in this study (78). Taken together, the marker-dependent strategy has allowed us to enrich putative PCSCs in PCa cell lines, xenograft models, and primary and metastatic patient samples.

PCSCs can also be enriched via marker-independent methods. For instance, it has been shown that ALDH-positive PCa cells are more tumorigenic and metastatic than the

ALDH-negative PCa cells (91, 93). Also, we have showed that LAPC9 SP cells are much more tumorigenic (>100-fold) than non-SP cells (86). Furthermore, we have revealed that the holoclones in PC3 cell cultures harbor stem cell-like PCa cells, compared to the isogenic meroclones and paraclones, manifested by their enhanced clonogenicity and tumorigenicity (82). Additionally, a recent study in primary HPCa samples has showed that *in vitro* serially passaged prostaspheres contained self-renewal cells expressing high levels of SC makers (i.e., $CD49b^{+}/CD49f^{+}/CD44^{+}/\Delta Np63^{+}/Nestin^{+}/CD133^{+}$) (90), suggesting that prostaspheres are likely to be enriched in PCSCs. Most recently, we have provided convincing evidence that the ($PSA^{-/lo}$) undifferentiated PCa cell population is enriched in PCSCs via a lentiviral reporter system from PCa cell lines, xenograft tumors as well as primary untreated patient samples (98). The $PSA^{-/lo}$ cells are significantly more clonal, clonogenic, quiescent, tumorigenic, stress-resistant and castration resistant than the isogenic differentiated bulk PSA^{+} cells. Furthermore, time-lapse videomicroscopy studies demonstrate that a portion of $PSA^{-/lo}$ PCa cells can undergo ACD to generate PSA^{+} cells, a cardinal feature for SCs (132). Moreover, $PSA^{-/lo}$ cells sustain long-term tumor propagation and can generate serially transplantable tumors that histologicially resemble their parental tumors. Collectively, these data unequivocally demonstrate the presence of the long-term PCSCs in the $PSA^{-/lo}$ PCa cell population, and highlight the importance of $PSA^{-/lo}$ cells as novel therapeutic targets.

What are the possible mechanisms to regulate PCSCs in human cancer? It has been shown that $CD133^{+}/CD44^{+}$ PCa cells (DU145 and PC3) are enriched in stem cell-like cells and can be propagated in sphere-forming conditions, in which PTEN/PI3K/AKT signaling is activated. Administration of the dual PI3K/mTOR inhibitor NVP-BEZ235 significantly inhibits tumor growth of $CD133^{+}/CD44^{+}$ PCa cells (89), raising a possibility that the

PTEN/PI3K/AKT pathway may be critical for PCSC properties. Our lab has recently shown that NANOG, a transcription factor essential for ESCs pluripotency and self-renewal (133), may play a role in regulating CSC properties as evidenced via loss and gain of function experiments (80, 81). Most recently, a subset of docetaxel-resistant PCa cells have been shown to harbor tumor initiating cells and overexpress Notch and Hedgehog signaling pathways. Specific targeting of these two pathways significantly inhibits tumor regrowth of these drug-resistant PCa cells, suggesting that Notch and Hedgehog signaling may represent therapeutic targets for PCSCs (105). Other studies have also implied alternative mechanisms, including the NF-κB pathway (94), and miR-34a (96).

1.8. Studies of mouse PCSCs

There have been several reports on mouse PCSCs. For example, Sca-1^{+}, but not Sca-1^{-} mouse prostate cells can lead to PIN after viral infection of AKT1, suggesting that Sca-1^{+}/$AKT^{+/hi}$ cells are endowed with high tumor-initiating capacity (33). A notable study from Wu and colleagues demonstrated that a subset of PCa cells from *PTEN*-null models possess heightened sphere-forming capacities and enhanced tumor-regenerative potentials, compared to other subsets of cells, which can be enriched by the phenotypic markers of Lin^{-} Sca-$1^{+}CD49f^{high}$ (LSC). Interestingly, tumors derived from LSC cells have been shown to mimic their parental tumors (134). Another study has demonstrated protospheres from *PTEN*/*TP53* null mice are enriched in tumor-initiating cells with enhanced levels of AKT and AR pathways in tumor growth, implying that these pathways may play roles in regulating mouse PCSCs (135).

1.9. Outline of Ph.D. projects: a brief overview

Although we and others have made significant contributions to identify and characterize PCSCs in both human and mouse tumor models, many unresolved issues and questions still exist. *First*, whether CSCs, in general, are resistant to chemo- and radio-therapies is controversial, let alone the murky relationship between PCSCs and therapy resistance. In Chapter 2, I will present results from our model, in which we established chronic drug-tolerant cancer cells from several cell lines (Du145, DLD1 and UC14), and uncovered their CSC properties *in vivo* and *in vitro*. To our surprise, we found that not all drug-tolerant cancer cells manifest CSC features. *Second*, the majority of our previous studies of human PCSCs used cultured cell lines as well as xenograft tumors. Although there is some evidence for the presence of PCSCs in primary HPCa patient samples, definitive evidence is lacking due to the aforementioned challenge of using primary HPCa cells. In Chapter 3, I will present data from our attempt to reconstitute PCa development in immunodeficient mice using single HPCa cells. *Finally*, as the majority of advanced PCa will eventually develop into the lethal and incurable CRPC, the mechanisms of CRPC regulation are not clear, and the cell-of-origin for CRPC (or CaRP-CSCs) have not been reported. In Chapter 4, I will present preliminary data from our *in vivo* and *in vitro* characterizations to show that we have found putative CaRP-CSCs phenotypically manifested by $ALDH^+CD44^+\alpha2\beta1^+$ (TM^+). Our mechanistic studies of these cells are currently ongoing, which will be one of our major projects in the future.

Chapter 2

Drug-tolerant cancer cells show reduced tumor-initiating capacity: depletion of $CD44^+$ cells and evidence for epigenetic mechanisms

2.1. Introduction

Therapy resistance is a common phenomenon in clinical cancer treatments. Most existing therapies that have been developed result in initial tumor shrinkage. However, most tumor treatments (e.g., chemo-, radio- and tumor-targeted agents) eventually fail, and tumors relapse and metastasize. The exact mechanisms behind therapy resistance in cancer are very complicated, and possible causes include: 1) ineffectiveness of therapy (e.g., delivery failure of the drug); 2) existence of therapy-resistant CSCs; 3) genetic and/or epigenetic influence on tumor cells (136).

As introduced in Chapter 1, the CSC model has been gaining much interest and attention, opening the possibility for more effective treatments against tumors. It is generally believed that the more aggressive a tumor is, the more CSCs it may contain (137, 138), and it is implied that such aggressive and advanced tumors tend to ultimately return (139). The phenomenon where tumors initially regress after treatment but eventually recur suggests that most existing therapies are likely to kill the bulk of tumor cells bearing limited proliferative capacities, but leave behind the CSCs, which are responsible for long-term tumor growth (6). Therefore, it is assumed that CSCs are therapy resistant. One corollary in support of this assumption is the observations that CSCs can be enriched by therapeutic treatments. For example, chemotherapy has been shown to increase breast CSCs (69). This, together with other studies, implies that therapy-tolerant cancer cells may possess CSC properties (140), although this assumption has not been rigorously examined.

What are the potential mechanisms regulating CSC therapy resistance? *First,* a large body of evidence has postulated that the quiescent and slow cycling CSCs may be resistant to therapy (49, 141), which has been exemplified in acute myeloid leukemia (AML) and

some solid tumors (49). As mentioned earlier in Chapter 1, a recent study using pulse-chase experiments (via CIdU and IdU, two BrdU analogues) have demonstrated the presence of a subset of GFP^+ glioma stem cells after TMZ treatments (126), providing strong support that therapy-resistant CSCs are slow cycling and quiescent. *Second,* CSCs, like their normal counterparts, may express high levels of ATP-binding cassette (ABC) drug efflux proteins. SP has been a useful tool to isolate both normal SCs (142) and CSCs (86), whose phenotype is mediated by ABC transporters associated with multidrug tolerance (143). Experimentally, SP utilizes a FACS-based Hoechst dye 33343 staining protocol, in which SCs pump out the dye, whereas the bulk of differentiated cells accumulate the dye, resulting in a small population of cells expressing $Hoechst^{-/lo}$ in the Flow chart, known as 'side population' cells. Because of this, it is believed that a similar trait is responsible for CSC drug tolerance. *Third,* enhanced expression of anti-apoptotic genes has been observed in normal SCs as well as CSCs. For example, a recent report has demonstrated that anti-apoptotic genes (i.e., CFLAR, Bcl-2, and Bcl2A1) are highly expressed in CSC-enriched SP populations in Ho-1-N-1 cells, a human oral squamous cell carcinoma cell line (144). More importantly, Ho-1-N-1 SP cells not only survive better than the non-SP cells after chemo- treatments (e.g., 5-fluorouracil and carboplatin), but also have sharply higher anti-apoptotic activities, providing direct evidence for anti-apoptotic mechanisms in chemotherapy resistance of CSCs (144). *Fourth,* CSCs may be inherently resistant to certain stresses, including reactive oxygen species (ROS), and DNA damage. For instance, mouse breast CSCs display lower levels of ROS compared to the bulk of non-tumorigenic cancer cells, which confers CSCs significantly higher clonogenic survival after ionizing radiation (145). In addition, treatment with the glutathione synthesis inhibitor BSO dramatically inhibits the clonogenicity of these

CSCs and increases their sensitivity to ionizing radiation (145). Another example comes from glioma stem cells, in which $CD133^+$ glioma stem cells are enriched after ionizing radiation compared to $CD133^-$ glioma cells, and the radio-resistance is mediated by enhanced activation of the DNA damage checkpoint in these $CD133^+$ CSCs. Using specific inhibitors of Chk1 and Chk2 kinases significantly inhibits these CSC survival after radiation (73). These studies suggest that CSCs have an innate ability to resist many therapies.

However, it is still debated whether all CSCs are therapy-resistant and, vice versa, whether drug-tolerant cancer cells possess CSC activities. For instance, testicular carcinoma and choriocarcinoma are derived from germ cells that are driven by undifferentiated tumor cells compared to the bulk of differentiated cells. However, both chemo- and radio-therapies tend to kill the undifferentiated portion, leaving the residual mass full of differentiated cells (146). This suggests that some undifferentiated tumor cell populations, in which CSCs are highly enriched, are sensitive to cancer therapies.

In PCa, the study of PCSCs and therapy tolerance is largely lacking. To address whether PCSCs, like CSCs in other cancer types, bear resistance to chemo- and radio-therapy, or whether drug tolerant PCa cells are enriched in PCSCs, we conducted studies presented herein. In our study, we created several lines of chronic 'drug-tolerant cells' (DTCs), and characterized their CSC properties: tumorigenicity and metastatic potential in xenograft models, and also clonogenicity and proliferative capacities *in vitro*. We initially *hypothesized* that DTCs in PCa are endowed with CSC traits both *in vivo* and *in vitro*.

2.2. Materials and Methods

Animal-related studies have been approved by the M.D Anderson Cancer Center Institutional IACUC committee (ACUF 08-05-08132). All other studies presented herein were the investigator-initiated and did not require approval from other regulatory bodies.

Cells, reagents, and animals

Du145, PC3, and UC14 cells were obtained from ATCC and cultured in RPMI containing 7% heat-inactivated FBS, 100 μg/ml streptomycin, and 200 U/ml penicillin (Gibco). DLD1 cells were obtained from ATCC and cultured in DMEM containing 7% FBS with antibiotics. Etoposide (VP16) and paclitaxel were purchased from Sigma. Doxorubicin (Dox) and staurosporine (STS) were bought from Biomol. WP1102 and WP1103 were two newly synthesized paclitaxel analogs with substitutions at the 2'-OH (by the Priebe group; details to be published elsewhere). Primary antibodies used in the current study included: rabbit mAb to CD44 (Abcam) for Western blotting (1:1,000), mouse mAb to CD44 (BD Pharmingen) for immunostaining (1:500), mouse mAb to ABCG2 (Abcam; 1:500), rabbit pAb to Bcl-2 (Santa Cruz; 1:500), mouse mAbs to p21 and p27 (Santa Cruz; 1:1,1000 for both), rabbit pAb to hTERT (Santa Cruz; 1:100), rabbit mAb to GAPDH (Cell Signaling; 1:2,000) and mAb to β-actin (Cell Signaling; 1:1,000). Secondary antibodies were purchased from GE Healthcare and ECL Plus reagents were from PerkinElmer Inc. NOD/SCID mice were initially purchased from the Jackson Laboratories (Bar Harbor, ME) and the breeding colonies established in our animal facility and maintained in standard conditions according to the institutional guidelines.

Establishment of DTCs and determination of IC50 values

Du145, DLD1, and UC14 cells were initially exposed to various drugs, in quadruplicate wells, at a range of concentrations, i.e., 0, 0.1 nM, 1 nM, 10 nM, 50 nM, 0.1 μM, 0.5 μM, 1 μM, 2 μM, 4 μM, and 10 μM. Drugs were replenished every 3 days and cells were treated continuously for 2 weeks. Cell survival and death were closely monitored under an inverted phase-contrast microscope. At the end of a 2-week treatment, 'optimal' drug concentrations were determined based on the criterion that drugs showed significant inhibitory effects on cell expansion but did not completely kill the whole population (~90% cell killing). The entire experiment was repeated once. These experiments led to the determination of optimal concentrations. Thereafter, cancer cells were continuously cultured in the medium containing the optimal concentration of drugs for a minimum of 3 months to establish the DTCs, which were designated as Du145-VP16 cells, Du145-Paclitaxel cells, so on and so forth. The DTCs were routinely cultured in the medium containing the optimal concentrations of individual drugs.

To determine the half-maximal concentrations of inhibition (i.e., IC50) of parental cancer cells and the DTCs, $2.5\text{-}3.0\times10^5$ cells were plated in quadruplicate in 24-well plates. After overnight culture, cells were treated with different concentrations of the initial selection drug or non-selecting drugs (to examine

potential cross resistance) for 24-48 h. At the end of treatment, viable cell numbers were counted using trypan blue assays and the GraphPad prism 5.0 software was used to analyze data and calculate the IC50 values.

Clonal and BrdU incorporation assays, immunofluorescence, and immunoblotting

Basic procedures for these experiments have been described in our earlier publications (80, 81, 85-87, 147). To determine total cell numbers, 5,000 cells were plated in triplicate or quadruplicate in 12-well plates and cultured for 10 days, with fresh medium fed every 3 days. At the end, viable cell numbers were counted using trypan blue. For BrdU assays, cells were plated in triplicate on glass coverslips (10,000 cells/coverslip) overnight and then pulsed with 10 μM BrdU for 4 h. At the end, cells were fixed in 4% paraformaldehyde containing 5% sucrose for 10 minutes. Cells were incubated for 20 min in 1% Triton-100 and then denatured, neutralized, blocked, and incubated with monoclonal anti-BrdU antibody (1:100) for 1 h at 37°C followed by goat anti-mouse IgGAlexa Fluor 594 (30 min at 37°C). A total of 500–1000 cells were counted per coverslip and two coverslips were counted for each cell type to determine the percentage of proliferating (i.e., $BrdU^{+}$) cells.

For clonal analysis, 100 cells were plated in triplicate in 6-well plates and cultured for 10 days with fresh medium fed every 3 days. At the end, both holoclones and meroclones (82) were enumerated and the results were presented as the cloning efficiency. Paraclones contained large and senescent cells (82) and generally had <20 cells and therefore were not quantified. Immunofluorescence staining of CD44 was performed as described (85, 147). For Western blotting. parental Du145 and various drug-tolerant Du145 cells were harvested to prepare whole cell lysate in Western blotting analysis of the molecules indicated in the figure panels. In some experiments, Du145-VP16 cells were first treated with various concentrations of trichostatin A (TSA) or 5'-aza-deoxycytidine (Aza) for 72 h.

Establishment of GFP-tagged drug-tolerant DU145 cells

Briefly, 293FT packaging cells (80) were transfected with pLL3.7-GFP lentiviral vector (80) together with the packaging plasmids using Lipofectamine. Virus-containing medium was collected 48-72 h later, centrifuged at 3,000 rpm, passed through a 0.45 μm filter to remove debris and finally subjected to ultracentrifugation (20,000 rpm×2 h at 4°C). Drug-tolerant DU145 cells were then infected with the virus at MOI (multiplicity of infection) of 20–25.

Subcutaneous (s.c) and orthotopic tumor experiments

Basic procedures were previously described (80, 82, 85-87, 96, 98). Briefly, parental and drug-tolerant Du145 (and other) cells at different numbers were injected in 50% Matrigel s.c into the flanks of NOD/SCID mice. When the largest tumor(s) in any group must be terminated by IACUC regulations or the tumor-bearing animals became moribund, all animals in that group were sacrificed and tumors harvested. For orthotopic implantation, animals were anesthetized and cells were injected in a 40-μl medium-Matrigel mixture (1:1) into the dorsal prostate. When tumor burden became obvious (by palpation), the experiment was terminated, animals sacrificed,

and primary tumors together with several organs (i.e., lung, liver, spleen, pancreas, kidney, etc) were dissected and examined for micro and macrometastasis (i.e., GFP^+ foci) under a Nikon epifluorescence microdissection microscope.

CD44 knockdown experiments

shRNA-mediated knockdown was performed as recently described (80, 96). Briefly, 293FT packaging cells were transfected with either pGIPz CD44-shRNA lentiviral vector or pGIPz-NS control vector. The virus-containing culture medium was collected 72 h post transfection, centrifuged at 3,000 rpm, filtered through a 0.45 μm-syringe filter, and finally subjected to ultracentrifugation (20,000 rpm×2 h at 4°C). The viral pellet was reconstituted in the OPTI-MEM medium and used to infect HT1080 fibrosarcoma cells to determine the viral titer. Then Du145 cells were infected with the pGIPz-NS or pGIPz-CD44shRNA viruses at an MOI of 20, and, 24–48 h later, were used in either *in vitro* characterizations or *in vivo* tumor experiments.

CD44 overexpression experiments

The basic retroviral procedure was previously described (96). Briefly, retroviral vectors, including control vector pBabe-GFP and pBabe-CD44 (Addgene, Cambridge, MA) were transfected into the Ampho-Phoenix 293 cells (ATCC). 48–72 h post transfection, virus-containing culture medium was collected, centrifuged at 3,000 rpm, filtered through a 0.45 μm-syringe filter, and finally subjected to ultracentrifugation (22,000 rpm×2 h at 4°C). The viral pellet was reconstituted in the OPTI-MEM medium and used to infect drug-tolerant Du145 cells for 24–48 h, which were then used in both *in vitro* and *in vivo* experiments.

Therapeutic treatment of orthotopic PC3 tumors with paclitaxel

The basic procedure for therapeutic experiments was recently described (96). Briefly, PC3-GFP cells were implanted in the dorsal prostate (DP) of male NOD/SCID mice (500,000 cells/DP; n =10). Three weeks later, 5 animals per group were injected, intravenously, with 15 mg/kg body weight of paclitaxel or vehicle control (PBS). The injections were repeated every week for two more weeks (i.e., a total of 3 injections) and animals were terminated 49 days after tumor cell implantation. The DP tumors were dissected out, imaged, and weighed whereas several organs, including the lung, pancreas, lymph node, liver, and brain, were examined for metastasis on a dissecting epifluorescence microscope (96).

Analysis of 'stemness' gene expression profiles by quantitative reverse transcriptase - polymerase chain reaction (qPCR)

The basic procedure for qPCR analysis was recently described (81, 96). Briefly, total RNA was extracted from Du145 and Du145-VP16 cells using an RNeasy RNA-purification kit (Qiagen, Valencia, CA). The ABI High-Capacity cDNA Archive Kit (Applied Biosystems, Carlsbad, CA) and random hexamers were used for cDNA synthesis. qPCR was performed by the M.D. Anderson Science-Park Molecular Biology Core Facility using an ABI Prism 7900HT (Applied Biosystems). File Builder 3.1 software (Applied Biosystems) was used to design PCR primers and

probes. Human gene-specific primer pairs were used for expression profiling by the SYBR® Green method. The experimental Ct (cycle threshold) was calibrated against that of 18S control product. All amplifications were performed in triplicate. The DDCt method was used to determine the amount of gene product relative to that expressed in parental Du145 cells (1-fold, 100%).

Statistical analyses

GraphPad prism 5.0 software and F-test were used to compare the IC50 values. Unpaired *t*-test was used to compare differences in cell numbers, $BrdU^+$% cells, cloning efficiency, $CD44^+$% cells, and tumor weights. Fisher's Exact Test was used to compare incidence and latency.

(The above Methods and Materials were taken from (148) with all authors' permission)

2.3 Results

Chronic sublethal drug treatment led to drug-tolerant cancer cells

Clinically, many cancer patients are often treated CHRONICALLY by anti-cancer therapeutics. The best example perhaps is CML (chronic myelogenous leukemia) patients who must take imatinib (Gleevec) continuously for years (149). Furthermore, metronomic chemotherapy - a form of chemo administration characterized by frequent, often daily, extended administration of small doses of conventional chemodrugs without major breaks (150), is emerging as a standard therapeutic regimen for many cancers. Based on the assumptions that CSCs may have a special advantage of surviving therapeutics and are likely the cells that mediate drug resistance, we tested whether cancer cells that have survived CHRONIC drug treatment may all possess CSC properties. We first treated Du145 prostate cancer (PCa) cells with two clinical drugs, i.e., etoposide (VP16) and paclitaxel (Taxol) as well as three experimental drugs, staurosporine (STS), a promiscuous protein kinase inhibitor, and two newly synthesized paclitaxel analogs termed WP1102 and WP1103. As described in Methods, we first treated Du145 cells with these five drugs at a range of 10 concentrations for 2 weeks to determine the 'optimal' sublethal concentrations at which drugs significantly inhibited tumor cell expansion but did not kill the entire population. Using this chronic treatment protocol that 'mimics' metronomic treatment in the clinic, we determined the optimal concentrations, in Du145 cells, of VP16, paclitaxel, STS, WP1102, and WP1103 at 1.25 μM, 50 nM, 7 nM, 5 nM, and 25 nM, respectively. Du145 cells were subsequently cultured, continuously, in the medium containing the optimal concentrations of drugs for ~3 months. The resultant drug-tolerant cell (DTC) lines were designated as Du145-VP16, Du145-Paclitaxel, Du145-STS, Du145-WP1102, and Du145-WP1103 cells, respectively.

To determine whether drug-tolerant Du145 cells were truly tolerant of the original selection drugs, we treated parental and drug-tolerant Du145 cells side-by-side with the respective five drugs. As shown in Figure 2-1, drug-tolerant Du145 cells were generally more resistant than parental Du145 cells to the selection drugs. Thus, Du145-VP16 cells were >10 times more resistant than Du145 cells to VP16 (IC50 values being 0.78 μM for Du145 and 9.17 μM for Du145-VP16 cells). Du145-Paclitaxel cells were ~7 times more resistant to paclitaxel than Du145 cells (Figure 2-1, A and C). Similarly, Du145-WP1103 cells were nearly 30 times more resistant to WP1103 than Du145 cells (Figure 2-1, B and C). Finally, Du145-STS and Du145-WP1102 cells were approximately 1.5 and 3 times more resistant to STS and WP1102, respectively, than unselected Du145 cells (Figure 2-1, B and C). Hence, the differential drug resistance among the established DTCs ranked Du145-WP1103>Du145-VP16>Du145-Paclitaxel>Du145-STS≈Du145-WP1102.

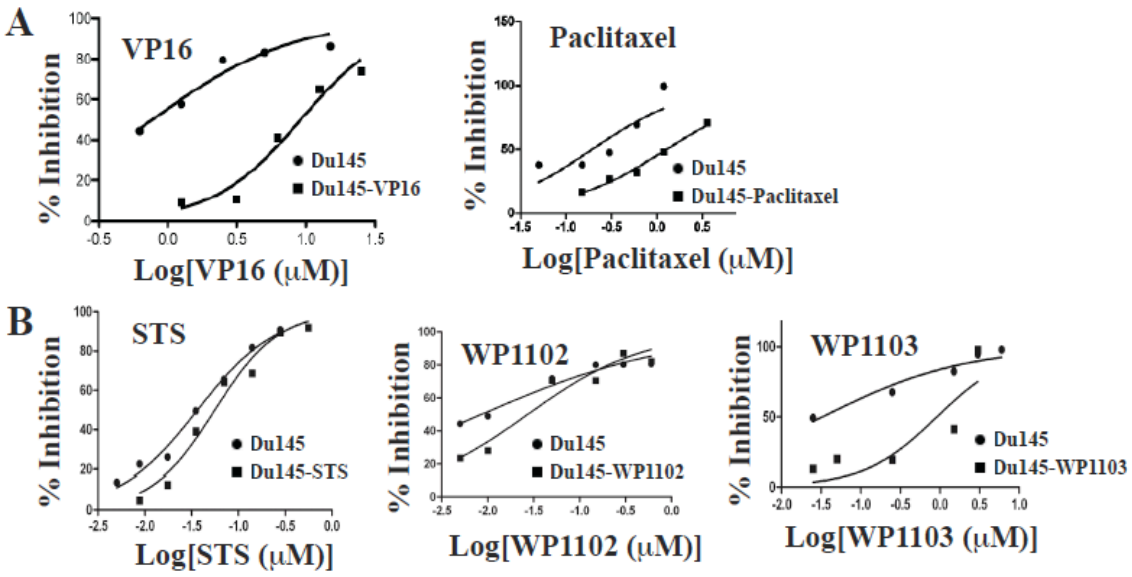

C

Cell type	*Drug*	*IC50 (μM)*	*95% CI*	*F value*	*P*
Du145	VP16	0.78 ± 1.21	0.42 – 1.42		
Du145-VP16	VP16	9.17 ± 1.13	6.15 – 13.67	79.89	0.0001
Du145	STS	0.04 ± 0.001	0.03 – 0.04		
Du145-STS	STS	0.06 ± 0.001	0.04 – 0.07	10.26	0.0094
Du145	Paclitaxel	0.19 ± 1.48	0.06 – 0.68		
Du145-Paclitaxel	Paclitaxel	1.28 ± 1.09	0.98 – 1.68	19.82	0.0043
Du145	WP1102	0.01 ± 1.27	0.004 – 0.02		
Du145-WP1102	WP1102	0.03 ± 1.29	0.01 – 0.05	9.85	0.0138
Du145	WP1103	0.03 ± 1.53	0.01 – 0.13		
Du145-WP1103	WP1103	0.91 ± 1.84	0.13 – 6.35	11.88	0.0137

Figure 2-1. Drug-tolerant Du145 cells were more resistant to the selection drugs. A-B. Parental Du145 and drug-tolerant Du145 cell lines selected with two clinical drugs (A) or three experimental drugs (B) were exposed, side-by-side, to the respective selection drugs (e.g., Du145-VP16 cells to VP16 and Du145-Paclitaxel cells to paclitaxel) at the concentrations (transformed into logarithm) indicated. Y-axis represents cell growth inhibition (%). C. Tabulated presentations of IC50 values and corresponding 95% CI (confidence interval) of Du145 cells and drugs-tolerant Du145 cells in response to the five drugs indicated. Values were calculated from data obtained in A and B. Taken from (148) with all authors' permission.

Subsequently, we exposed Du145-VP16 cells to three non-selecting drugs, i.e., paclitaxel, STS, and doxorubicin (Dox). As shown in Figure 2-2, Du145-VP16 cells were more resistant (than parental Du145 cells) to paclitaxel (~4 fold), STS (1.5 fold), and Dox (13 fold), suggesting that the DTCs were also cross-resistant to other non-selecting drugs.

Using similar strategies, we also established drug-tolerant DLD1 colon (Figure 2-3) and UC14 bladder (data not shown) cancer cells. In DLD1 cells, the optimal concentrations for VP16, paclitaxel, WP1102, and WP1003 were determined to be at 2.5 μM, 100 nM, 120 nM, and 100 nM, respectively. As shown in Figure 2-3, the established DLD1-VP16, DLD1-Paclitaxel, DLD1-WP1102, and DLD1-WP1103 cells were resistant to the respective selecting drugs. Furthermore, DLD1-VP16 cells also showed cross resistance to paclitaxel and Dox (Figure 2-3B). Drug-tolerant UC14 cells were similarly more resistant to the selection drugs (i.e., paclitaxel, STS, VP16, Dox, WP1102, and WP1103), than the parental UC14 cells (data not shown).

Drug-tolerant Du145 cells were surprisingly less tumorigenic than parental Du145 cells

We initially hypothesized that the DTCs might possess CSC properties and be more tumorigenic in vivo. Much to our surprise, all drug-tolerant Du145 cells subcutaneously (s.c) injected into the NOD/SCID mice demonstrated much reduced tumor-initiating capacity when compared to the same number of parental Du145 cells, which showed a tumor-initiating frequency (TIF) of ~1/175 (Table 2-1). Injection of increasing numbers of parental Du145 cells, expectedly, led to reduced latency (Table 2-1). In contrast, Du145-VP16 cells showed a TIF of ~1/62,000 and, at 100,000 cells injected, tumor latency was more than twice as long as for the same number of Du145 cells (Table 2-1). In fact, both Du145-Paclitaxel and Du145-WP1103 cells were non-tumorigenic up to 10,000 (for Du145-WP1103) and 100,000 (for Du145-Paclitaxel) cells implanted (Table 2-1). Even for Du145-STS and Du145-WP1102 cells, which showed the lowest IC50 differentials (Figure 2-1 B and C), reduced tumor incidence with TIF of 1/971 and 1/45,787, respectively, and smaller tumors were also observed (Table 2-1).

To determine whether tumor implantation site might have an effect on the differential tumorigenicity observed, we established GFP-tagged Du145 parental and drug-tolerant Du145 cells and implanted equal numbers (i.e., 500,000) of cells orthotopically in the dorsal prostate (DP) of the male NOD/SCID mice. When the experiment was terminated 75 days post tumor cell injections, we observed that Du145-VP16 and Du145-STS cells generated smaller tumors than parental Du145 cells (Figure 2-4A). In fact, both Du145-Paclitaxel and Du145-WP1103 cells were non-tumorigenic in the DP tumor regeneration model (Figure 2-4A). Significantly, parental Du145 cells metastasized to multiple organs including lymph nodes, kidney, pancreas, liver, lung, and spleen whereas drug-tolerant Du145 cells lacked apparent metastasis to any of these organs (Table 2-2; Figure 2-4; data not shown).

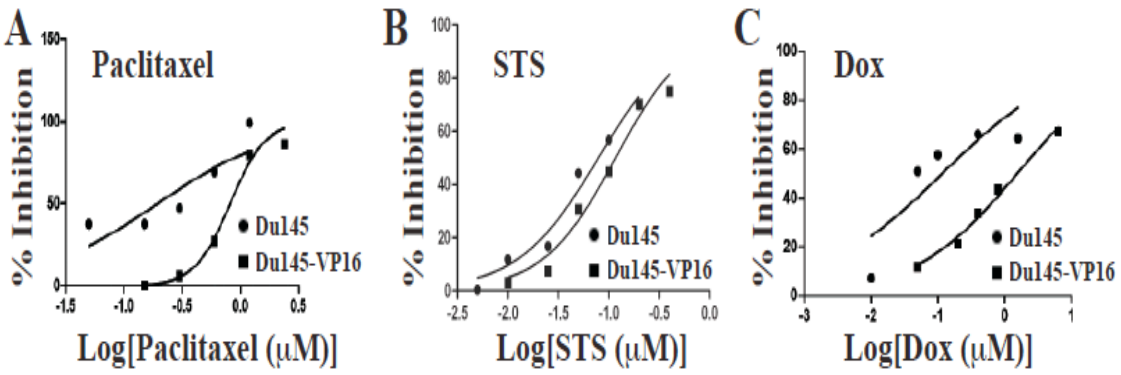

D

Cell type	*Drug*	*IC50 (μM)*	*95% CI*	*F value*	*P*
Du145	Paclitaxel	0.19 ± 1.48	0.06 – 0.68		
Du145-VP16	Paclitaxel	0.82 ± 1.08	0.64 – 1.04	15.14	0.0078
Du145	STS	0.08 ± 0.001	0.06 – 0.11		
Du145-VP16	STS	0.12 ± 0.001	0.09 – 0.16	5.92	0.041
Du145	Dox	0.12 ± 1.93	0.01 – 0.95		
Du145-VP16	Dox	1.56 ± 1.13	1.04 – 2.33	9.17	0.023

Figure 2-2. Drug-tolerant Du145 cells were cross-resistant to non-selecting drugs. Du145-VP16 cells were treated with paclitaxel (A), STS (B), and doxorubicin (Dox; C) at the concentrations [log] indicated. Results are presented as % inhibition and IC50 (D) were determined as in Figure 2-1. Taken from (148) with all authors' permission.

A

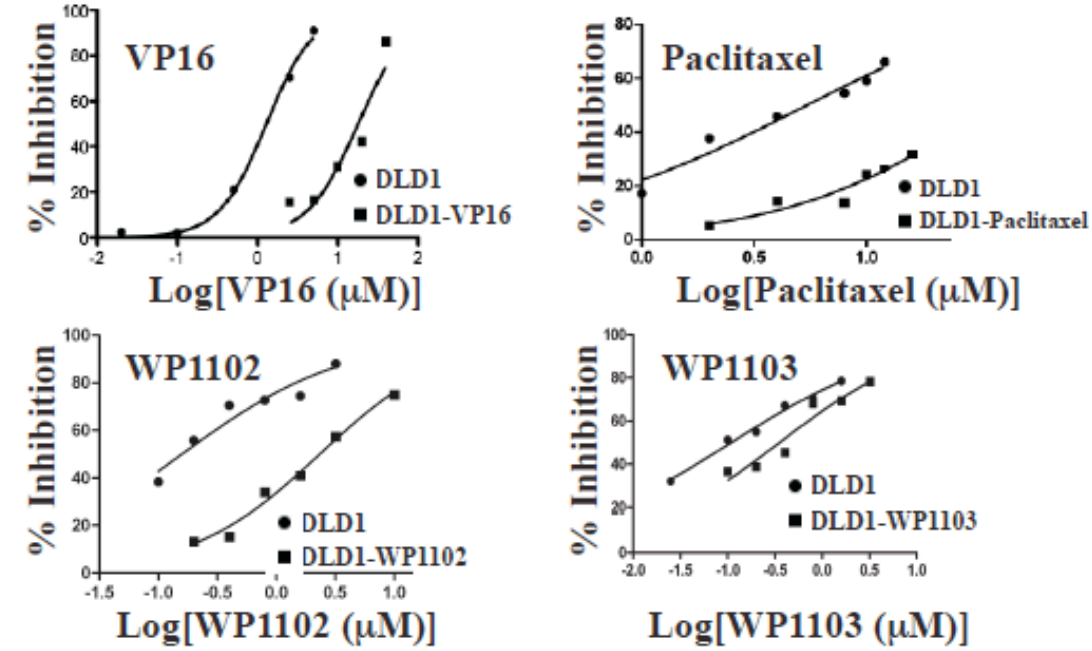

B

Cell type	*Drug*	*IC_{50} (μM)*	*95% CI*	*F value*	*P*
DLD1	VP16	1.29 ± 1.07	1.05 – 1.59		
DLD1-VP16	VP16	17.96 ± 1.22	9.57 – 33.71	65.14	0.0002
DLD1	Paclitaxel	5.44 ± 1.11	4.10 – 7.22		
DLD1-Paclitaxel	Paclitaxel	36.59 ± 1.32	16.96 – 78.95	66.84	<0.0001
DLD1	WP1102	0.16 ± 1.23	0.09 – 0.28		
DLD1-WP1102	WP1102	2.34 ± 1.09	1.83 – 2.99	154.70	<0.0001
DLD1	WP1103	0.11 ± 1.09	0.08 – 0.14		
DLD1-WP1103	WP1103	0.35 ± 1.19	0.22 – 0.57	26.45	0.0009
DLD1	Paclitaxel	3.54 ± 1.20	2.14 – 5.85		
DLD1-VP16	Paclitaxel	14.41 ± 1.17	8.68 – 23.94	22.58	0.0021
DLD1	Dox	0.24 ± 1.54	0.04 – 1.55		
DLD1-VP16	Dox	2.46 ± 1.12	1.51 – 4.02	39.38	0.0033

Figure 2-3. Drug-tolerant DLD1 cells were resistant to selecting and non-selecting drugs. Parental and drug-tolerant DLD1 cell lines selected with optimal concentrations of VP16, paclitaxel, WP1102, and WP1103, were exposed, side-by-side, to the respective selection drugs at the concentrations (transformed into logarithm) indicated (A). Y-axis represents cell growth inhibition (%). B. Tabulated presentations of IC50 values and corresponding 95% CI (confidence of intervals) of parental DLD1 cells and drug-tolerant DLD1 lines in response to both selecting and non-selecting drugs. Taken from (148) with all authors' permission.

Cell type[a]	Cell#	Incidence (%)[b]	TIF[c]	Latency(d)[d]	Termination(d)[d]	Weight (g)[e]
Du145	100	7/7 (100)	**1/175** (1/66–1/467)	63	90	0.07±0.03 (0.03–0.12)
	1000	7/8 (87.5)		36	60	0.42±0.33 (0.10–0.95)
	10000	8/8 (100)		27	59	0.50±0.35 (0.12–0.97)
	100000	7/8 (87.5)		21	52	0.39±0.17 (0.18–0.65)
Du145-VP16	100	1/8 (12.5)	**1/62,453** (1/26,455–1/147,436)	92	117	1.45
	1000	0/8**			60	
	10000	0/8**			59	
	100000	5/6 (83.3)		51**	52	0.06±0.05 (0.02–0.14)**
Du145-VP16 (2 mo.)#	1000	1/6 (16.7)*	**1/30,110** (1/7,199–1/125,948)	83	127	0.01
	10000	1/6 (16.7)*		45	127	0.2
Du145-STS	100	1/8 (12.5)	**1/971** (1/421–1/2,241)	52*	90	0.16
	1000	5/8 (62.5)		58*	66	0.07±0.02 (0.04–0.09)*
	10000	3/8 (37.5)*		48*	66	0.13±0.14 (0.05–0.29)*
Du145-Paclitaxel	100	0/8**			105	
	1000	0/8**			60	
	10000	0/8**			60	
	100000	0/6**			52	
Du145-WP1102	100	2/4 (50)	**1/45,787** (1/15,313–1/136,901)	58	90	0.03±0.01 (0.02–0.04)*
	1000	2/4 (50)		58**	66	0.37±0.13 (0.27–0.46)
	10000	2/4 (50)		58**	66	0.11±0.12 (0.02–0.19)*
	100000	3/4 (75)		31*	52	0.19±0.24 (0.01–0.46)
Du145-WP1103	100	0/8**			99	
	1000	0/8**			60	
	10000	0/8**			60	
Du145-WP1103 (2 mo.)#	1000	0/6**			108	
	10000	0/6**			108	

Table 2-1. Drug-tolerant Du145 cells possess much reduced tumorigenic potential. [a]Parental Du145 or drug-tolerant Du145 cells were s.c implanted in 50% Matrigel, at the numbers indicated, in NOD/SCID mice. In the two experiments marked by #, cells were first cultured in drug-free medium for 2 months prior to injections. [b]Tumor incidence (% of tumor development/injections). [c]Tumor-initiating frequency, as determined using the L-Calc^{TM} software (Stemcell Technologies). The ranges were indicated in the parentheses. [d]Tumor latency (mean time in days from injection to when tumors were first palpated) and termination time (days from injection to when animals were sacrificed). [e]Mean ± S.D (ranges in parentheses). Note that tumor weights sometimes varied greatly among different cell number groups. For statistical analyses, Fisher's Exact Test was used to compare tumor incidence and Student t-test was used to compare tumor weights and latencies. *P< 0.05; **P<0.01, when compared with the parental Du145 cells of the same number. Taken from (148) with all authors' permission.

Cell type (GFP-tagged)	Incidence (%)	Weight (g)
Du145	3/5 (60)	1.28 ± 1.04
Du145-VP16	3/5 (60)	0.41 ± 0.34
Du145-STS	3/5 (60)	0.67 ± 0.08
Du145-Paclitaxel	0/5	
Du145-WP1103	0/5	

Table 2-2. Reduced tumorigenic potential of orthotopically implanted drug-tolerant Du145 cells. GFP-tagged parental or drug-tolerant Du145 cells were implanted (500,000 cells/injection), in 50% Matrigel, in the DP of NOD/SCID mice. All animals were terminated 75 days post implantation. Shown are tumor incidence and tumor weights (mean ± S.D; statistics not applicable due to relatively small numbers of animals). Adapted from (148) with all authors' permission.

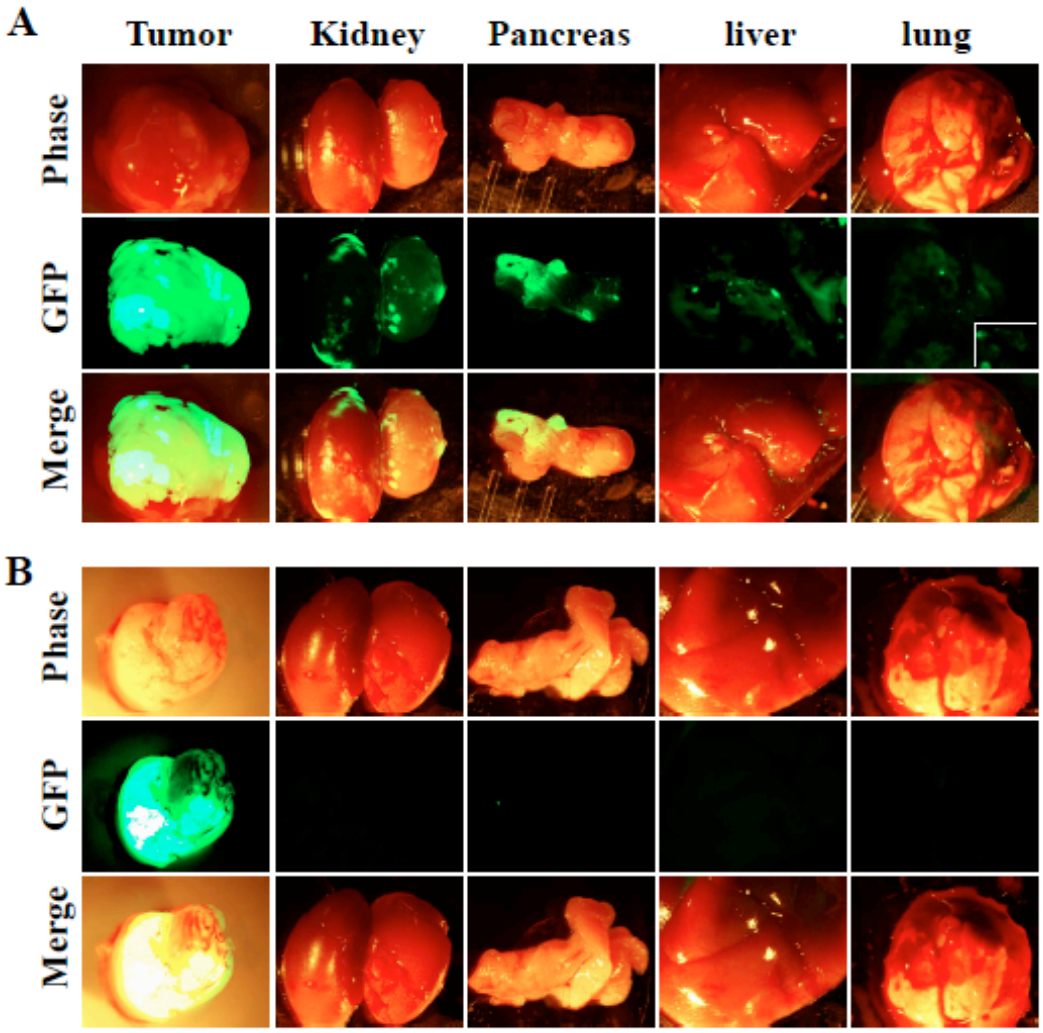

Figure 2-4. Orthotopically implanted drug-tolerant Du145 cells showed reduced tumorigenic and metastatic potential. Representative tumor and organ images from a tumor-bearing animal in the Du145 (A) and Du145-VP16 (B) group, respectively. All images were acquired using a Nikon microdissecting epifluorescence microscope at 0.75× and the boxed area in A (the lung GFP image) represents an enlargement showing GFP^+ spots in the lung. Adapted from (148) with all authors' permission.

Drug-tolerant DLD1 cells also showed reduced tumorigenicity whereas drug-tolerant UC14 cells demonstrated drug-dependent changes in tumor initiating capacity

To determine whether the reduced tumorigenicity associated with drug-resistant cells is restricted only to Du145 cells, we similarly injected, s.c., increasing numbers of parental DLD1 and four drug-tolerant DLD1 cell lines into the NOD/SCID mice. As shown in Table 2-3, the drug-tolerant DLD1 cells, though displaying similar tumor incidence, regenerated significantly smaller tumors compared to parental DLD1 cells at the same cell numbers.

We carried out similar limiting-dilution tumor experiments in 6 drug-selected UC14 cells (Table 2-4). In contrast to drug-tolerant Du145 and DLD1 cells, which uniformly demonstrated reduced tumorigenic potential, 4 of the 6 drug-tolerant UC14 cells (Table 2-4; shadowed brown) demonstrated enhanced tumor-regeneration capacity compared to the same number of parental UC14 cells. Interestingly, two drug-tolerant UC14 cell lines also regenerated much smaller tumors than the same number of parental UC14 cells (Table 2-4; shadowed pink). These results indicate that drug-tolerant UC14 cells are either more or less tumorigenic than the parental cells, depending on the initial selection drugs.

Drug-tolerant Du145 cells were less proliferative and showed low cloning efficiency

Since it was quite unexpected that some drug-tolerant cancer cells showed reduced tumor-regenerating capacity, we subsequently focused on drug-tolerant Du145 cells in attempt to uncover potential mechanisms. We consistently observed that most drug-tolerant Du145 cells seemed to proliferate more slowly compared to Du145 cells. Indeed, in a prospective 10-day experiment measuring live cell numbers, we observed that all drug-tolerant Du145 cells, except Du145-WP1102 cells, showed much lower end-point live cell numbers (Figure 2-5A), suggesting that DTCs were less proliferative and/or more susceptible to cell death. We then carried out BrdU incorporation experiments to directly measure cell proliferation. As shown in Figure 2-5B, drug-tolerant Du145 cells exhibited lower proliferative indices (i.e., % $BrdU^+$ cells). Interestingly, even Du145-WP1102 cells demonstrated a lower proliferative index (Figure 2-5B) although these cultures showed similar total live cell numbers to parental Du145 cells (Figure 2-5A). Remember that Du145-WP1102 cells also displayed relatively less reduction in tumor-initiating capacity compared to other drug-tolerant Du145 cells (Table 2-1). It is possible that Du145-WP1102 cells proliferated less but also had less spontaneous cell death, thus resulting in similar end-point live cell numbers (Figure 2-5A) and less pronounced decreases in tumorigenicity (Table 2-1). Indeed, we consistently observed that Du145-WP1102 cells, chronically selected using 5 nM WP1102 compound, showed less floating and apoptotic cells in the culture flasks compared with Du145-WP1103 cells (not shown), which were chronically selected using 25 nM WP1103 compound. Finally, we observed that all drug-tolerant Du145 cells demonstrated lower cloning efficiencies than the parental Du145 cells (Figure 2-5C).

Cell line	Cell#	Tumor incidence (%)	Termination (days)	Weights (g)
DLD1	1000	8/8 (100)	45	0.58 ± 0.22 (0.28-1.03)
	10000	8/8 (100)	30	0.60 ± 0.25 (0.31-0.97)
	100000	6/6 (100)	30	0.88 ± 0.18 (0.75-1.24)
DLD1-VP16	1000	7/8 (87.5)	45	0.09 ± 0.11 (0.01-0.31)**
	10000	7/8 (87.5)	30	0.08 ± 0.07 (0.01-0.21)**
	100000	6/6 (100)	30	0.41 ± 0.10 (0.26-0.56)**
DLD1-Paclitaxel	1000	8/8 (100)	45	0.40 ± 0.22 (0.13-0.80)
	10000	6/8 (75)	30	0.34 ± 0.15 (0.15-0.54)*
	100000	6/6 (100)	30	0.65 ± 0.17 (0.49-0.87)*
DLD1-WP1102	1000	8/8 (100)	45	0.36 ± 0.21 (0.11-0.59)*
	10000	8/8 (100)	31	0.37 ± 0.18 (0.07-0.60)*
DLD1-WP1103	1000	8/8 (100)	45	0.46 ± 0.15 (0.21-0.66)
	10000	8/8 (100)	31	0.28 ± 0.18 (0.04-0.55)**

Table 2-3. Reduced tumorigenic potential in drug-tolerant DLD1 cells. Parental or drug-tolerant DLD1 colon cancer cells were implanted, in 50% Matrigel, at various cell numbers s.c in NOD/SCID mice. Presented are tumor incidence (% tumor development), termination time (days since tumor cell injection when animals were sacrificed), and tumor weights (mean ± S.D; ranges in parentheses). *P< 0.05 and **p<0.01, compared with the parental DLD-1 cells of the same numbers. Taken from (148) with all authors' permission.

Cell line[a]	Cell#	Tumor incidence[b] (%)	Latency[c] (days)	Termination[c] (days)	Tumor weight[d] (grams)
UC14	1,000 10,000 100,000	6/8 (75.0) 8/8 (100) 5/6 (83.3)	23 15 13	38 29 24	0.15±0.16 (0.01-0.41) 0.32±0.10 (0.11-0.46) 0.23±0.17 (0.09-0.43)
UC14-Paclitaxel	1,000 10,000 100,000	8/8 (100) 8/8 (100) 5/6 (83.3)	20# 15 13	38 29 24	0.66±0.37 (0.18-1.16)** 0.42±0.15 (0.15-0.60) 0.38±0.13 (0.20-0.54)
UC14-STS	1,000 10,000 100,000	5/8 (62.5) 8/8 (100) 6/6 (100)	26 18 18	38 29 24	0.08±0.06 (0.03-0.16) 0.33±0.27 (0.09-0.81) 0.53±0.16 (0.30-0.76)**
UC14-Dox	1,000 10,000 100,000	4/8 (50) 8/8 (100) 6/6 (100)	N.D 22## 13	38 29 24	0.01±0.01 (0.01-0.02)* 0.12±0.09 (0.02-0.27)** 0.27±0.13 (0.16-0.45)
UC14-VP16	1,000 10,000 100,000	0/8 (0)- 6/8 (75) 5/6 (83.3)	20# 13	29 24	0.04±0.04 (0.01-0.09)** 0.08±0.02 (0.05-0.09)
UC14-WP1102	1,000 10,000 100,000	4/8 (50) 5/6 (83.3) 6/6 (100)	27 19 13	38 29 24	0.17±0.18 (0.01-0.35) 0.28±0.25 (0.02-0.61) 0.42±0.14 (0.21-0.59)*
UC14-WP1103	1,000 10,000 100,000	8/8 (100) 7/8 (87.5) 6/6 (100)	22 18 13	38 29 24	0.34±0.37 (0.01-1.15) 0.57±0.22 (0.24-0.96)* 0.48±0.09 (0.39-0.64)*

Table 2-4. Drug-tolerant UC14 cells demonstrate drug-dependent changes in tumorigenicity. [a]Parental UC14 or drug-tolerant UC14 cells were implanted s.c, in 50% Matrigel, at the numbers indicated, in NOD/SCID mice. [b]Tumor incidence (% of tumor development/injections). Δ, P< 0.05, compared with UC14 at the same cell dose. [c]Tumor latency refers to mean time in days from injection to when tumors were first palpated. Δ, P< 0.05, and ΔΔ, P<0.01, when compared with UC14 at the same cell doses. All animals injected with the same number of tumor cells were terminated at the same time. [d]Mean ± S.D (ranges in parentheses). *, P< 0.05, and **, P<0.01, compared with UC14 at the same cell doses. For statistical analyses, Fisher's Exact Test was used to compare tumor incidence and latency and Student *t*-test was used to compare tumor weights and latencies. Taken from (148) with all authors' permission.

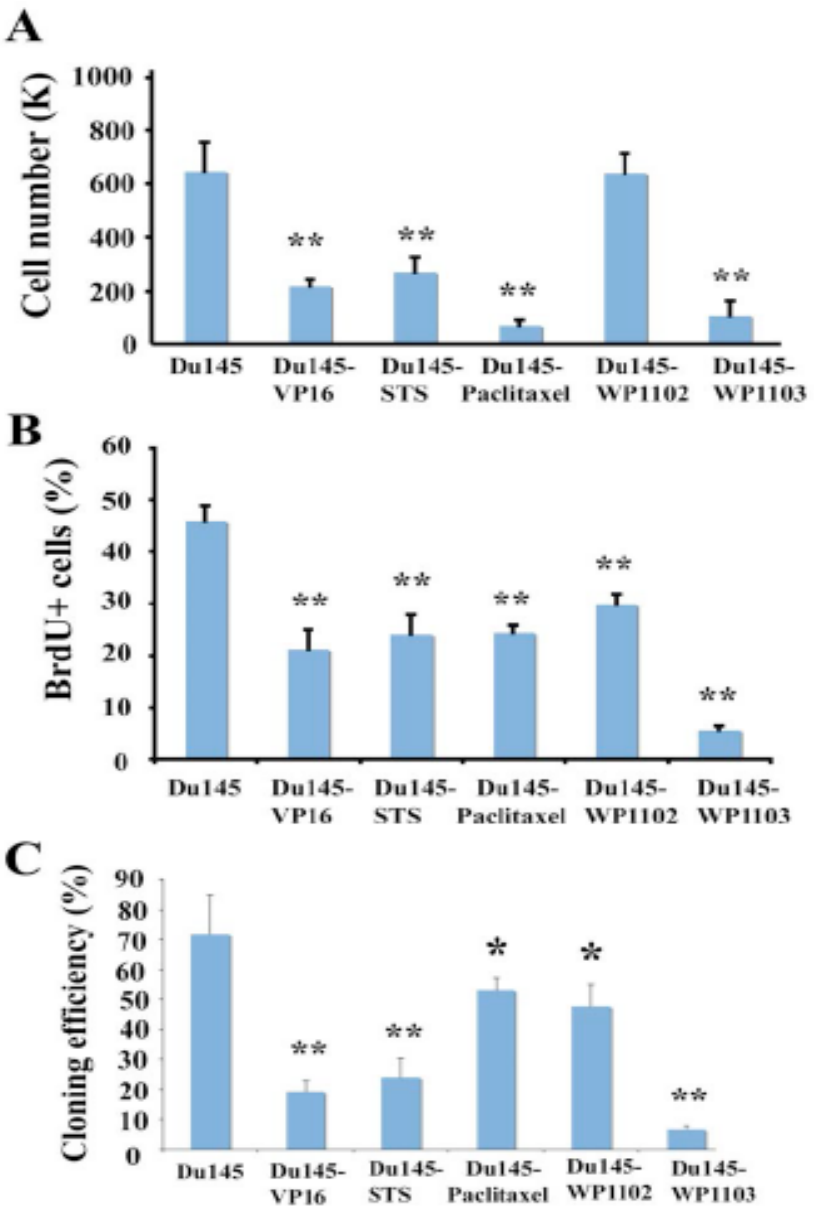

Figure 2-5. Drug-tolerant Du145 cells were less proliferative and showed low cloning efficiency. (A). Quantification of numbers of viable cells. Parent and drug-tolerant Du145 cells were plated, in quadruplicate, in 12-well plates (5,000 cells/well) and viable cells were quantified using Trypan blue exclusion assay 10 days post plating. (B). Quantification of % $BrdU^{+}$ cells. (C). Determination of cloning efficiency. Parent and drug-tolerant Du145 cells were plated, in quadruplicate, in 6-well plates (100 cells/well) with fresh medium replenished every 3 days. The numbers of holoclones and meroclones were determined 10 days post plating. In all data, bars represent the mean ± S.D and statistical analyses were conducted using Student *t*-test (*, $P<0.05$; **, $P<0.01$). Taken from(148) with all authors' permission.

Consistent with reduced cell proliferation, drug-tolerant Du145 cells showed increased levels of two cyclin-dependent kinase inhibitors, p21 and p27, especially in Du145-Paclitaxel and Du145-WP1103 cells (Figure 2-6A), the two cell lines that completely lacked tumorigenicity (Table 2-1). The p27 levels were also elevated in all three other drug-tolerant Du145 cell lines (Figure 2-6A). Intriguingly, the significantly increased p27 protein band in Du145-Paclitaxel and Du145-WP1103 cells migrated slightly faster than the protein in other cell lines (Figure 2-6A). Future studies will clarify this potentially interesting observation. In contrast to p21 and p27, Bcl-2, an anti-apoptotic protein, showed less, albeit dramatic decrements, again, in the two non-tumorigenic Du145 lines, i.e., Du145-Paclitaxel and Du145-WP1103 (Figure 2-6A).

Drug-tolerant Du145 cultures showed reduced numbers of, or were devoid of, $CD44^+$ cells

Several pieces of evidence suggest that diminished tumor-regenerating capacity in drug-tolerant Du145 cells may involve, in addition to compromised proliferative potential perhaps mediated by increased p21 and p27, drug-induced defects in tumor-initiating cells. When we examined drug-tolerant Du145 cells for the levels of hTERT, which is essential for normal prostate stem/ progenitor cells as shown by our recent studies (147), we found that Du145-Paclitaxel and Du145-WP1103 cells, which lacked tumorigenic potential, lost hTERT expression (Figure 2-6A). Our previous studies have demonstrated that the clonogenic and tumorigenic potential of Du145 cells largely resides in the $CD44^+$ cell fraction (15, 85) and it has recently been shown by one of our groups that paclitaxel conjugated to hyaluronic acid, designed to specifically target the CD44-expressing cells, exhibited potent anti-ovarian cancer effects (151).

The above discussions raised the possibility that perhaps $CD44^+$ cells and/or CD44 expression were reduced or ablated in drug-tolerant Du145 cell lines. To test this possibility, we carried out both Western blotting and immunofluorescence experiments. Remarkably, both Du145-Paclitaxel and Du145-WP1103 cultures completely lacked $CD44^+$ cells (Figure 2-6; Figure 2-7; Figure 2-8). Du145-VP16 and Du145-STS cultures also showed reduced CD44 protein levels (Figure 2-6) and numbers of $CD44^+$ cells (Figure 2-6; Figure 2-7; Figure 2-8). By contrast, Du145-WP1102 cells, which retained some tumor-initiating capacity (Table 2-1), showed similar levels of CD44 protein expression to (Figure 2-6B) or slightly more $CD44^+$ (many faintly positive) cells (Figure 2-7; Figure 2-8) than parent Du145 cultures. Hence, the extent to which $CD44^+$ cells were ablated in drug-tolerant Du145 cultures appeared to correlate well with the level of reduction in their tumorigenic potential. In contrast to CD44, ABCG2 protein (Figure 2-6) or $ABCG2^+$ cells (data not shown), which constituted ~1% of total Du145 cells (86), did not show consistent and significant changes in drug-tolerant Du145 cells.

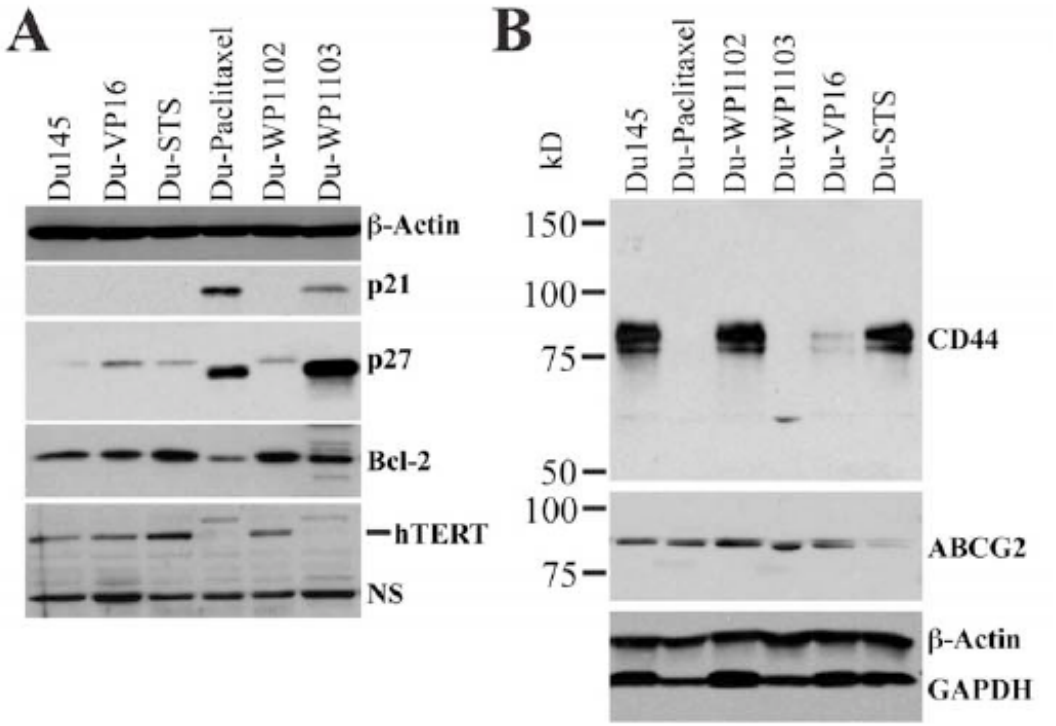

Figure 2-6. Western blotting of different molecules in drug-tolerant Du145 cells cultures. (A). Whole cell lysate from the cell types indicated was used in Western blotting of p21, p27, Bcl-2, and hTERT and the blot was reprobed for β-actin. NS, non-specific. (B). Analysis of CD44 and ABCG2. The blot was reprobed for β-actin and GAPDH. Adapted from (148) with all authors' permission.

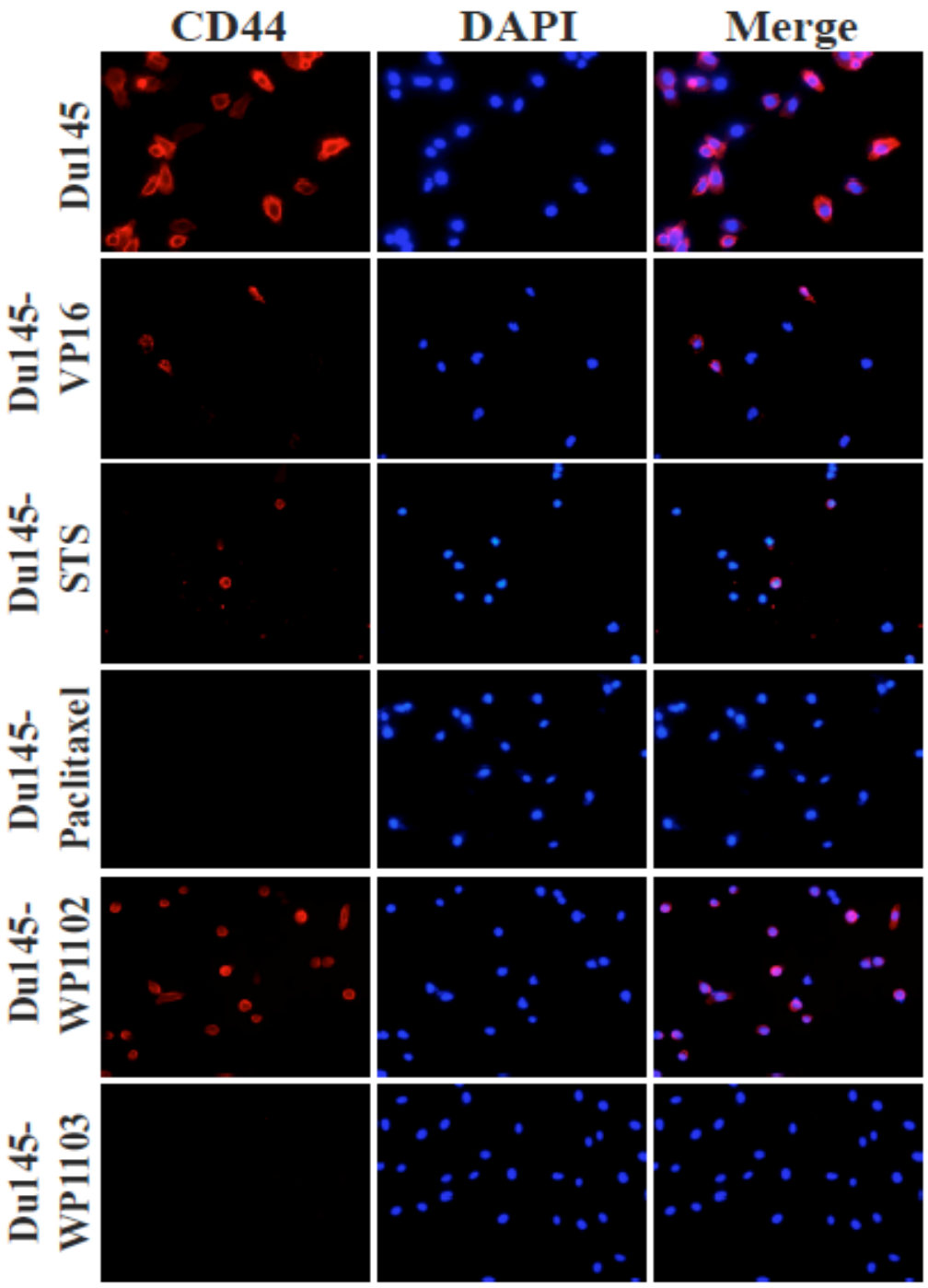

Figure 2-7. Representative images of immunofluorescent staining of CD44 in drug-tolerant Du145 cells cultures. Du145 and drug-tolerant Du145 cells were plated on glass coverslips and stained for CD44 using monoclonal antibody. Adapted from (148) with all authors' permission.

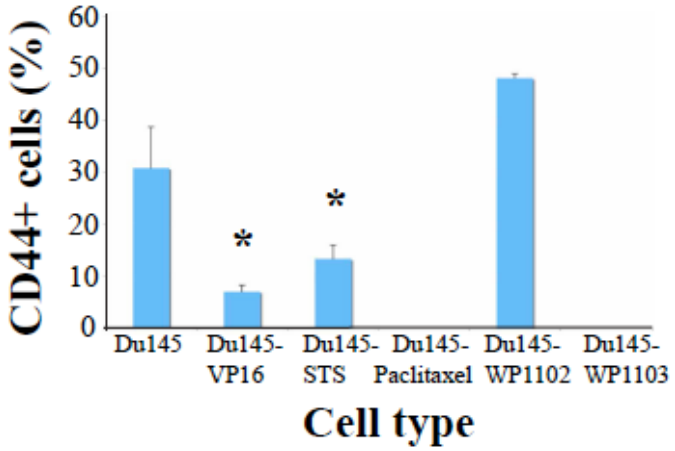

Figure 2-8. Quantification of CD44^{+} cells in drug-tolerant Du145 cells cultures. The quantification was based on IF staining in Figure 2-7. Adapted from (148) with all authors' permission.

Requirement of CD44 in Du145 cell tumorigenicity

The above surprising finding that drug-induced reduction/loss of $CD44^+$ cells correlates with reduction/loss of tumorigenic potential in Du145 DTCs, is fully consistent with our earlier studies showing that the $CD44^+$ PCa cells are more tumorigenic and metastatic than the corresponding $CD44^-$ cells (85, 87). To prospectively determine whether CD44 is causally involved in PCa cell tumorigenicity, we infected parental Du145 cells with a lentiviral vector encoding CD44 shRNA (CD44-shRNA) or a nonsilencing shRNA (NS-shRNA). CD44-shRNA reduced CD44 protein (Figure 2-9A, inset) and inhibited Du145 cell proliferation as evidenced by reduced % of $BrdU^+$ cells (Figure 2-9A–B) resulting in reduced live cell numbers (Figure 2-9C). When implanted either s.c or orthotopically, the CD44-shRNA infected Du145 cells generated significantly smaller tumors (Figure 2-10).

We then performed the reciprocal gain-of-function experiments by overexpressing CD44 in drug-tolerant Du145 cells. Specifically, we infected the Du145-VP16 cells with pBabe-CD44, which led to increased CD44 expression compared to Du145-VP16 cells infected with pBabe-GFP (Figure 2-11, inset). CD44 re-expression in Du145-VP16 cells enhanced cell proliferation as revealed by BrdU incorporation assays (Figure 2-11), resulting in increased live cell numbers (Figure 2-11). Pilot studies indicated that CD44 overexpression in Du145-VP16 slightly increased tumorigenicity (tumor incidence was 1/4 vs. 4/6 in Du145-VP16/pBabe.GFP and Du145-VP16/pBabe.CD44, respectively).

The above results suggest that a reduction in $CD44^+$ cells is, at least partially, involved in the reduced tumorigenicity of drug-tolerant Du145 cells. These observations also imply that conventional drugs such as etoposide and Taxol may directly target tumor-initiating cells. To further explore this latter point, we employed PC3 cells, which are all $CD44^+$ (85), to establish orthotopic tumors in the mouse prostate. After tumors developed for ~3 weeks, we then performed a therapeutic experiment via i.p (intra-peritoneal) injection of paclitaxel. Consistent with the idea that Taxol may directly target $CD44^+$ PCa cells, the intravenously injected paclitaxel greatly inhibited PC3 tumor growth (Figure 2-12A) as well as metastasis to the lung (Figure 2-12B), pancreas and many other organs (data not shown).

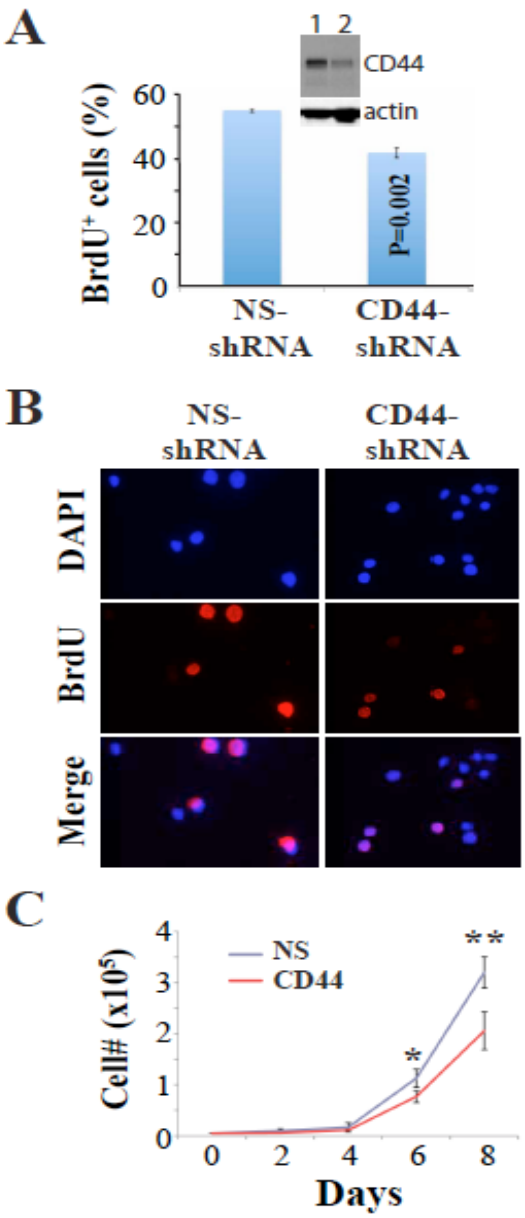

Figure 2-9. CD44 knockdown in Du145 cells and *in vitro* characterizations. Du145 cells infected with the control (NS) or CD44 shRNA lentivectors (MOI 20; 72 h) were plated (10,000/well) in triplicate, pulsed by BrdU for 4 h, and processed for BrdU staining. Shown in (A) is the quantification of $BrdU^+$ cells from a total of 500 cells counted for each and in (B) are representative images (×400). Inset, Western blot showing reduced CD44 protein expression in Du145 cells infected with CD44-shRNA (lane 2) compared with the cells infected with NS-shRNA (lane 1). For experiments in C, Du145 cells infected with the control (NS) or CD44 lentivector were plated (5,000/well) in quadruplicate on day 0. At the end of day 2, 4, 6, and 8, cells were dissociated and counted by Trypan blue exclusion. Plotted are the live cell numbers (mean ± SD) as a function of time. *P = 0.019; **P = 0.003 (Student's *t*-test). Adapted from (148) with all authors' permission.

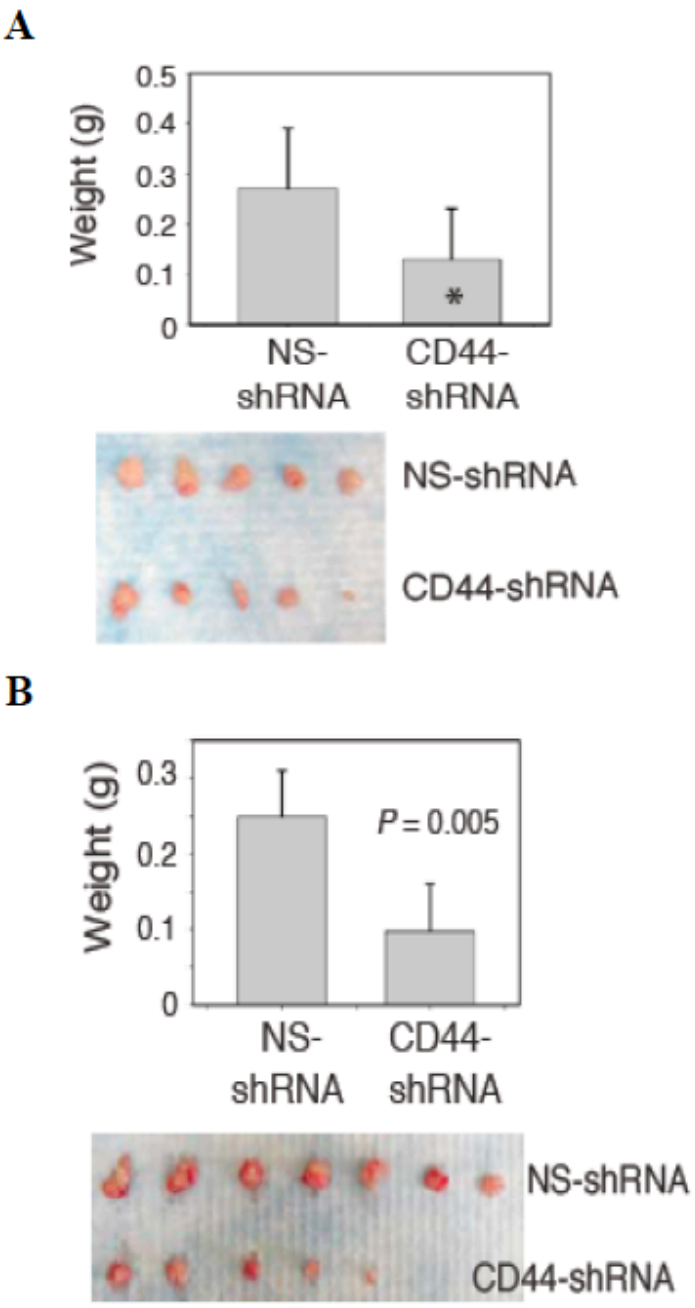

Figure 2-10. CD44 knockdown in Du145 cells and *in vivo* characterizations. (A) Shown are the weights (above; mean ± s.d, *P < 0.05) and images (below; incidence, 5/5 for both groups) of subcutaneous tumors derived from Du145 cells infected with NS-shRNA or CD44-shRNA (MOI 20, 72 h; harvested at 56 d). (B) Shown are the weights (above; mean ± s.d) and images (below) of orthotopic tumors derived from Du145 cells infected with NS-shRNA or CD44-shRNA (harvested at 41 d). Tumor incidence for the NS-shRNA and CD44-shRNA group was 7/7 and 5/8, respectively. Adapted from (96) with permission from Nature Publishing Group.

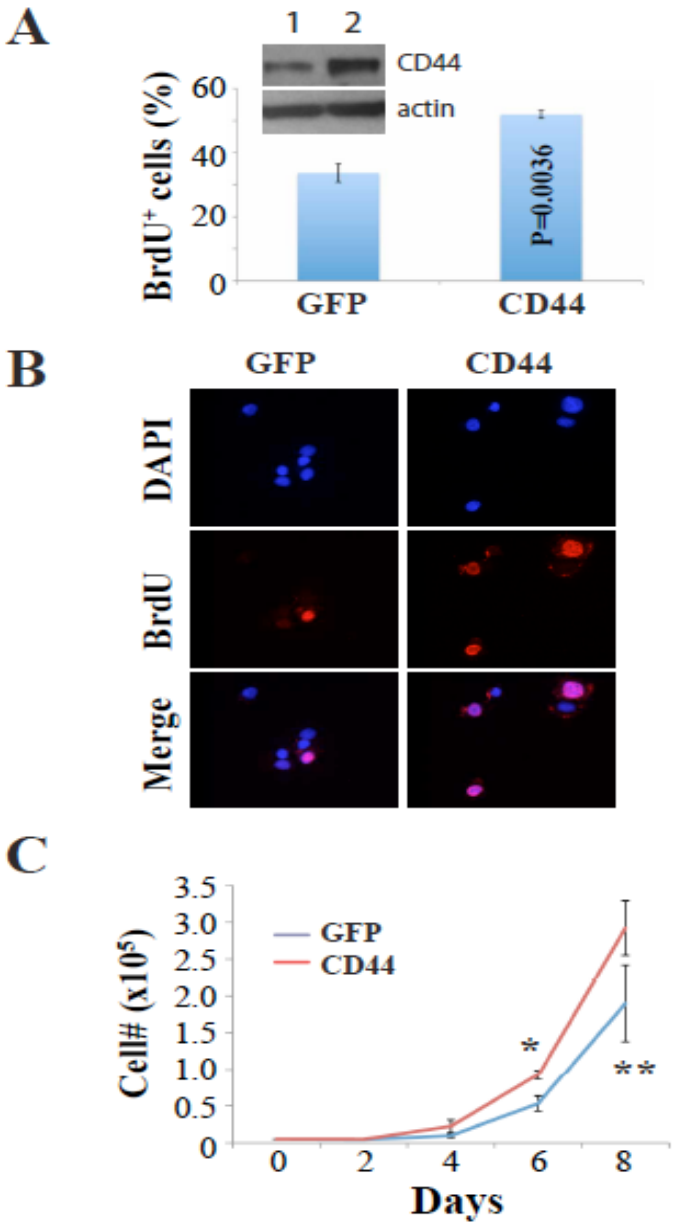

Figure 2-11. CD44 overexpression in Du145 cells and *in vitro* characterizations. Du145-VP16 cells infected with GFP or CD44 retroviral vectors (MOI 20; 72 h) were plated (10,000/well) in triplicate, pulsed by BrdU for 4 h, and processed for BrdU staining. Shown in (A) is the quantification of $BrdU^+$ cells from a total of 500 cells counted for each condition and in (B) are representative images (×400). Inset, Western blot showing increased CD44 protein expression in Du145-VP16 cells infected with pBabe-CD44 (lane 2) compared with the cells infected with pBabe-GFP (lane 1). For experiments in C, Du145-VP16 cells infected with the GFP or CD44 retroviral vectors were plated (5,000/well) in quadruplicate on day 0. At the end of day 2, 4, 6, and 8, cells were dissociated and counted by Trypan blue exclusion. Plotted are the live cell numbers (mean ± SD) as a function of time. *P = 0.035; **P = 0.028. Adapted from (148) with all authors' permission.

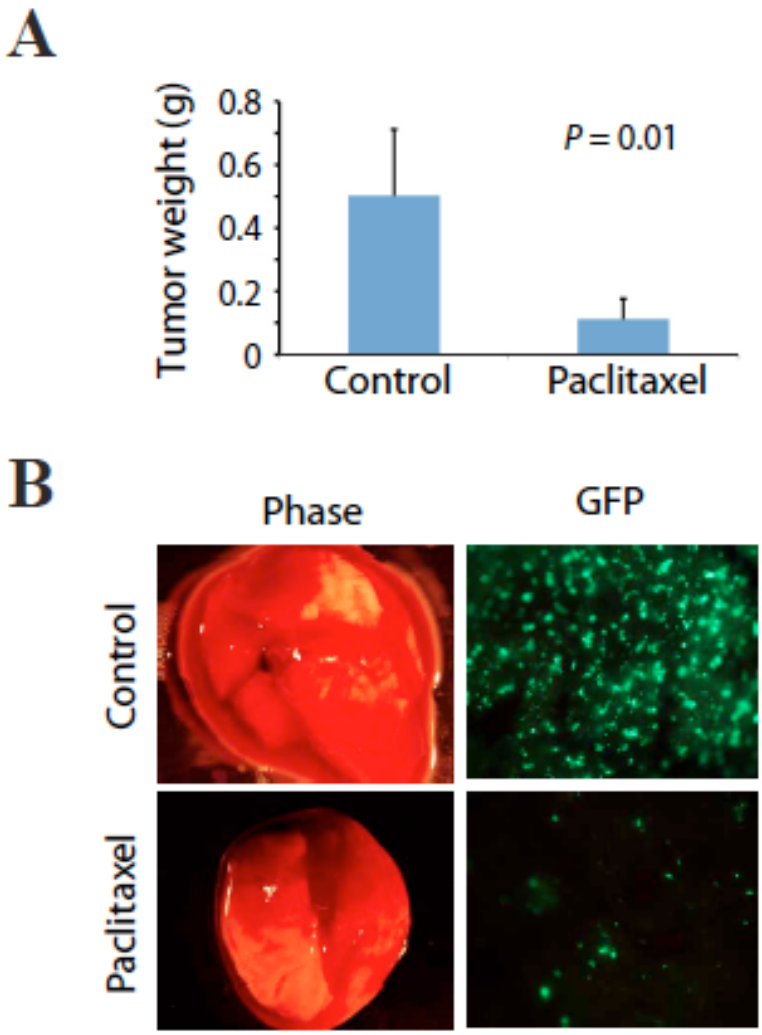

Figure 2-12. Paclitaxel inhibits PC3 orthotopic tumor growth and metastasis. Presented in (A) is the tumor weight (mean ± S.D; n = 5 for each group). Tumor incidence is the same (i.e., 5/5) for both groups. Shown in (B) are representative phase and GFP microphotographs of lung metastases, i.e., GFP^+ foci. Adapted from (148) with all authors permission.

Gene expression changes in drug-tolerant Du145 cells

To further understand what molecular changes might have occurred in drug-tolerant cells, we performed a stem cell SuperArray gene expression analysis of ~20 'stemness' genes, including ALDH1A1 (the major isoform that mediates the Aldeflour phenotype), BCL-2, CD24, CD29 (integrin β1), CD44, CD49b (integrin α2), c-KIT, CSF-1R, CXCR4, ITGB3 (integrin β3), NANOG, NKX3.1, OCT-4, PROM-1 (CD133), SOX2, hTERT, TGFB1, TGFBR2, and WNT4, in Du145 and Du145-VP16 cells. Consistent with our Western blotting and immunostaining results (Figure 2-6), CD44 mRNA was significantly lower in Du145-VP16 cells. The mRNA levels of c-KIT and TGFBR2 were also significantly reduced (Figure 2-13). The mRNA levels of NANOG and CSF-1R showed a reducing trend but the decrease was not statistically significant. Most surprisingly, 6 molecules analyzed, ALDH1A1, BCL-2, CXCR4, OCT-4, SOX2, and WNT4, showed significantly increased mRNA levels in Du145-VP16 cells (Figure 2-13). These results indicate that the drug-tolerant PCa cells show both decreases and increases in 'stemness' genes.

Evidence for epigenetic mechanisms in generating DTCs

Recently, it has been reported that while modeling the acute response of human lung cancer cells to chemotherapeutic drugs, a small population of reversibly drug-tolerant cells that possessed an altered chromatin state that involved the KDM5A histone lysine demethylase can be detected (152). To determine whether our DTCs were 'permanently' changed by chronic drug exposure, we cultured Du145-VP16 and Du145-WP1103 cells in drug-free (DF) medium for 2 months and performed tumor experiments. Such DF-2 month 'reversion' experiments revealed that Du145-VP16 cells were still much less tumorigenic and Du145-WP1103 cells still failed to regenerate tumors (Table 2-1, marked by #; Figure 2-14A). However, when we cultured the Du145-VP16 cells in DF medium for 3 months and injected 10,000 such cells into the NOD/SCID mice, we observed 6/8 tumors (Figure 2-14A) with mean tumor weight of 0.76 ± 0.24 g, of which both tumor incidence and weight were close to those in the parental Du145 cells (Table 2-1). The above tumor experiments suggest that the reduced tumorigenicity of drug-tolerant Du145 cells is reversible and may also involve epigenetic mechanisms. To explore this point, we treated Du145-VP16 cells with HDAC (histone deacetylase) inhibitor TSA (trichostatin A) or DNA methyltransferase inhibitor 5'-aza-deoxycytidine (Aza), as we previously described (80). Both treatments significantly increased the protein levels of CD44, E-cadherin, and KDM5A (Figure 2-14B and C). When we injected 10,000 Aza-treated Du145-VP16 cells, we observed 3/10 tumors (Figure 2-14A). These results thus implicate epigenetic mechanisms in chronic drug-induced DTC generation.

(The above results were adapted from (148) with all authors' permission)

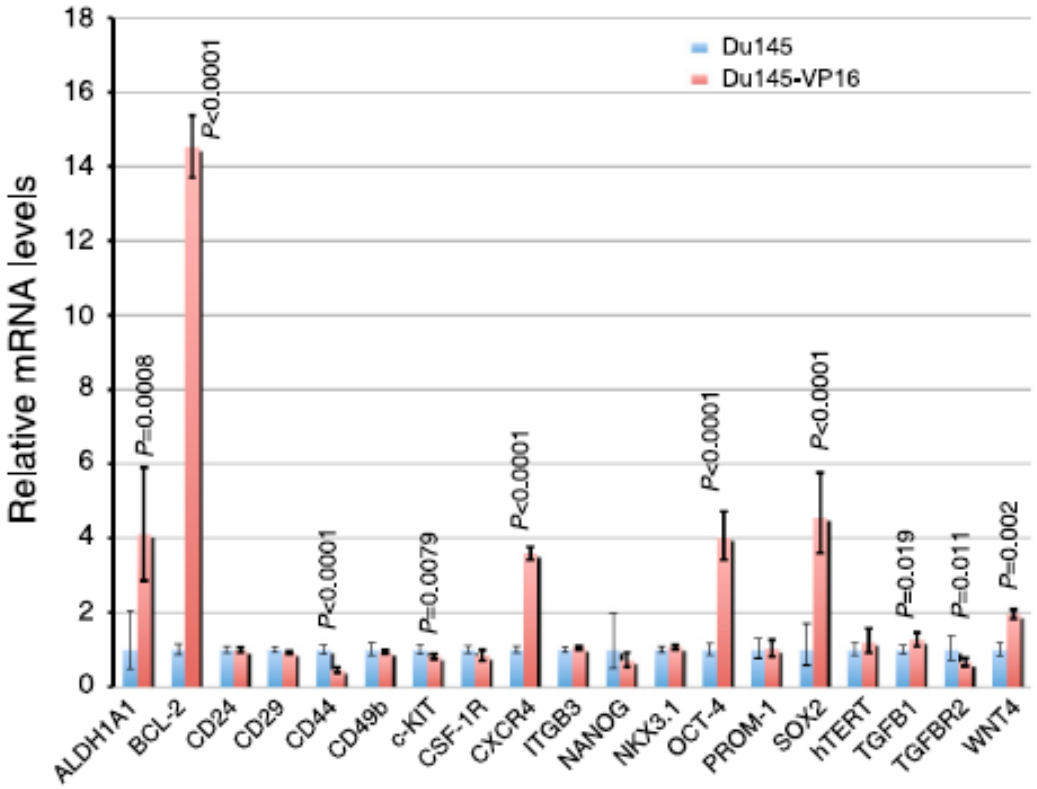

Figure 2-13. 'Stemness' gene expression profiles in Du145-VP16 cells. Du145-VP16 cells show both decreases and increases in stemness gene expression levels. The mRNA levels of the indicated genes in parental Du145 (set at 1, blue bars) and Du145-VP16 (red bars) cells were determined by qPCR. P values were indicated for those genes that showed statistically significant differences. Adapted from (148) with all authors' permission.

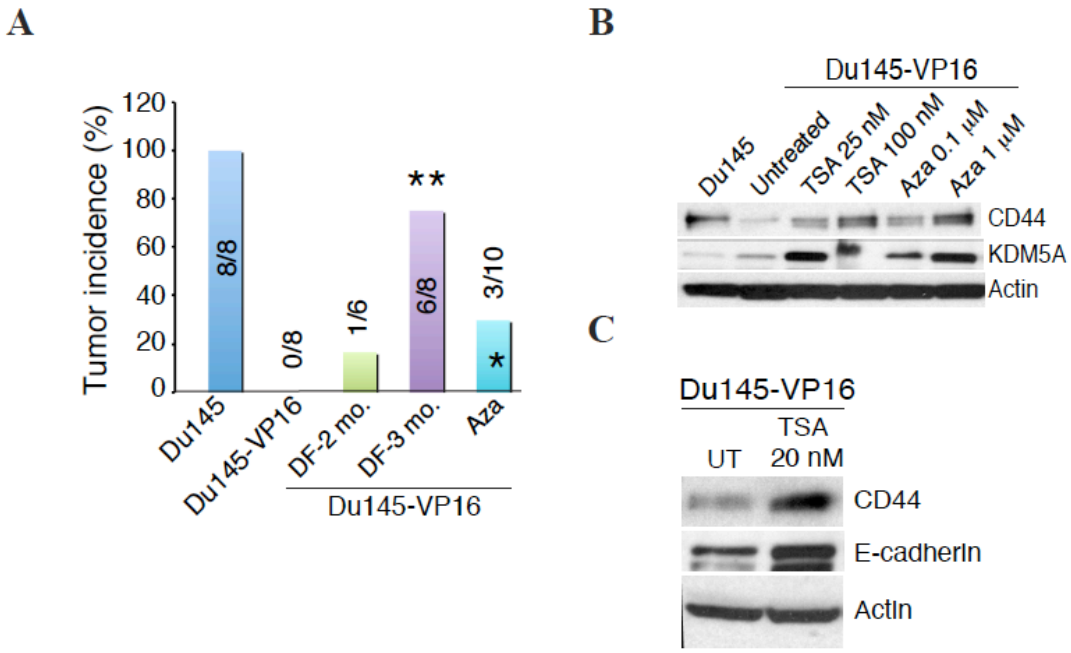

Figure 2-14. Epigenetic mechanisms in Du145-VP16 cells. (A) Tumor incidence in various types of Du145-VP16 cells implanted (10,000) in NOD/SCID mice. As shown in Table 2-1, parental Du145 cells showed 100% incidence at 10,000 cells whereas Du145-VP16 cells failed to initiate tumors. When cultured in drug-free (DF) medium for 2 and 3 months, increased tumor incidence was observed (**$P < 0.01$ compared with Du145-VP16). When Du145-VP16 cells treated with Aza (0.1 μM, 72 h) were injected, increased tumor incidence was also observed (*$P < 0.05$ when compared with Du145-VP16 cells). (B-C). Du145-VP16 cells treated with the indicated chemicals (72 h) were used in Western blotting analysis of CD44, KDM5A, and E-cadherin. β-Actin was used as loading control. UT: untreated. Adapted from (148) with all authors' permission.

2.4. Discussion

The correlation of PCSCs and therapy tolerance is largely unknown. Many previous studies of CSCs and therapy resistance in other tumor systems have shown that CSCs appear to resist chemo- and radio- therapy, whereas therapy resistant cancer cells possess enhanced CSCs properties (73, 145). However, in nearly all these studies, cancer cells were treated with these therapies for only a few days, or at most 2 weeks, which only represents a short-term drug tolerant state. In our current study, after chronic (>3 months) selection using 5 chemotherapy drugs (i.e., two clinical drugs: VP16 and Taxol; and three experimental drugs: STS, WP1102, and WP1103), we have established several lines of DTCs from 3 different tumor types: Du145 (prostate), DLD1 (colon) and UC14 (bladder). Contrary to previous findings that therapy-resistant cancer cells may possess enhanced CSC properties and to our initial hypothesis that DTCs in PCa may be enriched in CSCs, we have obtained somewhat different and intriguing findings, which I will discuss below.

Firstly, most of our DTCs show decreased CSC properties manifested as diminished proliferative, clonogenic, tumorigenic and metastatic potentials. For instance, all Du145-DTCs are much less tumorigenic than parental Du145 cells, and, in fact, both Du145-paclitaxel and Du145-WP1103 cells are nearly non-tumorigenic. Similarly, all DLD1-DTCs generate much smaller tumors than the parental DLD1 cells. In contrast, 2 out of the 6 UC14-DTCs (UC14-Dox and UC14-VP16) generate much smaller tumors than the same number cells from parental UC14 cells. However, the remaining 4 drug-tolerant cell lines show enhanced tumorigenic potential, which is consistent with the general assumption that therapy-resistant cells possess CSC properties (6). Consequently, we have focused on Du145 PCa cells for functional and mechanistic studies. Collectively, our results suggest that not all

DTCs are CSCs, and some DTCs may manifest greatly reduced CSC activity both *in vivo* and *in vitro*. On a facial value, our observations are consistent with reports that some CSCs or CSC activities can be targeted and eradicated by certain therapies. For example, a recent study, using a high- throughput chemical compounds screening (~16,000 compounds), identifies salinomycin to specifically target breast CSCs ($CD44^+CD24^-$) that seem to be intrinsically chemotherapy resistant (153). The therapeutic effects of salinomycin on the breast CSCs are much more significant (>100-fold) compared to paclitaxel, a clinical anti-cancer drug for breast cancer. As a result, salinomycin reduced mammosphere formation as well as tumor regenerative and metastatic potentials (153). Another study has shown that at an optimized concentration, TMZ, a common chemotherapeutic agent for glioblastoma can directly target $CD133^+$ glioma stem cells and significantly inhibit their clonogenicity and tumor-initiating capacities (154). Similar anti-CSC activities have also been reported in other cancer types (155-158). Interestingly, docetaxel-resistant Du145 and 22Rv1 cells after a 9-month and 6.5-month drug selection, respectively, appear to contain enhanced tumor-initiating ability (105), which suggests that whether DTCs contain CSCs is likely to be cell- and drug- dependent phenomenon.

Secondly, we have noticed that most of the chemotherapeutic reagents we studied can eliminate $CD44^+$ cells and that the reduced levels of CD44 correlate well with the decreased levels of tumorigenicity and clonogenicity in our DTCs. Thus, both Du145-Paclitaxel and Du145-WP1103 cells completely devoid of $CD44^+$ cells display non-tumorigenic properties. Du145-VP16 and Du145-STS cells that have partially depleted their $CD44^+$ cells exhibit partially reduced tumorigenicity and clonogenicity. In contrast, Du145-WP1102 cells that appear to have stable or slightly higher levels of CD44, remain somewhat

tumorigenic. These data in Du145-DTCs strongly suggest that CD44 may play a causal role in the clonogenicty and tumorigenicity of PCa cells. To support this notion, we have performed a CD44 knockdown experiment in several PCa cells lines (PC3, Du145, LAPC9, etc), and observed that knocking down CD44 expression significantly inhibits tumor growth, metastasis and sphere formation in these cells (96). In reciprocal experiments, overexpression of CD44 can enhance the proliferative and tumorigenic potentials in some Du145-DTCs. In summary, our current study further substantiates the importance of CD44 in regulating PCa development and PCSC activities. However, we have not yet found a similar reduction of CD44 levels in DLD1 cells (unpublished data), implying that chemotherapy-induced reduction of $CD44^+$ cancer cells may be cell type-dependent. The reason that DLD1-DTCs manifest reduced tumorigenicity is likely related to other mechanisms that need future clarification.

Thirdly, we have noted both increased and decreased levels of SC-related genes in DTCs, and the state of drug tolerance seems to be 'reversible', which implies some epigenetic mechanisms in generating DTCs. For example, we cultured the Du145-DTCs in drug free medium for ~2-3 months before conducting a limiting dilution tumor experiment. Initially, Du145-VP16 cells continuously cultured in VP16-containing medium were non-tumorigenic at 10,000-cell injection. However, the same cells cultured in VP16-free medium gradually regained their tumorigenicity, with tumor incidence of 1/6 and 6/8 if cultured at 2 months and 3 months, respectively, at 10,000-cell injection. Moreover, when we treated the DTCs with a DNA methyltransferase inhibitor, Aza, the tumorigenicity of Du145-VP16 cells can be partially restored, with tumor incidence up to 3/10. In addition, after treatment with Aza and a histone deacetylase inhibitor, TSA, the reduced CD44 levels in some DTCs

rebounded in a dose-dependent manner. Furthermore, TSA and Aza treatment in DTCs can also increase the expression levels of E-cadherin and KDM5A. Reduced E-cadherin levels have been associated with the invasiveness and metastasis of cancer cells (159), which can be attributed to DNA methylation (160, 161) and histone deacetylation (162). Our data supports the idea that epigenetic regulation is important in suppressing E-cadherin expression. Of particular interest, a recent report has shown that KDM5A, a histone demethylase, plays a vital role in directly mediating a drug tolerant phenotype in lung cancer cells (152). Our DTCs also show enhanced levels of KDM5A: after TSA and Aza treatments, KDM5A protein levels in Du145-DTCs increase significantly, implying that this histone demethylase itself may be regulated by novel epigenetic mechanisms yet to be uncovered. Whether KDM5A-mediated drug tolerance in lung cancer cells is also involved in the reduced levels of CD44 in PCa DTCs will be an interesting subject to explore.

In this study, we have shown that the clinically used chemotherapy drugs, VP16 and Taxol, can significantly ablate $CD44^+$ Du145 PCa cells, which are known to be enriched in CSCs. However, why do these drugs fail to cure PCa patients by wiping out CSCs? One possibility is that delivery of these drugs is not efficient enough to effectively reach and target $CD44^+$ CSCs in the prostate tumors. The second possibility is that because CSCs are heterogeneous (7), even if these commonly used chemotherapy drugs are capable of eliminating $CD44^+$ CSCs, other CSC populations may be spared, which may drive tumor relapse and metastasis. Finally, it is also possible that $CD44^+$ PCa cells may represent a population of intermediate cycling cells (85) that can be targeted by chemotherapeutic drugs. However, more quiescient tumor cells still exist after clinical treatments, which may be therapy-resistant and sustain tumor propagation. It is crucial that a long-term study should

be conducted to clarify what is occurring in these instances. Therefore, identifying the long-term slow cycling/quiescent PCSCs will be significant not only for our understanding of the disease, but also for possible future therapy development.

2.5. Future Studies

For this project, one of the most interesting questions to be addressed in the future is to understand how $CD44^+$ Du145 cells are ablated by the chronic drug exposure. One potential mechanism relates to epigenetic regulation by molecules such as KDM5A. In Du145-VP16 cells, CD44 protein levels decrease accompanied by increased KDM5A, suggesting that KDM5A, as a histone lysine demethylase, might directly target CD44 gene and regulate its expression. To test this suggestion and to determine the relationship between the two molecules, we will *first* use qPCR to examine the basal expression levels of KDM5A and CD44 using Du145 and Du145-DTCs (e.g., Du145-VP16). The purpose is to determine whether the reciprocal changes in the two molecules take place at the transcriptional level. *Then,* KDM5A will be knocked down in Du145-DTCs, followed by examination of the expression levels of CD44 at both mRNA and protein levels. If KDM5A is causally involved in shutting down CD44, its knockdown is predicted to boost CD44 mRNA and protein levels. Tumor-initiating experiments using LDA and *in vitro* proliferation (i.e., Ki67 or BrdU incorporation assays) and sphere-formation experiments will be used to determine the effects of KDM5A knockdown, which we expect should 'phenocopy' CD44 overexpression in these cells. *Subsequently*, in a reciprocal experiment to further confirm the gene knockdown results, a lentiviral-mediated gene overexpression of KDM5A will be conducted in Du145 cells, followed by characterization of CD44 expression and tumor-initiating and clonogenic capacities. *Finally*, to test whether KDM5A is directly involved in epigenetic regulation of CD44 transcription, a chromatin immunoprecipitation (ChIP) assay will be performed to examine the recruitment of KDM5A to the endogenous promoter region of CD44. We expect to see that KDM5A will bind to the promoter region of

CD44 and regulate CD44 expression by inhibiting its transcription. Collectively, the above-proposed experiments will allow us to obtain a better understanding of the epigenetic mechanisms regulating CD44 expression in our drug-tolerant PCa cells.

Chapter 3

Dissociated Primary Human Prostate Cancer Cells Coinjected with the Immortalized Hs5 Bone Marrow Stromal Cells Generate Undifferentiated Tumors in NOD/SCID-IL2Rγ$^{-/-}$ Mice

3.1. Introduction

As introduced earlier in Chapter 1, the majority of studies on PCSCs have used long-term cultured PCa cells or xenograft tumors (7). A KEY unanswered question is whether similar stem-like PCa cells with enhanced tumor-propagating properties also exist in primary human PCa (HPCa) samples. The reason that this important question has dodged a definitive answer lies in the fact that we have yet to establish a RELIABLE assay system that can REPRODUCIBLY and FAITHFULLY reconstitute tumor regeneration from single HPCa cells (83). Most currently used PCa models are derived from either genetically modified mice where specific genes are overexpressed or knocked out or from xenografts by using human cancer cell lines or tumor pieces inoculated orthotopically or ectopically into the immunodeficient mice (2). For many reasons, mouse models of PCa possess histopathological characteristics that are not entirely representative of human PCa, which are often characterized by multiple genetic alterations that are beyond the ability of any genetically engineered models may recapitulate. Moreover, a specific genetic mutation may result in distinct biological and histological phenotypes in animals versus in human (163). In contrast, xenograft models are widely studied for the ease of use. They are of human origins and therefore are believed to better recapitulate human tumors in terms of the histopathological and molecular characteristics (2).

Several widely used PCa xenografts, such as the LAPC and LuCaP series (164-166), have been established by implanting human prostate tumor pieces in immunodeficient mice. PCa xenografts can also be created by injecting established PCa cell lines such as PC-3 (bone metastasis), Du145 (brain metastasis), and LNCaP (lymph nodes metastasis) (131). Due to the well-known fact that localized PCa or PCa cells rarely form tumors in

immunodeficient mice (131), the above-mentioned examples of xenografts or cell lines were all established from metastases, and they only represent a minority of surgically removed human PCa and do not completely reflect the heterogeneity of the disease. Recently, efforts have been made to generate PCa xenografts by grafting localized PCa pieces (167, 168) or primary PCa cells recombined with neonatal mouse mesenchyme (169) in the renal capsule. The regenerated xenografts appear to resemble, histopathologically, the donor patient tumors, but whether they could be serially passaged is unknown.

The main goal of our current project is to establish a reliable assay system that would allow us to reproducibly and faithfully reconstitute human prostate tumor regeneration in mice using patient tumor-derived HPCa single cells. We have previously made some efforts towards this goal but most of our reconstitution protocols completely failed to regenerate tumors (83). Here, we have utilized many of the 114 untreated prostatectomy samples, ranging from Gleason Score (GS) 6 to 10, to prepare single epithelial cancer cells, which were recombined with different stromal cells including rUGM, carcinoma-associated fibroblasts (CAFs), or immortalized bone marrow-derived stromal cells (Hs5), and implanted at different anatomical sites in either NOD/SCID or NOD/SCID-IL2R$\gamma^{-/-}$ (NSG) mice. Below we present the results of our comprehensive studies.

3.2. Materials and Methods

Cells, reagents, and animals

PC3, DU145, LNCaP, and Swiss 3T3 cells were obtained from ATCC. Hs5 cells were kindly provided by Dr. M. Andreeff (M.D Anderson Cancer Center). Carcinoma associated fibroblasts (CAFs) were prepared as previously reported (170). All cells were cultured in recommended media containing 7% heat-inactivated FBS, 100 μg/ml streptomycin, and 200 U/ml penicillin (Gibco). Testosterone was purchased from Sigma. The TRPC xenograft line was provided by Dr. Palapattu (171). Immunodeficient mice (NOD/SCID, NSG, Rag2; (83)) were initially purchased from the Jackson Laboratories (Bar Harbor, ME) and the breeding colonies were established in our animal facility and maintained in standard conditions according to the institutional guidelines. Antibodies used in this study are presented in Table 3-1.

Histological and immunohistochemical (IHC) analyses

Tumor tissues harvested from patient tumors and reconstituted xenografts were fixed in formalin for 24 h followed by 70% ethanol and embedding in paraffin. Sections (4 μm) were cut and stained with hematoxylin and eosin (HE). For IHC, sections were deparaffinized and hydrated and endogenous peroxidase activity was blocked with 3% H_2O_2 in water for 10 min. Antigen retrieval was performed with 10 mM citrate buffer (pH 6.0) for 10 min in a microwave oven followed by a 20-min cool down and thorough wash. Slides were incubated with Biocare Blocking Reagent (#BS966M with casein in the buffer) for 10 min to block non-specific binding. Slides were incubated with various primary antibodies

for 30 min at room temperature, and washed in phosphate buffer twice and then incubated in biotinylated goat-anti-rabbit or mouse IgG (Vector Laboratories, Burlingame, CA) at a 1:500 dilution for 30 min at room temperature. After thorough washing, they were incubated with SA-HRP (BioGenex, San Ramon, CA) for 30 min at room temperature followed by washing. Finally, these slides were incubated with BioGenex DAB substrate (color development closely monitored under a microscope) and lightly counterstained with hematoxylin. Images were captured using a MagnaFire Camera, and the whole mount slides were scanned using an Aperio ImageScope system.

Aperio-assisted morphometric analysis

HE or IHC stained glass slides containing patient or xenograft tumors were scanned by using the Aperio Scanscope imaging platform (Aperio Technologies, Vista, CA, USA) with a 20× objective at a spatial sampling period of 0.47 μm per pixel. Whole slides images were viewed and analyzed by using desktop personal computers equipped with the free ScanScope software.

Purification of tumor cells from primary patient samples and xenograft tumors

Basic procedures have recently been described in Chapter 2. Primary PCa samples were obtained at radical prostatectomy with patients' consent according to the MDACC Institutional Review Board guidelines (IRB LAB04-0498). None of the patients received any treatment prior to surgery. *For patient samples*, tumor tissues freshly obtained from prostatectomy were minced into ~1 mm^3 pieces and tissues are subjected to enzymatic digestion (type I collagenase plus DNase at 50 U/ml) for 8-10 h at 37ºC. Upon digestion,

epithelial organoids are enriched by a brief centrifugation followed by trypsin digestion (0.05%, Gibco) on a rocker at 37ºC for 15-30 min to release epithelial cells. *For xenografts*, tumor tissues were incubated with 1x Accumax (1200–2000 U/ml proteolytic activity containing collagenase and DNase; Innovative Cell Technologies, Inc) at 10 ml per gram tissue for 30 min at room temperature under rotating conditions. Single-cell suspension was obtained by filtering the supernatant through a pre-wetted 40-μm cell strainer and cell suspension was then gently loaded onto a layer of Histopaque-1077 (Sigma) gradient purification step to remove the majority of red blood cells, dead cells and debris. Finally, the resultant cell mixture was subjected to a MACS lineage cell depletion kit (Miltenyi Biotec) and the cocktail (anti-CD3, 14, 16, 19, 20, 45, 56, and 140b for patient tumors; $H2K^d$ for xenografts) to remove the Lin^+ cells including hematopoietic, endothelial, and other stromal cells (smooth muscle, myoepithelial, fibroblast, etc) for patient samples, or mouse stromal cells for xenograft tumors, respectively.

Tumor transplantation experiments

Purified PCa cells (above), either alone or in combination with helper cells including rUGM, CAFs, or Hs5 cells, are implanted either subcutaneously (s.c) or under the kidney capsule (KC) of immunodeficient mice. Alternatively, pieces or fragments of HPCa were grafted subcutaneously, under the KC, or in the mouse anterior prostate (AP). Basic procedures for these transplantations have been previously described (83). Briefly, *for s.c implantations*, tumor cells were injected, in 40 μl of medium containing 50% Matrigel, subcutaneously into 6-8 week old male mice supplemented with exogenous testosterone pellets. *For KC transplantations*, PCa cells were mixed with 250,000 rUGM cells and tissue

recombinants were made in rat-tail collagen and incubated overnight. The tissue recombinants were transplanted next morning under the renal capsule of recipient male mice supplemented with testosterone pellets. *For AP grafting*, small pieces of HPCa tissues were directly implanted. In some cases, HPCa cells at different numbers were first mixed with rat collagen and incubated in a tissue culture plate at 37° for 10-15 min. Then the solidified cell pellets were gently covered in medium and cultured for 4 h to overnight prior to implantation. A transverse incision was made in the lower abdomen to expose the AP by partially pulling the bladder, seminal vesicles and prostate out of the abdominal cavity. A 2-3 mm incision was made in the AP through the tubule between the two main ducts with the aid of a 22-gauge needle. Using a fire-rounded glass pipette tip, the collagen dots were inserted into a pocket formed under the prostate tubule. Then the organs were replaced and the body wall and skin closed.

In all above experiments, tumor development was monitored starting from the second week. Tumorigenicity was measured mainly by tumor incidence (i.e., the number of tumors/number of injections), latency (i.e., time from injection to detection of palpable tumors), tumor volume, and endpoint tumor weight.

Fluorescence-Activated Cell Sorting (FACS) and purification of EpCAM$^+$ cells

HPCa/Hs5 tumors cells were treated with FcR blocking agent (Miltenyi Biotec) for 10-15 min at 4°C and stained with PerCP-eFluor 710 conjugated anti-EpCAM antibody and biotinylated mouse H-2K[d] antibody for 30 min at 4°C. Cells were then washed with PBS and labeled with Alexa Fluor 405 conjugated streptavidin (Invitrogen, S-32351) for 10 min

at 4°C. $EpCAM^+$ and $EpCAM^-$ cells were further purified using FACS (96, 98). Post-analysis revealed purities of both populations being >98%.

Sphere-Formation Assays

Basic procedures for sphere-formation assays were previously described (96, 98). We purified $EpCAM^+$ HPCa/Hs5 cells via MACS, and cultured them up in serum-free prostate epithelial basal medium (PrEBM) containing B27 (Invitrogen), 20 ng/ml EGF and bFGF in Purecol (Advanced BioMatrix, #5005-B) coated T-25 flasks. When these cells were confluent, we harvested the cells via 0.05% trypsin/EDTA, and plated the single cells in 6-well ULA plates at the density of 5,000–10,000 cells/well. Spheres were scored in ~2 weeks. For serial sphere-formation assays, the first-generation spheres were harvested with 0.025% trypsin/EDTA, triturated with a 27-G needle, filtered through a 40-μm strainer, and replated as above. This process was repeated for up to 3-4 generations.

Western blotting

Whole cell lysates were prepared in complete RIPA buffer (50 mM Tris-HCl, pH 7.5, 150 mM NaCl, 1% Nonidet P-40, 0.5% sodium deoxycholate, 0.5% Triton X-100, 10 mM EDTA) containing protease inhibitor mixture. Protein concentrations were determined by MicroBCA kit (Pierce). Various amounts of proteins were loaded on a 15% SDS-PAGE. Western blotting was performed as standard using ECL Plus (PerkinElmer).

Reverse transcription (RT)-PCR analysis

Total RNA was extracted from tumor pieces or cultured cancer cells using Trizol (Invitrogen), and used in RT-PCR analysis. The PCR primers included human AR (sense: 5'-GCTAAAGACTCGGAGGAAGCAAG-3'; antisense: 5'-TGGGGGAAAACAGAGGGTTC-3'); PSA (sense: 5'-TGGGAGTGCGAGAAGCATTC-3'; antisense: 5'-GCTGTGGCTGACCTGAAATACC-3'); β-actin (sense:5'-CTGGCACCACACCTTCTACAATG-3'; antisense: 5'- AATGTCACGCACGATTTCCCGC-3').

Karyotyping and genomic instability

Cells were exposed to Colcemid (0.04 μg/ml) for 25 min at 37°C and then to a hypotonic solution (0.075 M KCl) for 20 min at room temperature. Cells were fixed in a methanol and acetic acid (3:1 by volume) mixture for 15 min, and washed three times in the fixative. The slides were air-dried, optimally aged, and G-banded using trypsin solution and stained in Giemsa following the routine procedure. Images were captured using a Nikon 80i microscope equipped with karyotyping software from Applied Spectral Imaging (ASI) Inc., Vista, CA. and a minimum of 15 G-banded metaphases were karyotyped.

Statistic analysis

Limiting dilution analyzes were carried out using ELDA (http://bioinf.wehi.edu.au/software/elda/). Tumor-initiating cell frequencies were compared using likelihood ratio tests. Differences in tumor-take rate were determined by the Proportion test. Statistical significance was defined as $P < 0.05$.

Antibody	Host/Type	Catalog #	Company	Application	Remarks
AR	mouse monoclonal	sc-7305	Santa Cruz	WB	Clone 441
AR	rabbit polyclonal	ab74272	Abcam	IHC	
PSA	mouse monoclonal	ab2218	Abcam	WB	Clone A67-B/E3
PSA	rabbit polyclonal	N1517	Dako	IHC	
Racemase	mouse monoclonal	sc-81710	Santa Cruz	WB	Clone 2A10F3
Racemase	rabbit monoclonal	M3616	Dako	IHC	Clone 13H4
p63	mouse monoclonal	#559951	BD Pharmingen	WB	Clone 4A4
p63	mouse monoclonal	sc-8431	Santa Cruz	IHC	Clone 4A4
CK5	rabbit polyclonal	#PRB-160P	Covance	IHC	
CK8	rabbit polyclonal	Troma-1	DSHB	IHC	
CK18	rabbit polyclonal	sc-28264	Santa Cruz	WB	
β-actin	rabbit polyclonal	#4967	Cell Signaling	WB	
GAPDH	rabbit polyclonal	ab9485	Abcam	WB	
Ki-67	mouse monoclonal	M7240	Dako	IHC	Clone MIB-1, human specific
Ki-67	rat monoclonal	M7249	Dako	IHC	Clone TEC-3, mouse specific
mitochondria	mouse monoclonal	MAB1273	Millipore	IHC	Clone 113-1, human specific
EpCAM	mouse monoclonal	130061101	Miltenyi Biotec	MACS	Microbeads conjugated
EpCAM	mouse monoclonal	469326	eBioscience	FACS	PerCP-eFluor 710 conjugated
H-2K[d]	mouse monoclonal	553564	BD Pharmingen	FACS	Clone SF1-1.1, Biotinlyated
CD44	mouse monoclonal	555478	BD Pharmingen	FACS	FITC conjugated

Table 3-1. Primary antibodies used in Chapter 3.

3.3. Results

HPCa piece xenotransplants show higher tumor takes at subcutaneous site than at other sites

Our lab has so far worked on 114 patient samples freshly obtained from prostatectomy. Some of these samples have been used in our previous studies (83, 96, 98) and most of them were used in the current project. Of the 114 HPCa samples, 15.8% had combined Gleason Score (GS) 6, 52.6% GS7, 11.4% GS8, and 20.2% GS9. In general, the HPCa samples were used in 2 types of experiment: either transplanted, as small pieces, in male immunodeficient mice to generate xenografts or used to make single-cell suspension for in vitro and in vivo studies (Figure 3-1).

For xenograft studies, we implanted tumor pieces (~2-3 mm^3) at three different anatomical sites (83), i.e., subcutis (s.c), kidney capsule (KC), or anterior prostate (AP) in one of the three immunodeficient mouse strains, i.e., NOD/SCID, $Rag2^{-/-}$, or NSG mice. NOD/SCID mice lack both T and B cells and have functional deficit (though not complete deficiency) in NK cells and $Rag2^{-/-}$ mice also lack T and B cells whereas the NSG mice are the most immunodeficient lacking T, B, and NK cells (83, 122). As summarized in Table 3-2, in every strain of mice and with every grade of HPCa, the s.c implants showed the highest tumor take compared to KC and AP xenotransplants. Furthermore, in NOD/SCID mice, which were used most often, we observed increasing tumor takes with increasing tumor grade at s.c and KC sites (Table 3-2). Interestingly, the tumor grade-associated increase in tumor takes was not observed in Rag2 and NSG mice and HPCa samples xenotransplanted in NSG mice did not exhibit an increase in tumor takes compared to those implanted in

NOD/SCID mice (Table 3-2).

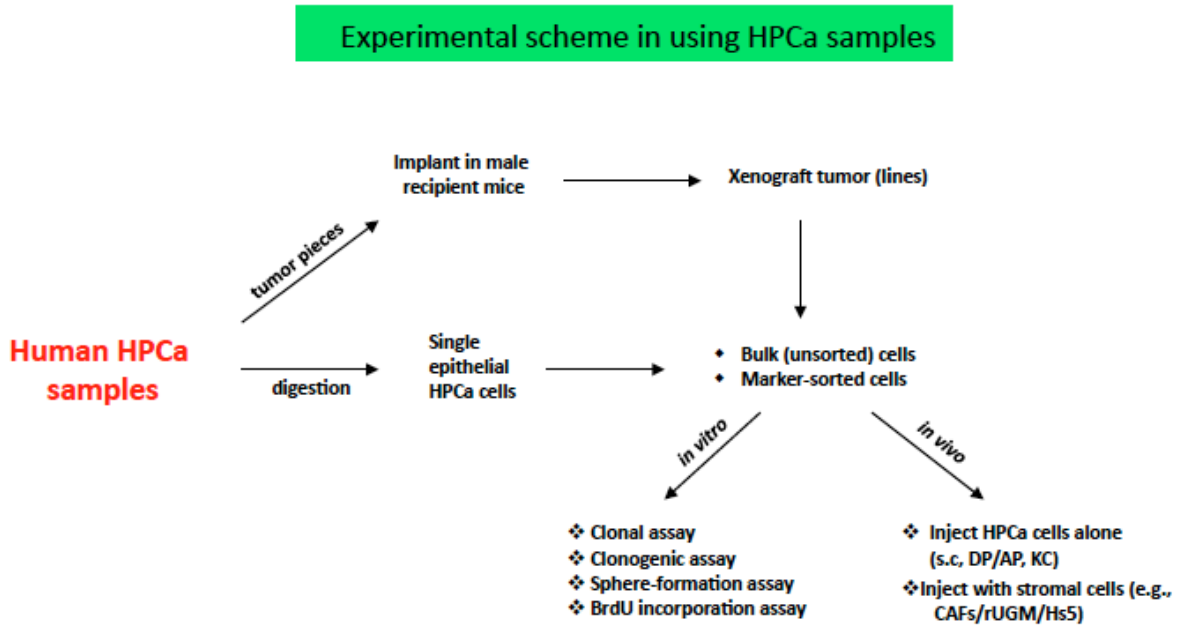

Figure 3-1. Experimental scheme in using HPCa samples.

HPCa[a] (Gleason)	Number	Harvest time[b] (days)	Host	Tumor take (%)		
				s.c	KC	AP
GS6	6	175	N/S	8/16 (50)[#$]	2/26 (7.7)[¶$]	2/11 (18.2)[@$]
GS7	29	151	N/S	68/115 (59.1)[#&]	20/59 (33.9)[¶&]	1/20 (5)[@&]
	4	114	Rag2	14/22 (63.6)	-	-
	9	252	NSG	31/42 (73.8)	-	-
GS8	6	148	N/S	36/40 (90)[#*]	6/15 (40)[¶*]	3/14 (21.4)[@*]
	2	151	Rag2	5/8 (62.5)	2/2 (100)	-
	2	248	NSG	7/9 (77.8)	-	-
GS9	12	142	N/S	45/57 (78.9)[#§]	6/12 (50)[¶§]	4/10 (40) [@§]
	1	258	Rag2	1/2 (50)	-	-
	7	237	NSG	29/38 (76.3)	-	-

Table 3-2. HPCa xenotransplantation using tumor pieces in immunodeficient mice. [a]HPCa pieces (~2-3 mm^3) were implanted in the indicated strains of male immunodeficient mice supplemented with testosterone pellets. For s.c experiments, tumor pieces soaked in 50% Matrigel were surgically implanted. For KC experiments, tumor pieces were directly implanted in the kidney capsule of the host. For AP implantation experiments, tumor pieces were surgically grafted in the AP tubules. "-", not done. [b]Average time in days from the start of tumor piece implantation to the day of harvest. [c]Tumor take refers to the number of tumors observed/number of implants. N/S: NOD/SCID mice. $^{\#}P = 0.0003$; $^{¶}P = 0.023$; $^{@}P = 0.13$; $^{\$}P = 0.006$; $^{\&}P = 3.719e\text{-}06$; $^{*}P = 1.464e\text{-}06$; $^{§}P = 0.01$ (all conducted by Proportion test).

HPCa cells, unlike HPCa pieces, failed to re-initiate tumors in NOD/SCID mice: No significant effects with rUGM, CAFs, and immortalized human (bone marrow) stromal (Hs5) cells

Subsequently, we asked whether freshly isolated HPCa cells, rather than tumor pieces, could also regenerate tumors in any of the immunodeficient mice. In the very beginning, we recombined HPCa cells with rUGM for KC transplantations or mixed the HPCa cells in 50% Matrigel for s.c injections in male NOD/SCID mice (83). In 3 GS6 HPCa (HPCa9, 10, and 16) samples, when 10,000 to 100,000 HPCa cells recombined with rUGM were implanted under the KC, we observed 0/30 outgrowth (83). Similarly, in 2 GS7 HPCa (HPCa11 and 14) samples, when 10,000 to 200,000 HPCa cells recombined with rUGM were implanted under the KC, we observed 0/17 outgrowth (83). Finally, when 1 million of HPCa18 (GS7) cells were injected s.c in 50% Matrigel, there was no single tumor out of 4 injections (83). We then purified $CD44^+$, $CD133^+$ or $CD44^+CD133^+$ (and corresponding marker-negative) HPCa cells from 4 GS6 tumors (HPCa 9, 10, 13, and 16), 4 GS7 tumors (HPCa4, 6, 8, and 12), and 1 GS9 tumor (HPCa42) and implanted increasing numbers of cells (from 1,000 to 2 million) subcutaneously (for the GS9 HPCa cells) or in the KC or AP (for the rest) of the male NOD/SCID mice and we observed 0/225 outgrowths (83). We also purified $CD44^+/CD44^-$ HPCa cells from 3 GS8 (HPCa25, 32, and 33) and 1 GS9 (HPCa24) primary (1º) xenografts and implanted 1,000 to 500,000 cells in 50% Matrigel at the most sensitive site, i.e., subcutis of male NOD/SCID mice. Again, we did not observe any tumor regeneration out of 52 implantations (83). Finally, when unsorted HPCa cells purified from 3 GS6 tumors (HPCa2, 10, and 16), 4 GS7 tumors (HPCa3, 11, 14, and 18), 2 GS8 tumors (HPCa15 and 37), and 2 GS9 (HPCa5 and 21), either injected alone in

Matrigel s.c or recombined with rUGM and then transplanted under the KC, gave rise to 0/92 tumors (83). In all these transplantation experiments, the male NOD/SCID mice were supplemented with exogenous testosterone pellets.

Next, we co-injected unsorted or marker-sorted HPCa cells with carcinoma-associated fibroblasts (CAFs), which have been reported to promote tumor development in some experimental systems (172), either subcutaneously or under the KC of testosterone-supplemented male NOD/SCID mice. We observed 3 outgrowths out of total 56 injections (Table 3-3). Nevertheless, the 3 outgrowths were not serially transplantable (Table 3-3).

Recently, human bone marrow derived mesenchymal stromal (or stem) cells (MSCs) have been shown to integrate into the tumor-associated stroma and promote breast cancer cell metastasis (173). We wondered whether MSCs might facilitate tumor reconstitution by primary HPCa cells. The Hs5 cell line, generated from human bone marrow, was immortalized by transduction with human papilloma virus E6/7 genes (174), and shown to support proliferation of PCa cells in cultures (175, 176). We thus subcutaneously coinjected unsorted or marker-sorted (i.e., CD44) HPCa cells (from 2 GS6, 3 GS7, 4 GS8 and 1 GS9) with 100,000 Hs5 cells into NOD/SCID mice. We observed 4 tumors in a total of 54 injections (Table 3-4). Again, the 4 regenerated tumors could not be serially transplanted (not shown). Hs5 cells alone did not generate tumors in NOD/SCID mice at ≤ 100,000 cells.

Taken together, our prior (83) and current studies indicate that NOD/SCID mice are not permissive for reconstituting transplantable tumors from primary HPCa cells, even in the presence of rUGM, CAFs, or MSCs such as Hs5.

HPCa sample	Marker/cell number	Site/Harvest time (d)	Incidence
HPCa71 (GS6)	Unsorted/250k (1x), 500k (1x), 1000k (1x)	s.c (180)	0/3
HPCa34 (GS7) - 1^{0} xenograft	CD44+/1k (3x), 10k (3x), 50k (1x)	s.c (139)	0/7
	CD44-/1k (2x), 10k (2x), 50k (3x), 500k (1x)	s.c (139)	0/8
HPCa39 (GS7) - 1^{0} xenograft	CD44+/1k (8x), 10k (8x), 100k (2x)	s.c (147)	1/4
	CD44-/1k (6x), 10k (6x), 100k (6x)	s.c (147)	2/6
HPCa52 (GS8)	CD44+/100k (1x)	s.c (163)	0/1
	CD44-/100k (2x)	s.c (163)	0/2
	Unsorted /500k (1x)	s.c (163)	0/1
HPCa27 (GS8) - 1^{0} xenograft	CD44+/1k (5x), 10k (4x), 50k (1x)	s.c (150)	0/10
	CD44-/1k (2x), 10k (2x), 50k (2x), 100k (2x)	s.c (150)	0/8
HPCa45 (GS9) - 1^{0} xenograft	CD44+/1k (2x), 50k (1x)	KC (113)	0/3
	CD44-/50k (1x)	KC (113)	0/1
	Unsorted /300k (2x)	KC (113)	0/2
			Total: 3/56 = 5.4%

Table 3-3. Unsorted or marker-sorted HPCa cells mixed with CAFs fail to initiate transplantable tumors in NOD/SCID mice. For s.c injections, cells were mixed with 100,000 CAFs and implanted subcutaneously in 50% Matrigel; For KC transplantations, cells were first recombined with 250,000 CAFs and then transplanted under the kidney capsule. All injections/transplantations were carried out in 6-8 week old male NOD/SCID mice supplemented with testosterone pellet.

HPCa sample	Marker/cell number	Harvest time (d)	Incidence
HPCa71 (GS6)	Unsorted/250k (2x), 500k (2x), 1M (2x)	131	0/6
HPCa82 (GS6)	Unsorted/10k (2x), 100k (1x)	273	0/3
HPCa70 (GS7)	$CD44^+$/10k (6x)	175	0/6
	$CD44^-$/10k (6x), 100k (2x)	175	0/8
HPCa83 (GS7	Unsorted/10k (5x)	185	0/5
HPCa93 (GS7)	Unsorted/1k (2x), 10k (2x), 40k (2x)	261	1/6
HPCa52 (GS8)	Unsorted/500k (1x)	163	0/1
	$CD44^+$/100k (1x)	163	1/1
	$CD44^-$/100k (2x)	163	2/2
HPCa69 (GS8)	Unsorted/960k (1x)	178	0/1
HPCa75 (GS8)	Unsorted/25k (1x)	203	0/1
HPCa91 (GS8)	Unsorted/100 (1x), 1k (1x), 10k (1x), 50k (1x)	123	0/4
HPCa87 (GS9)	Unsorted/1k (4x), 10k (4x), 100k (2x)	272	0/10
			Total: 4/54 = 7.4%

Table 3-4. Unsorted or marker-sorted HPCa cells mixed with Hs5 cells fail to initiate transplantable tumors in NOD/SCID mice. Unsorted or purified $CD44^+$/$CD44^-$ HPCa cells were mixed with 100,000 Hs5 cells and injected subcutaneously in 50% Matrigel in 6-8 weeks old male NOD/SCID mice supplemented with testosterone pellet.

Hs5 cells induce HPCa cells to initiate transplantable tumors in NSG mice

What if we utilize more immunodeficient mice? We first injected freshly purified primary HPCa cells from 5 patients (2 GS7, 1 GS8, 2 GS9) subcutaneously into NSG mice. In a total of 37 injections, we did not observe any tumor growth after 8 months (Table 3-5). Since Hs5 cells slightly increased tumor regeneration of HPCa cells in NOD/SCID mice (Table 3-4), we therefore *hypothesized* that subcutaneous coinjection of primary HPCa cells with Hs5 cells into NSG mice will allow us to reconstitute HPCa in immunodeficient mice using patient cells.

In 9 patient samples, this modified 'recombination protocol' remarkably induced tumor formation in 41/59 injections (i.e., ~70%; Table 3-6). HPCa cells derived from 3 GS9, 1 GS8, and 4 GS7 tumors all regenerated tumors when coinjected with Hs5 cells (Table 3-6). We also established 1º xenografts in Rag2 mice from pieces of 3 other HPCa tumors (i.e., HPCa57, 58, and 70). When the 1º xenograft cells were purified out and coinjected with Hs5 cells into male Rag2 or NSG mice, we readily obtained the 2º xenografts ((96, 98); data not shown). In total, we have established 11 HPCa/Hs5 xenografts from 7 GS7 (HPCa57, 58, 70, 83, 84, 85, and 92), 1 GS8 (HPCa91), and 3 GS9 (HPCa80, 87, and 96) tumors. These results seem to suggest that Hs5 cells highly efficiently promote tumor regeneration from fresh HPCa cells in NSG mice.

The reconstituted tumors were highly tumorigenic and could be passaged indefinitely (Table 3-7; data not shown). Also, the regenerated tumors were able to give rise to transplantable tumors independently of Hs5 cells (Table 3-7). Moreover, unsorted or CD44-sorted (both $CD44^+$ and $CD44^-$) HPCa cells were able to re-initiate tumors both subcutaneously and in the dorsal prostate (DP) and, significantly, HPCa cells purified from

the xenografts initially established in NSG mice could regenerate tumors in NOD/SCID mice (Table 3-7; data not shown).

Reconstituted "prostate" tumors are of human origin and present an undifferentiated and epithelial morphology: IHC, biochemical, and molecular characterizations

We first carried out histological and IHC analyses of the reconstituted tumors. As expected, the HPCa57 patient tumor exhibited typical GS7 histology with crowded tumor glands, in which most cells stained positive for luminal prostate epithelial cell markers PSA, nuclear AR, and cytokeratin 8 (CK8) (Figure 3-2A). Also, tumor glands showed positive staining for racemase (alpha-methylacyl-CoA racemase, also known as AMACR or P504S; encoded by the *AMACR* gene), negative (or weakly positive) staining for CK5 (a prostate basal epithelial marker), and negative for p63 (another basal cell marker) (Figure 3-2A). The HPCa57/Hs5 reconstituted tumors in NSG mice appeared completely undifferentiated and lacked glandular structures and PSA expression (Figure 3-2B). The cells looked overall epithelial, as supported by the presence of some $CK8^+$ and sporadic $CK5^+$ cells (Figure 3-2B). Interestingly, scattered AR^+ and $p63^+$ cells could be observed (Figure 3-2B). Staining with human-specific antibodies against mitochondria and Ki-67, both of which did not stain mouse tissues (Figure 3-3), confirmed the human origin of the regenerated HPCa57 tumor (Figure 3-2B). Similar patterns of morphology and marker expression were observed in Hs5-reconstituted HPCa58 (Figure 3-4) and 9 other HPCa samples, i.e., HPCa70, 80, 83, 84, 85, 87, 91, 92, 96 (data not shown).

Sample	Cell number (# injections)	Harvest (days)	Incidence
HPCa84 (GS7)	12.5k (1x), 50k (1x), 100k (1x)	177	0/3
HPCa85 (GS7)	100k (1x), 200k (1x), 500k (1x)	160	0/3
HPCa91 (GS8)	100 (3x),1k (3x), 10k (3x), 50k (1x)	123	0/10
HPCa87 (GS9)	1k (4x), 10k (5x), 100k (3x), 300k (1x)	143	0/13
HPCa89 (GS9)	1k (2x), 10k (2x), 100k (2x), 1M (2x)	248	0/8
			Total: 0/37

Table 3-5. Freshly purified and unsorted HPCa cells injected in NSG mice. Freshly purified and unsorted HPCa cells were subcutaneously injected in 50% Matrigel in 6-8 week old male NSG mice supplemented with testosterone pellet.

HPCa sample	Cell number	Harvest time (d)	Incidence
HPCa82 (GS6)	10k (2x), 100k (1x)	272	0/3
HPCa83 (GS7)	10k (5x)	185	5/5
HPCa84 (GS7)	12.5k (1x), 50k (1x), 100k (1x)	185	2/3
HPCa85 (GS7)	100k (1x), 200k (1x), 500k (1x)	160	3/3
HPCa92 (GS7)	1k (2x), 10k (2x), 100k (2x), 500k (2x)	149	5/8
HPCa91 (GS8)	100 (3x), 1k (3x), 10k (3x), 50k (1x)	154	9/10
HPCa80 (GS9)	1k(2x), 10k(2x), 30k(1x), 300k(1x)	147	4/6
HPCa87 (GS9)	1k (4x), 10k (5x), 100k (3x), 300k (1x)	143	7/13
HPCa96 (GS9)	1k (2x), 10k (2x), 100k (2x), 500k (2x)	161	6/8
			Total: 41/59 = 69.5%

Table 3-6. HPCa cells mixed with Hs5 cells initiate serially transplantable tumors in NSG mice. Freshly purified and unsorted HPCa cells at the indicated numbers were recombined with 100,000 Hs5 cells and then subcutaneously injected in 50% Matrigel in 6-8 week old male NSG mice supplemented with testosterone pellet.

HPCa sample	Marker/Cell number	Co-injection	Injection site/ Precondition/Host[#]	Harvest time (days)	Incidence[c]
HPCa57 (GS7)-2º	Unsorted/200k (2x), 500k (2x), 1M (2x)	100k Hs5	s.c/NSG	31	3/3
	$CD44^+$/1k (3x), 100k (6x)	100k Hs5	s.c/NSG	35	5/6
	$CD44^-$/1k (3x), 100k (3x), 1M(2x)	100k Hs5	s.c/NSG	35	5/6
HPCa57 (GS7)-3º	$CD44^+$/1k (4x), 5k (4x), 10k(2x), 50k (2x)	100k Hs5	s.c/NSG	77	8/8
	$CD44^-$/1k (7x), 10k (1x)	100k Hs5	s.c/NSG	77	4/8
HPCa57 (GS7)-4º	Unsorted/10k (6x), 100k (5x)	100k Hs5	s.c/NSG	56	8/9
	Unsorted/10k (6x), 100k (4x)	-	s.c/NSG	56	3/8
HPCa57 (GS7)-5º	Unsorted/1k (2x), 10k (2x), 100k (2x)	-	s.c/NSG	37	6/6
	$CD44^+$/100 (2x), 1k (2x), 10k (2x), 100k (2x)	-	s.c/NSG	37	8/8
	$CD44^-$/1k (2x), 10k (2x), 100k (2x)	-	s.c/NSG	37	6/6
HPCa80 (GS9)-1º	Unsorted/400k(4x)	100k Hs5	DP/NSG	35	4/4
	Unsorted/400k(2x)	-	DP/NSG	35	1/2
HPCa80 (GS9)-2º	Unsorted/300k(2x)	-	DP/NSG	50	2/2
	Unsorted/400k(3x)	-	DP/NSG	50	2/3
HPCa70 (GS7)-2º	Unsorted/1M (2x), 500k (4x), 100k (4x)	100k Hs5	s.c/NS	63	8/10
HPCa70 (GS7)-3º	Unsorted/500k(5x)	100k Hs5	s.c/NS	33	5/5
	Unsorted/500k (5x)	-	s.c/NS	33	5/5
HPCa70 (GS7)-4º	Unsorted/100k (5x)	-	s.c/NS	46	5/5

Table 3-7. Reconstituted 'prostate' tumors are independent of Hs5 cells, host, and injection site. Bulk or $CD44^+$/$CD44^-$ HPCa cells were purified from primary (1º) xenografts and used in subsequent (2º, 3º, etc) xenotransplantations (either s.c or DP) in the presence or absence (-) of 100,000 Hs5 cells in male NOD/SCID (NS) or NSG mice supplemented with testosterone pellet.

Consistent with the IHC results, RT-PCR analysis using human-specific primers revealed that none of the HPCa/Hs5 xenografts expressed *PSA* but most expressed different levels of *AR* mRNA (Figure 3-5). Notably, cultured murine fibroblasts (Swiss 3T3) and Hs5 cells were negative for both *AR* and *PSA* mRNAs (Figure 3-5). Western blotting experiments for 4 luminal cell markers, racemase, PSA, AR, and CK18 confirmed lack of PSA expression and revealed varying levels of the other 3 markers in different xenografts (Figure 3-6). Note that cultured Hs5 cells and Hs5 tumors (see below) did not express CK18 (Figure 3-6C, arrow) although they expressed low levels of racemase (Figure 3-6). Occasionally, Hs5 tumors were found to express low levels of AR protein (Figure 3-6B) although they expressed barely detectable *AR* mRNA (Figure 3-5). Most HPCa/Hs5 xenografts expressed higher levels of racemase than PC3 cells (Figure 3-6A). Interestingly, western blotting for p63 revealed very high levels in PC3 and LNCaP cells, readily detectable expression in HPCa57 and HPCa96 xenografts, and very low levels in several other HPCa xenografts (HPCa58,70, and 91) (Figure 3-6A). These results overall suggest that the *HPCa/Hs5 xenografts contain human prostatic epithelial cells*. As further support, western blotting of AR and CK18 on a series of HPCa57/Hs5 xenograft tumors, from the 1º generation (P1) to the 4º generation (P4), derived from s.c or DP implantations, showed that all these tumors were positive for AR and CK18 (Figure 3-6D).

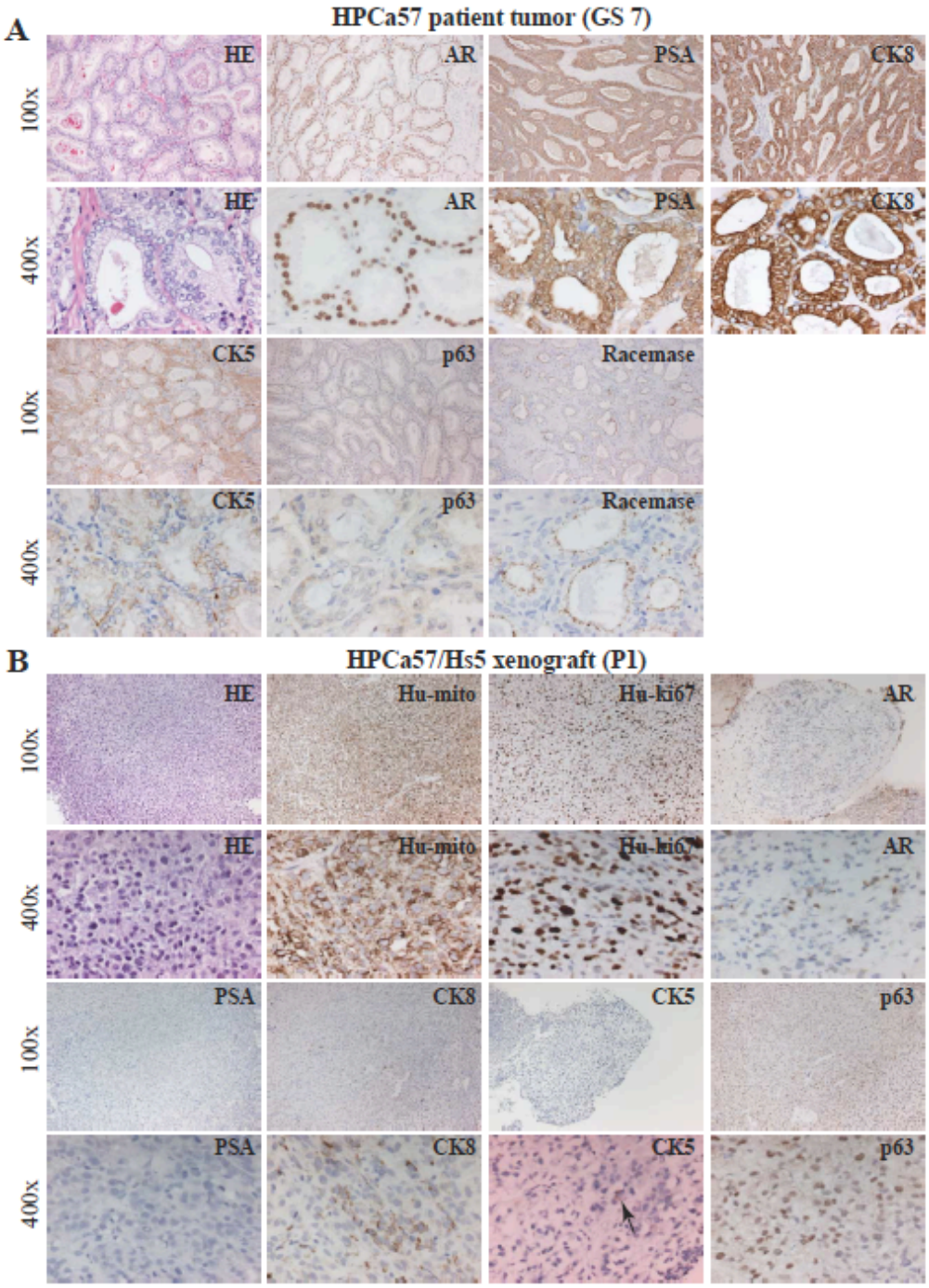

Figure 3-2. IHC analysis of HPCa57 patient sample (GS7) and its xenograft tumor. (A) Staining of HE, AR, PSA, CK8, CK5, p63 and Racamase in HPCa57 patient sample. (B) HPCa57P1 xenograft tumor, derived from coinjection with 100,000 Hs5 cells, was used to make serial sections, which were stained for HE, Hu-mito, Hu-ki67, AR, PSA, CK8, CK5 and p63. Both low (i.e., 100x) and high-power (i.e., 400x) magnifications were shown. The arrow indicates a $CK5^{+}$ cells.

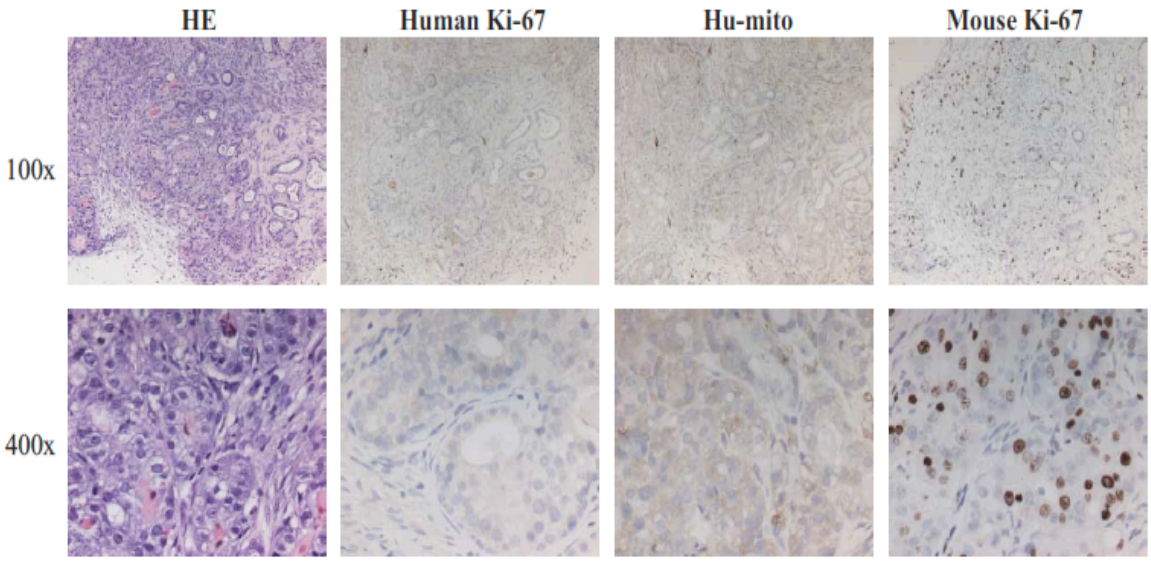

Figure 3-3. Testing antibody specificity in mouse prostate tumors. Serial sections from the Hi-Myc mouse prostate tumors were stained for HE, Hu-ki67, Hu-mito, or mouse-ki67 antibodies. Both low (i.e., 100x) and high-power (i.e., 400x) magnifications were shown. Note that although mouse-specific Ki-67 antibody stained positively, the human-specific anti-Ki67 and anti-mitochondria antibodies did not manifest any specific staining.

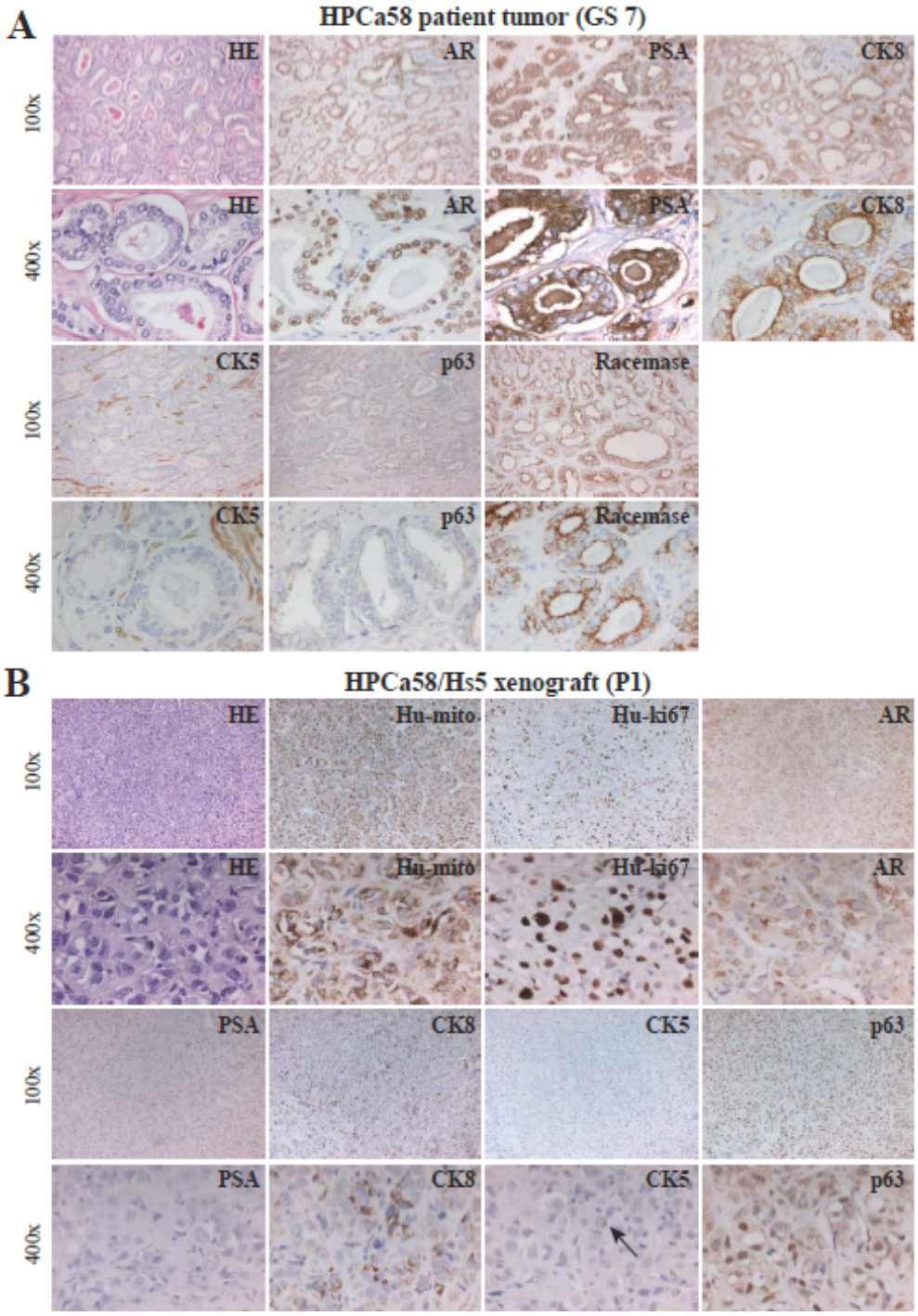

Figure 3-4. IHC analysis of HPCa58 patient sample (GS7) and its xenograft tumor. (A) Staining of HE, AR, PSA, CK8, CK5, p63 and Racamase in HPCa58 patient sample. (B) HPCa58P1 xenograft tumor, derived from coinjection with 100,000 Hs5 cells, was used to make serial sections were stained for HE, Hu-mito, Hu-ki67, AR, PSA, CK8, CK5 and p63. Both low (i.e., 100x) and high-power (i.e., 400x) magnifications were shown. The arrow indicates a $CK5^{+}$ cells.

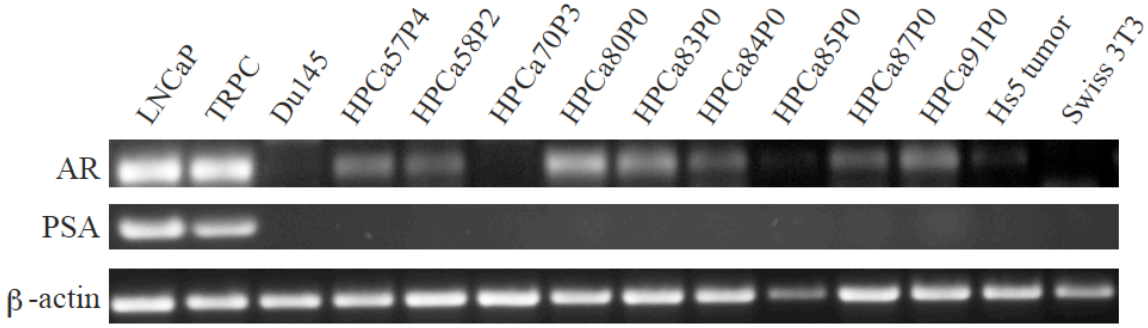

Figure 3-5. RT-PCR characterization of HPCa/Hs5 xenograft tumors. RT-PCR results of AR, PSA, and β-actin using human-specific primers. LNCaP, TRPC (treatment-refractory prostate cancer; (171)) and Du145 cells were used as controls.

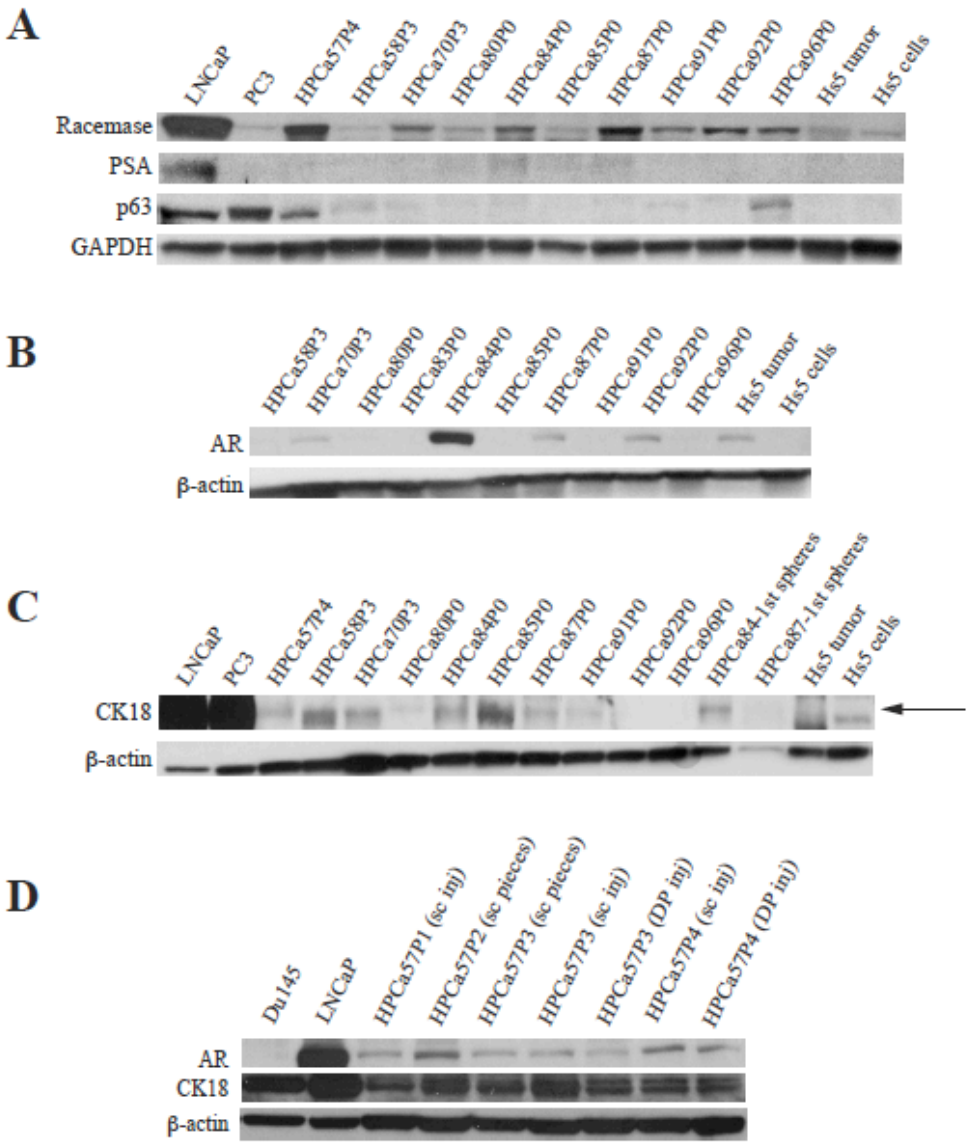

Figure 3-6. Western blotting characterizations of HPCa/Hs5 xenograft tumors. (A-C) Western blotting of Racemase, PSA, p63, AR and CK18 on HPCa-Hs5 xenograft tumors and the tumor cell-derived spheres. GAPDH and β-actin were used as loading controls. The arrow in C indicated the CK18 protein band (note that Hs5 cells and Hs5 tumor had some non-specific lower M.W bands). (D) Western blotting of AR, CK18 and β-actin in HPCa57/Hs5 serial xenograft tumors (P1-P4) from either subcutaneous or orthotopical (DP) injections. LNCaP and Du145 cells were used as controls.

Cytogenetic evidence for presence of human PCa cells in HPCa/Hs5 xenograft tumors and physical contributions of Hs5 cells to the xenografts

Our cytogenetic analyses (Figure 3-7) provided further evidence for the conclusion that HPCa/Hs5 xenografts contain human prostatic epithelial cells. The cultured Hs5 cells showed multiple chromosomal abnormalities with at least 5 marker chromosomes, i.e., M1 [del(1p)], M2 [del(2p)], M3 [der(2)], M4 [der(11)], and M5 [13q+] (Figure 3-7A). HPCa70 cells derived from either tumor piece implant (Figure 3-7B) or Hs5 coinjections (Figure 3-7C) showed similar karyotypic features that were distinct from the cytogenetic makeup of Hs5 cells. Specifically, tumor cells from both HPCa70/Hs5 coinjections and pieces implant showed a deletion at chromosome 10, which is a common chromosomal abnormality in PCa (177-179).

On the other hand, when we performed similar cytogenetic analysis in cells derived from HPCa57/Hs5 and HPCa87/Hs5 coinjections, most cells we were able to karyotype showed karyotypic features similar to those of Hs5 cells (not shown), suggesting that epithelial human PCa cells in these tumors represented the minority with Hs5 cells being the majority. Also, the overall histological and structural dissimilarities between the HPCa/Hs5 xenografts and the corresponding patient tumors made us wonder whether Hs5 cells might have physically contributed to the establishment of the xenografts. In partial support of this conjecture, Hs5 cells injected alone were capable of initiating tumor development in NSG mice with a grafting efficiency at ~52.5% (Table 3-8). Both Hu-mito and Hu-Ki67 staining of the Hs5 cell-derived tumors was positive (Figure 3-8, top), confirming their human origin. The Hs5 tumors manifested a stromal morphology, and IHC staining of these tumors was completely negative for PSA, CK8, CK5 and p63 (Figure 3-8), consistent with RT-PCR and

western blotting results (Figure 3-5; Figure 3-6). AR staining was observed in some cells but only in the cytoplasm (Figure 3-8). These data, taken together, suggest that Hs5 cells were tumorigenic in the highly immunodeficient NSG mice, but tumors derived from these cells were distinct from HPCa/Hs5 xenograft tumors.

The reconstituted HPCa/Hs5 tumors contain EpCAM$^+$ epithelial cancer cells that can regenerate tumors that contain both epithelial and mesenchymal-like cells

To provide further evidence that reconstituted HPCa/Hs5 tumors contain epithelial cells, we analyzed the expression of epithelial cell adhesion molecule (i.e., EpCAM) and detected a small percentage of EpCAM$^+$ cells in the HPCa/Hs5 (e.g., ~0.2% in HPCa58/Hs5) tumors (Figure 3-9A; data not shown). To functionally analyze these EpCAM$^+$ PCa cells, we purified out EpCAM$^+$ and isogenic EpCAM$^-$ cells from HPCa58/Hs5 tumors and injected them into male NSG mice. Interestingly, the EpCAM$^+$ cells in HPCa58/Hs5 tumors were capable of regenerating tumors with as few as 100 cells, and, importantly, the EpCAM$^+$ cell-derived tumors comprised both epithelial- and stromal-like cells (Figure 3-9B). In contrast, EpCAM$^-$ cells gave rise to tumors consisting of only stromal-like cells (Figure 3-9B).

We also sorted out EpCAM$^+$ cells from HPCa58/Hs5 tumors via Magnetic Activated Cell Sorting (MACS), cultured them in PrEBM medium in collagen treated plates, and, finally, tested their sphere-forming capacities (Figure 3-9C). We observed that most EpCAM$^+$ cells attached and proliferated to give rise to cells that were capable of generating serially passageable spheres in the ultra-low attachment plates (Figure 3-9D). Importantly, these spheres were positive for CK18 (Figure 3-6C). Taken together, these results further

indicate that the reconstituted HPCa/Hs5 tumors contain a subset of epithelial ($EpCAM^{+}$) PCa cells that are clonogenic as well as tumorigenic.

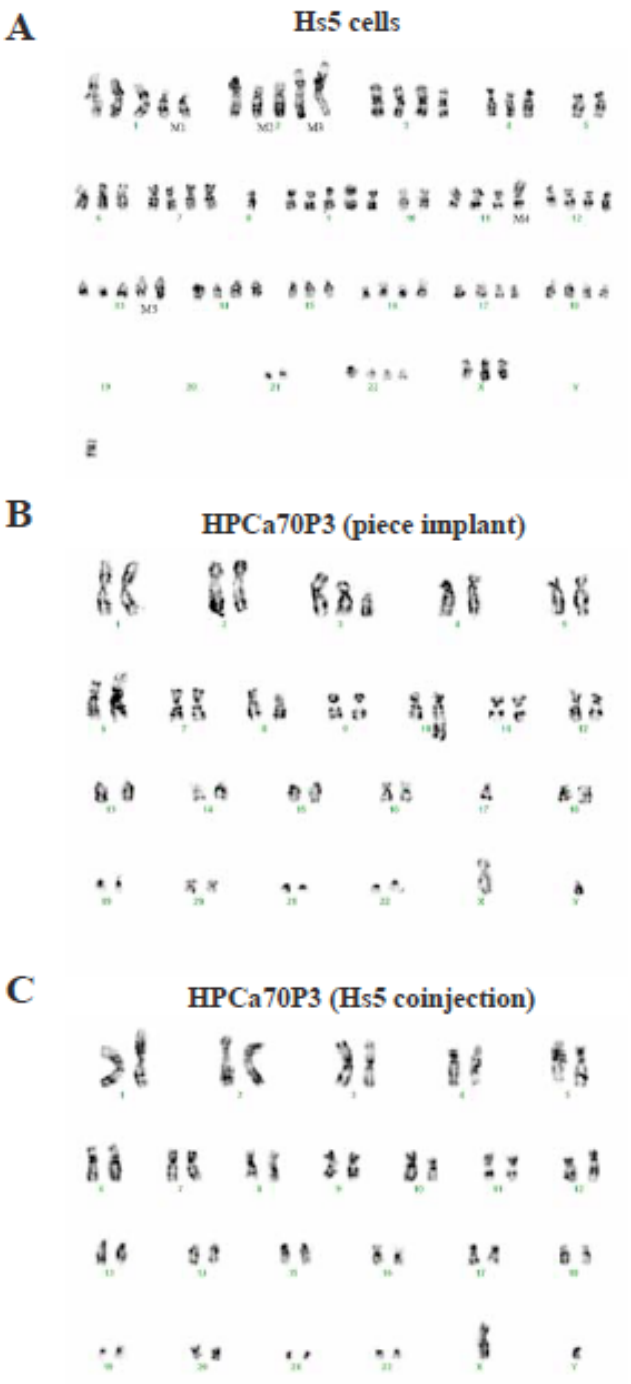

Figure 3-7. Cytogenetic analysis of HPCa/Hs5 xenograft tumors. (A) An example of Hs5 cell karyotype. (B-C) Karyotypes of xenograft cells derived from HPCa70 piece implantation (B) or from HPCa70/Hs5 coinjections (C).

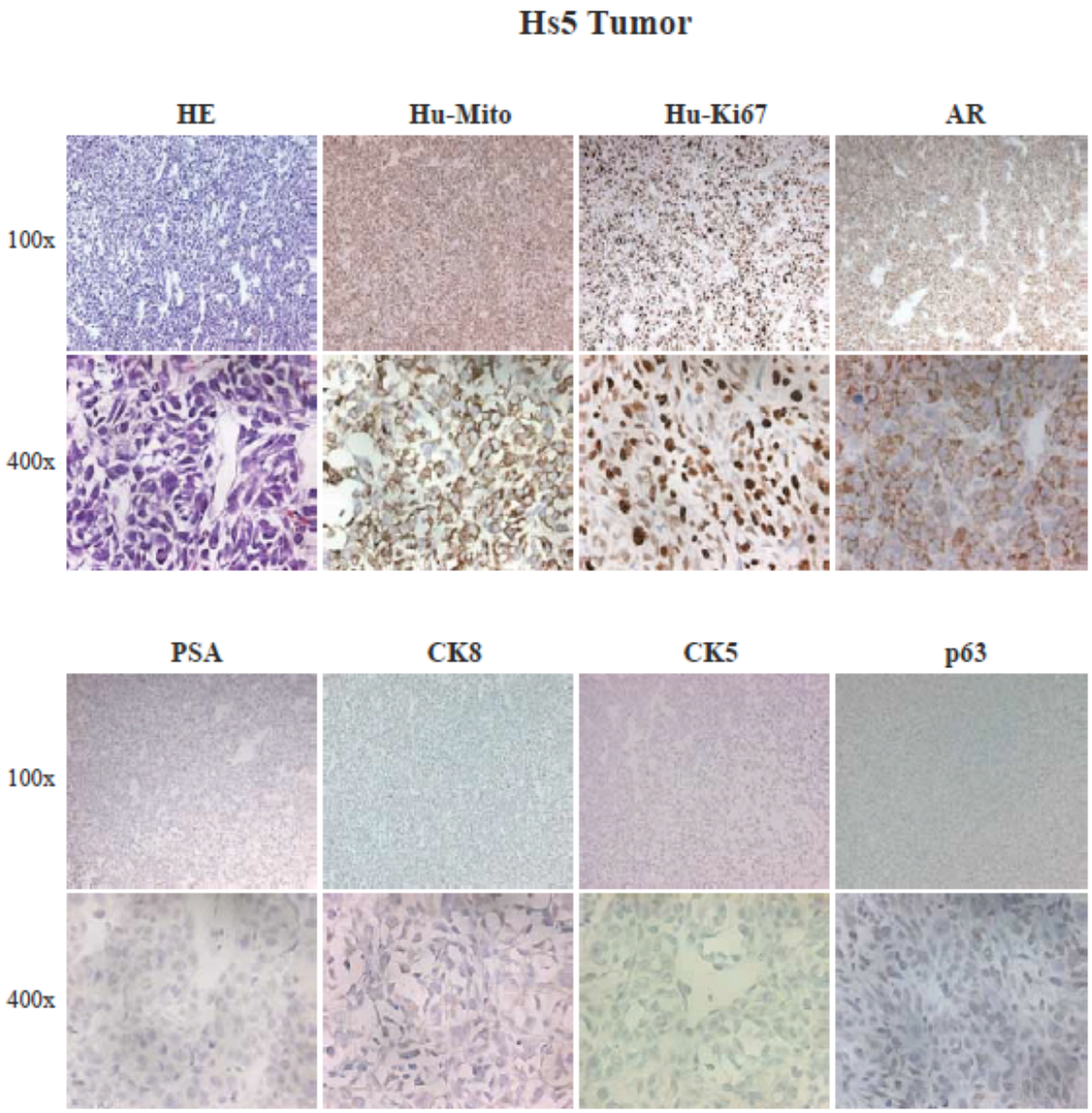

Figure 3-8. Histological analysis of Hs5 tumors. Serial sections were stained for HE, Hu-mito, Hu-ki67, AR, PSA, CK8, CK5 and p63. Both low (i.e., 100x) and high-power (i.e., 400x) magnifications were shown.

Cell number	Harvest Time (days)	Incidence
100k (2x)	232	1/2
100k (2x)	34	0/2#
100k (2x)	153	1/2
100k (1x)	180	1/1
100k (2x)	42	0/2#
100k (2x)	150	1/2
100k (2x)	197	2/2
100k (2x)	140	2/2
100k (4x)	139	4/4
100k (2x)	104	1/2
100k (2x)	149	0/2
100k (2x)	133	1/2
50k (2x), 10k (2x), 1k (2x)	232	2/6
500k (6x), 100k (6x), 10k (6x), 1k (6x), 100 (6x)	147	16/30
		Total: 32/61 = 52.5%

*Hs5 cells were subcutaneously injected in 50% Matrigel into 6-8 week old NSG mice supplemented with testosterone pellet.
#Mice died and no tumor was found.

Table 3-8. Cultured Hs5 cells initiate tumor development in NSG mice. Hs5 cells were subcutaneously injected in 50% Matrigel into 6-8 week old NSG mice supplemented with testosterone pellet.

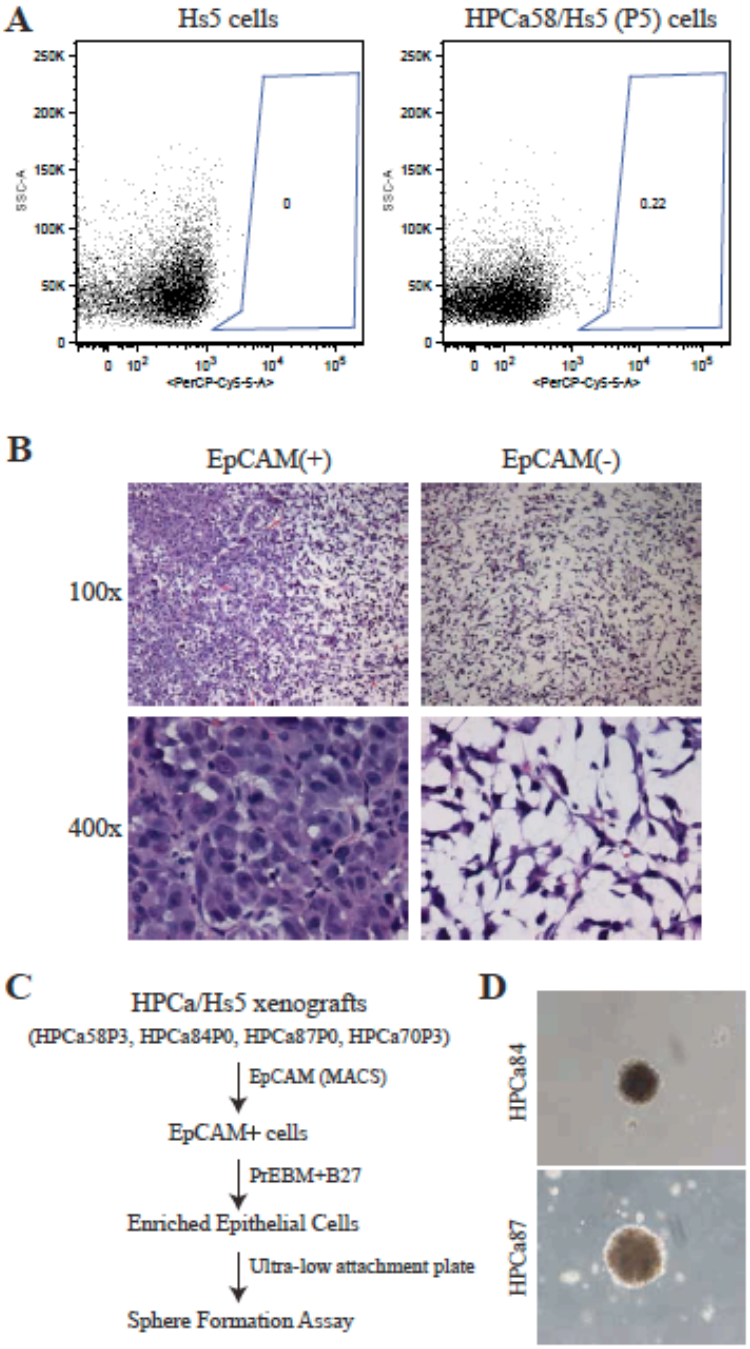

Figure 3-9. Functional characterizations of EpCAM$^+$ cells in HPCa/Hs5 tumors. (A) FACS analysis of EpCAM expression in cultured Hs5 cells and tumor cells harvested from HPCa58P/Hs5 tumors (P5). (B) HE staining of tumors derived from 100 EpCAM+ and EpCAM- cells from HPCa58/Hs5 tumors. (C) Scheme of sphere formation assays using HPCa/Hs5 xenograft tumor cells. (D) Representative images of spheres derived from EpCAM+ HPCa84 and HPCa87 tumor cells (100x).

Evidence that undifferentiated HPCa cells might be the cells that reconstituted the HPCa/Hs5 tumors

The observations that GS7 tumors such as HPCa57 and HPCa58, which contained well-differentiated glandular structures, nevertheless reconstituted tumors as fully undifferentiated tumors (Figure 3-2; Figure 3-4) are rather intriguing. When the whole-mount sections were analyzed under Aperio ScanScope, we observed discernible regions of poorly differentiated or undifferentiated tumor cells in all GS7 tumors such as HPCa57 (Figure 3-10), HPCa58 (Figure 3-11), and HPCa70 (Figure 3-12). On the other hand, although most tumor cells in GS9/10 tumors were poorly differentiated or undifferentiated, differentiated areas with glandular structures could clearly be observed (e.g., HPCa101; Figure 3-13). These cellular and structural heterogeneities in patient prostate tumors raised a possibility that undifferentiated HPCa cells might be the cells that survived in the tumor microenvironment and gave rise to transplantable xenograft tumors in the presence of Hs5 cells.

As indirect support for this possibility, we have successfully established two "pure" HPCa xenograft lines, i.e., HPCa70 and HPCa101 that were derived from primary tumor pieces implanted subcutaneously into the NSG mice. In HPCa70 patient tumor, most tumor cells were highly positive for luminal markers AR, PSA, CK8, and racemase but weakly positive for CK5 and negative for p63 (Figure 3-14A). Strikingly, the HPCa70 xenograft tumor, which was established by implanting tumor pieces without Hs5 cells presented a fully undifferentiated morphology and IHC staining was negative for PSA and weakly positive for AR (Figure 3-14B). The tumor piece-derived xenograft tumors were expectedly of the human origin (Hu-ki67$^+$, Hu-mito$^+$) and contained CK8$^+$ and CK5$^+$ cells (Fig. 3-14B).

Similarly, in the HPCa101 patient tumor (GS9), most tumor cells were positive for nuclear AR but moderately positive for CK8 and PSA, perhaps due to their overall poorly differentiated nature (Figure 3-15A). As expected, the corresponding HPCa101 xenograft tumor derived from pieces implant showed an undifferentiated morphology, was negative for PSA and p63 and weakly positive for AR, and contained $CK8^+$ and $CK5^+$ epithelial cells (Figure 3-15B). These striking observations in two tumor pieces-derived xenograft tumors, which histologically and immunophenotypically resembled the HPCa/Hs5 reconstituted xenograft tumors, raised the possibility that undifferentiated HPCa cells might have a survival advantage to regenerate tumors.

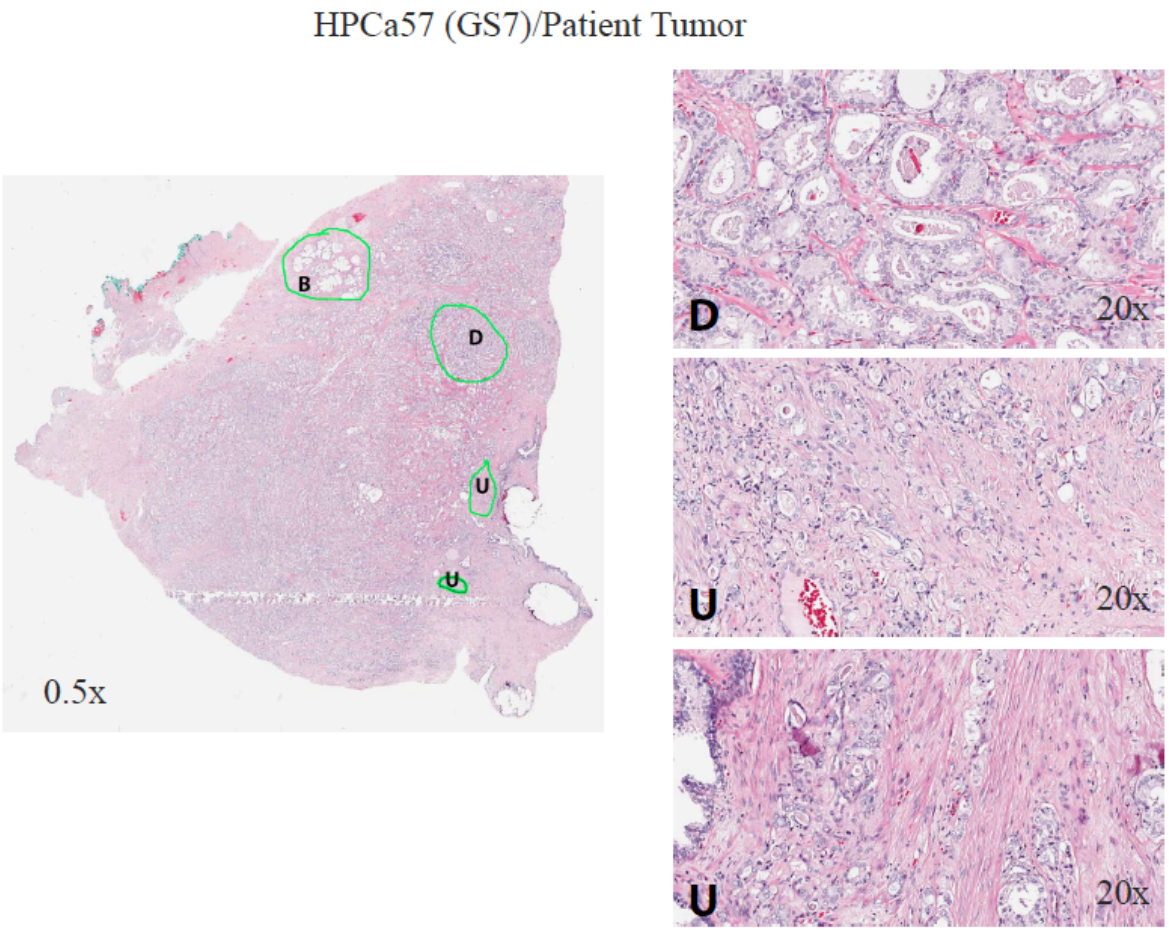

Figure 3-10. Histological and cellular heterogeneity in HPCa57 (GS7) prostate tumors. Shown are whole-mount Aperio Scanscope images of HPCa57 patient tumors, in which benign (B) glands, differentiated (D), and undifferentiated (U) tumor areas can be identified. Enlarged images of one differentiated and two undifferentiated areas are shown on the right. The magnifications of the original objectives are indicated.

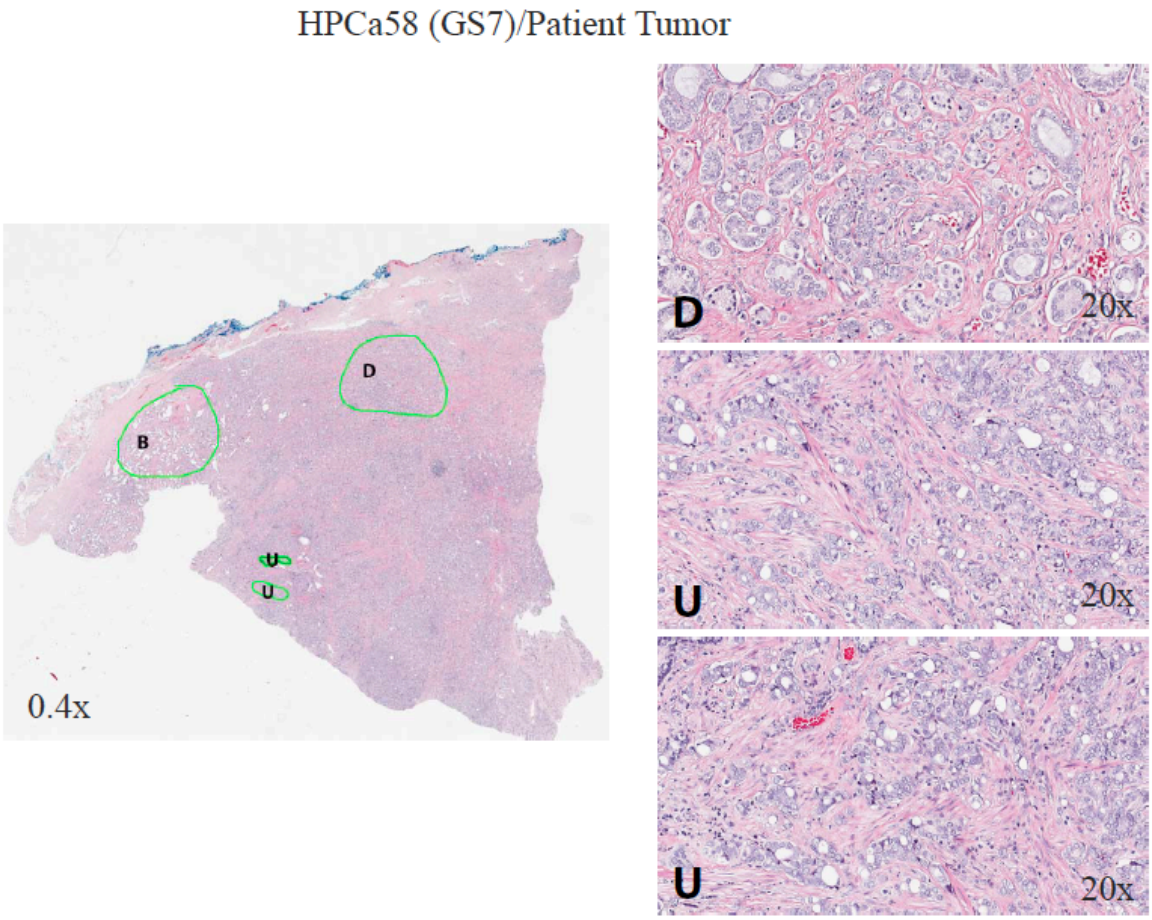

Figure 3-11. Histological and cellular heterogeneity in HPCa58 (GS7) prostate tumors. Shown are whole-mount Aperio Scanscope images of HPCa58 patient tumors, in which benign (B) glands, differentiated (D), and undifferentiated (U) tumor areas can be identified. Enlarged images of one differentiated and two undifferentiated areas are shown on the right. The magnifications of the original objectives are indicated.

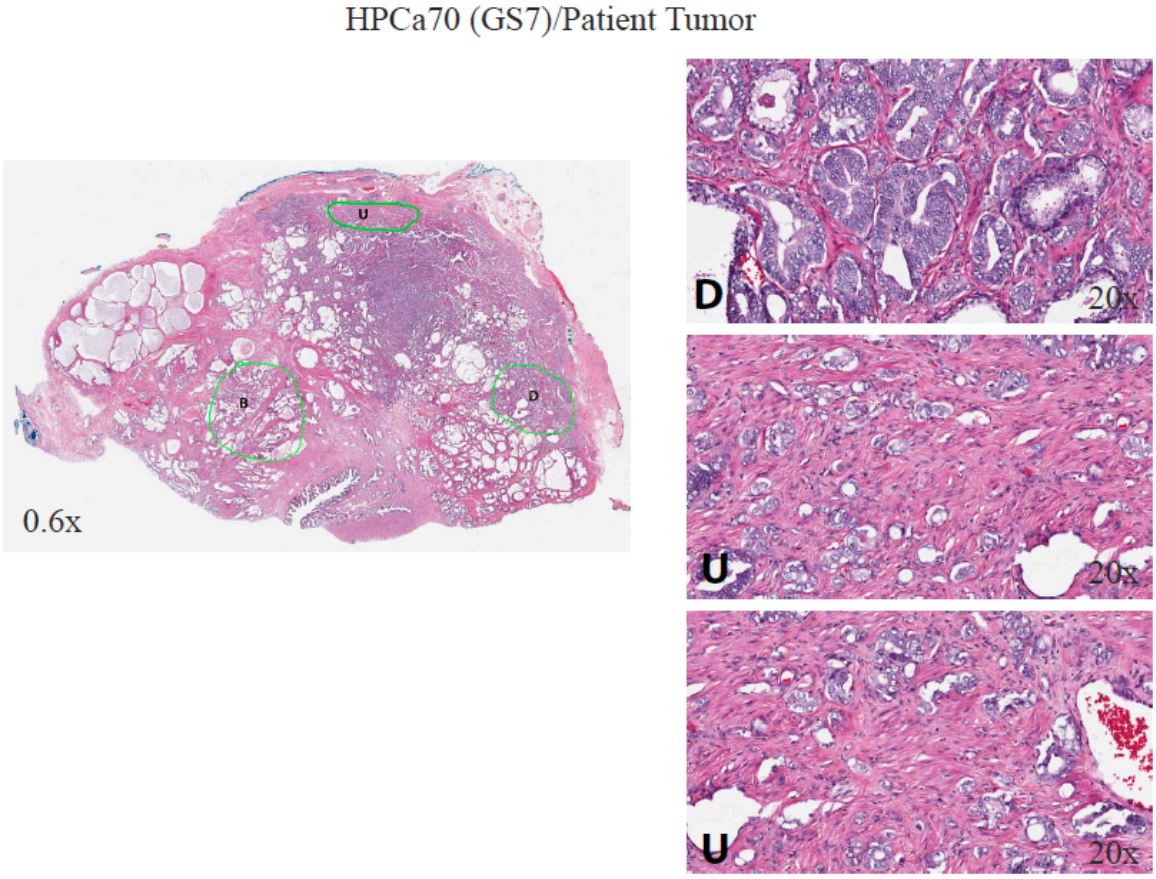

Figure 3-12. Histological and cellular heterogeneity in HPCa70 (GS7) prostate tumors. Shown are whole-mount Aperio Scanscope images of HPCa70 patient tumors, in which benign (B) glands, differentiated (D), and undifferentiated (U) tumor areas can be identified. Enlarged images of one differentiated and two undifferentiated areas are shown on the right. The magnifications of the original objectives are indicated.

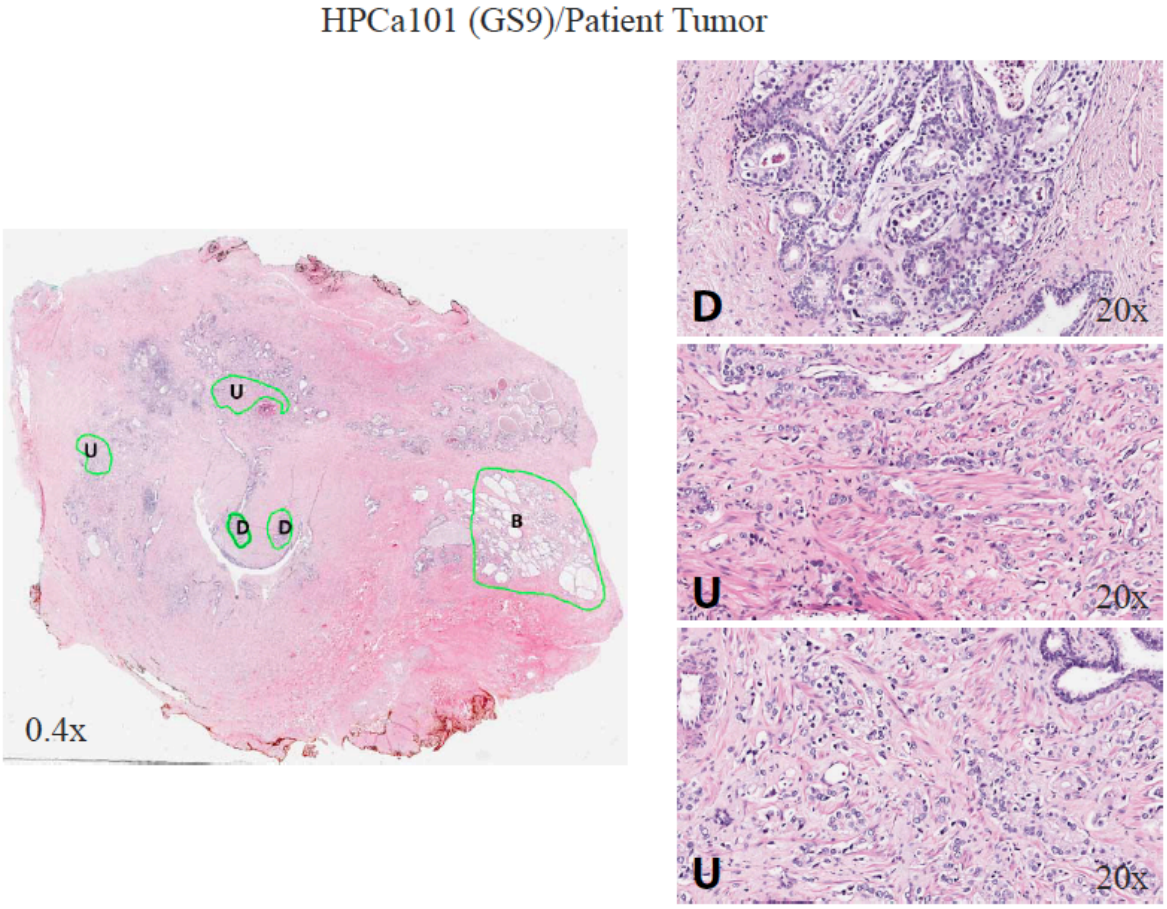

Figure 3-13. Histological and cellular heterogeneity in HPCa101 (GS9) prostate tumors. Shown are whole-mount Aperio Scanscope images of HPCa101 patient tumors, in which benign (B) glands, differentiated (D), and undifferentiated (U) tumor areas can be identified. Enlarged images of one differentiated and two undifferentiated areas are shown on the right. The magnifications of the original objectives are indicated.

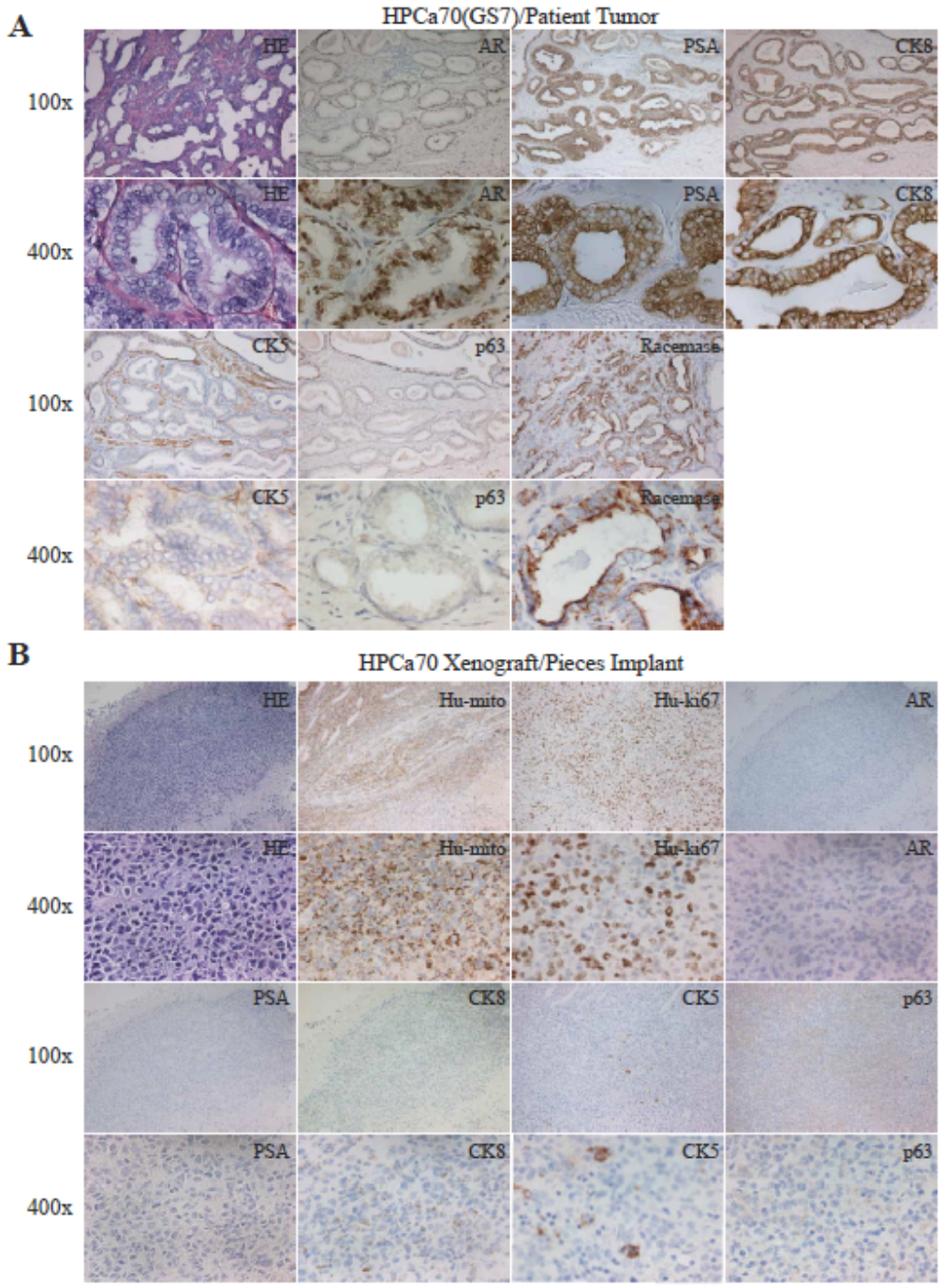

Figure 3-14. Histological analysis of HPCa70 (GS7) patient sample and its piece implant-derived xenograft tumor. (A) Staining of HE, AR, PSA, CK8, CK5, p63 and Racamase in HPCa70 patient sample. (B) HPCa70 xenograft tumor, derived from primary HPCa70 tumor pieces implantation, was used to make serial sections, which were stained for HE, Hu-mito, Hu-ki67, AR, PSA, CK8, CK5 and p63. Both low (i.e., 100x) and high-power (i.e., 400x) magnifications were shown.

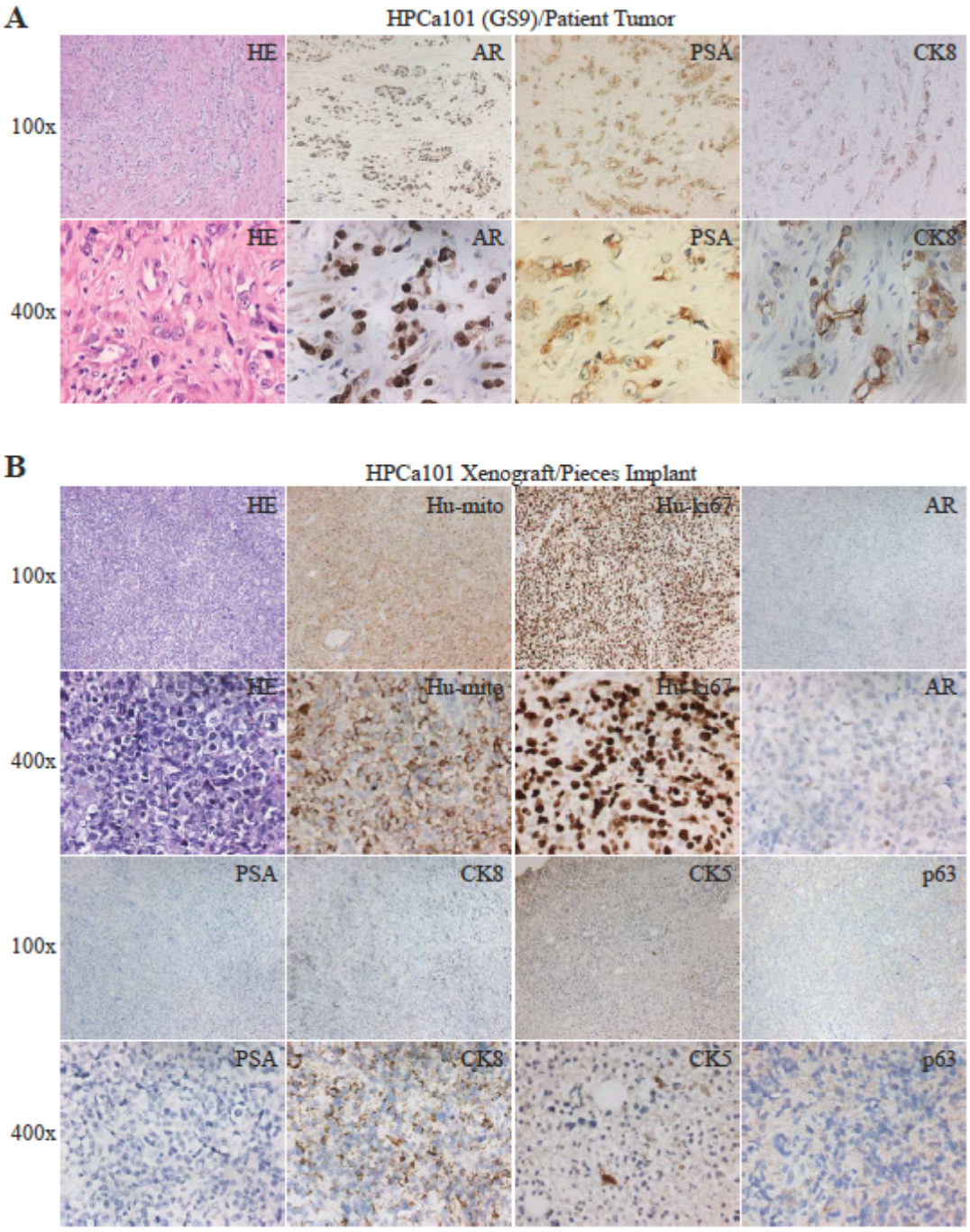

Figure 3-15. Histological analysis of HPCa101 (GS9) patient sample and its piece implant-derived xenograft tumor. (A) Staining of HE, AR, PSA, CK8, CK5, p63 and Racamase in HPCa101 patient sample. (B) HPCa101 xenograft tumor, derived from primary HPCa101 tumor pieces implantation, was used to make serial sections, which were stained for HE, Hu-mito, Hu-ki67, AR, PSA, CK8, CK5 and p63. Both low (i.e., 100x) and high-power (i.e., 400x) magnifications were shown.

3.4. Discussion

The PCa field has long been hampered by the paucity of suitable xenograft models. There are two lines of studies that attempt to reconstitute human PCa development in immunodeficient mice, i.e., tumor piece implantation and cell injection. In the past, PCa xeonografts from either way were mainly derived from metastasis (164-166). It is conceivable that more challenges exist to establish xenografts using single cells derived from primary human PCa samples in that many factors will contribute to the complexity of reconstitution such as Gleason score, tumor type, relative abundance of tumor cells, host, applied methodologies, etc (83). As a result, tumor piece implantation has been used more widely. It is believed that such "tumorgrafts" should recapitulate primary patient tumors histopathologically and molecularly (180), at least to a certain degree.

Various groups have attempted to establish HPCa xenograft models by using tumor piece implantation. For example, Wang and colleagues compared the efficiency and histopathologic patterns of xenografting both benign and malignant human prostate tissue (low- to mid-grade) into different sites (subrenal, orthotopic and subcutaneous) of SCID mice, and they showed that both subrenal capsule and orthotopic sites could be used for HPCa xenograft studies with respect to high take rate and histopathologic differentiation (181). More recently, Priolo and colleagues implanted 30 primary localized prostate tumor pieces into the KC site of Nu/Nu or NOD/SCID mice, and they obtained a 56% tumor take with very low tumor take from subcutaneous and orthotopic implantations (167). The xenografts from subrenal site maintained both grading and expression of phenotypic markers of the parental patient tumors (167). Also, a tissue slice graft model has been developed by subrenal implantation of fresh thin, precision-cut tissue slices derived from 2 primary patient

adenocarcinomas into RAG2-γ mice, and this model has been advocated as a tool to model all stages of PCa (168). Most of these implantations have been done in the subrenal site, in which tumor growth is somewhat limited. Also, whether these grafted tumors can be serially transplanted remains unknown. In our study, we implanted primary tumor pieces from 78 untreated patients (ranging from GS6-GS9) into the male NOD/SCID, Rag2, or NSG mice supplemented with testosterone at 3 different sites (i.e., SC, KC and/or AP) (Table 3-2). Our results reveal the subcutaneous site to be the most sensitive in NOD/SCID mice in allowing tumor piece grafting. In addition, tumor grade positively correlates with tumor take at the subcutaneous site. Importantly, we have established two serially transplantable xenograft models from two primary patient samples using subcutaneous tumor piece implantation, i.e., HPCa70 (GS7) and HPCa101 (GS9) (Figure 3-14 and Figure 3-15). To our knowledge, these two xenograft lines are among the few serially transplantable PCa models that originate from primary patient tumors.

Reconstitution of PCa in the immunodeficient mice from patient-derived HPCa single cells is much more challenging, explaining, partially, why there is a limited number of PCa cell lines currently available (182). This challenge is also the underlying reason why it has yet to be demonstrated that human PCa cells freshly purified from patient tumors contain stem-like cancer cells that can initiate serially transplantable tumors, a gold standard to functionally characterize CSCs in vivo, although such studies have been done with many PCa xenograft models or cultured cell lines (see Introduction). It is rather striking how indolent primary PCa cells are compared to many other tumor cells such as melanoma, colorectal cancer, and glioblastoma cells, which, when freshly purified from patient tumors and implanted in Matrigel in immunodeficient mice, can readily regenerate xenograft tumors

that even have defined structures (e.g., glands) (7, 122). In sharp contrast, acutely purified HPCa cells, either bulk or marker-enriched, are virtually non-tumorigenic when implanted in Matrigel in NOD/SCID or NSG mice, even in the presence of "helpers" such rUGM and CAFs ((83); this study).

There are several novel and important findings from our current study. *First*, bulk or marker-sorted HPCa cells, when injected alone in 50% Matrigel, cannot induce tumor growth, even in the highly immunodeficient NSG mice, supporting the notion that HPCa cells are quite indolent. These results also suggest that either primary HPCa cells need special microenvironment to maintain their growth in vivo, or they need manipulations to enhance their tumor-initiating potential. About this latter point, it has been recently shown that basal cells from primary benign human prostate tissues are capable of initiating PCa in NSG mice upon overexpressing 3 oncogenic molecules (i.e., AKT, ERG, and AR) (183).

Second, although HPCa cells coinjected with rUGM, CAFs, or Hs5 cells do not regenerate serially transplantable tumors in NOD/SCID mice after 6-9 months, Hs5 cells significantly enhance the ability of HPCa cells to initiate serially transplantable tumors in NSG mice (~10-fold increase compared to in NOD/SCID mice). Thus, our results in PCa substantiate that more immunodeficient mice dramatically increase primary tumor take/incidence, as shown in melanoma (122). Furthermore, our study hints that certain microenvironments (e.g., coinjection of 'helper' cells) may likely help primary HPCa cells set a foothold in vivo. To our knowledge, our work is the first in the field to systematically compare tumor take/incidence in both NOD/SCID and NSG mice by using patient-derived HPCa single cells.

Third, recent evidence suggests that bone marrow-derived human MSCs increase tumor grafts of human breast cancer cells by promoting angiogenesis (184) as well as enhance metastatic capacities (173). Here we report, for the first time, that the immortalized human MSCs (i.e., Hs5) reliably promote human prostate tumor reconstitution in NSG mice. Several pieces of evidence support the presence of epithelial PCa cells in the reconstituted HPCa/Hs5 tumors: most tumor cells present an epithelial morphology; $CK8^+$ and $CK5^+$ cells can be observed; RT-PCR and/or western analyses reveal AR and CK18 expression in most tumors; karyotyping analysis shows cytogenetic abnormalities characteristic of human PCa cells; and presence of $EpCAM^+$ cells that are both clonogenic and tumorigenic.

Intriguingly, all HPCa/Hs5 tumors, including those from GS7 tumors, present a fully undifferentiated histology lacking glandular structures. Consistent with the undifferentiated tumor histology, all HPCa/Hs5 tumors lack PSA and only express very low levels of AR. These results suggest that Hs5 cells fail to fully reconstitute the original patient tumor histology. The fact that prostate tumors are extremely heterogeneous leads us to propose that it is perhaps only the undifferentiated PCa cells in the primary tumors that have the ability to reconstitute tumor formation in highly immunodeficient mice. As indirect support for this proposal, we have recently provided evidence that undifferentiated (i.e., $PSA^{-/lo}$), compared to differentiated (PSA^+) PCa cells, are enriched in prostate CSCs that possess long-term tumor-propagating capacity (98). As further support, the phenotype of "undifferentiation" in our HPCa/Hs5 reconstituted tumors is similar to that in xenograft tumors derived from HPCa70 and HPCa101 tumor pieces. In fact, it has been reported that subcutaneous transplantation of primary PCa pieces into nude mice leads to xenograft tumors composed entirely of undifferentiated cells (185).

The exact mechanisms by which Hs5 cells support HPCa tumor regeneration need further investigation. One possibility is that Hs5 cells secrete critical cytokines such as IL-6 that help maintain the survival of undifferentiated PCa cells. Another possibility is that Hs5 cells promote HPCa tumor reconstitution via cell-cell fusion as we have demonstrated that prostatic epithelial cells and fibroblasts have a high propensity to fuse with each other (186). It has also been reported that MSCs from FSP1-Cre/Rosa 26 mice were recruited to the prostate and could fuse with local prostate epithelial cells from β-actin-GFP mice, manifested by co-expression of β-galactosidase and GFP during prostate regrowth after castration (187). In addition, the authors found that MSCs were able to home to C4-2B xenograft tumors and enhance Wnt signaling activity (187). Using a co-culture model, Wang and colleagues found that some of the cancer-stromal hybrids could survive and led to colony formation in the co-culture, and these colonies featured with androgen-independent phenotypes (188). It has been reported that coinjection of tumorigenic rat prostatic fibroblasts enhanced tumor formation of otherwise non-tumorigenic adjacent prostatic epithelial cells via paracrine signaling, leading to the formation of carcinosarcoma (189). The Hs5 cells utilized herein are tumorigenic whereas HPCa cells are non-tumorigenic in NSG mice, but HPCa/Hs5 coinjections initiate serially transplantable tumors. Importantly, the HPCa/Hs5 tumors, to a certain degree, resemble carcinosarcomas reported earlier (189). Cell fusion and carcinosarcoma formation can probably help explain why in general the $EpCAM^+$ cells in HPCa/Hs5 tumors are rare (i.e., ~0.2% or less). It is interesting that tumors derived from $EpCAM^+$ cells contain both epithelial and mesenchymal-like cells, suggesting that $EpCAM^+$ cells might possess some bi-potential differentiation capacity.

A recent study reported that PCa can be reconstituted from primary HPCa single cells by coinjecting with neonatal mouse mesenchyme under kidney capsule, which significantly increased xenografting rate to 32% compared to 0% without the mesenchyme (169). It remains unclear whether the reconstituted tumors are serially transplantable. More recently, it has been reported that less differentiated HPCa cells marked by low levels of HLA expression and injected in Matrigel can initiate serially transplantable tumors in NSG mice, although the efficiency is rather low, i.e., <10% (105). This study (105) is fully consistent with ours (98), which, coupled with our current study, strongly suggest that undifferentiated PCa cells are endowed with the unique capability to regenerate PCa in immmunodeficient hosts. Future research will focus on better characterizing the immunophenotypes of undifferentiated PCa cells, which should lead to much improved tumor reconstitution protocols.

3.5. Future studies

From our and others' studies, it is of the utmost importance that we explore and optimize protocols that may allow us to reliably establish HPCa development in immunodeficient mice using single patient PCa cells, and that the reconstituted tumor will, at least partially, restore tumor heterogeneity of the parental tumor. To achieve this, there are several critical factors that need to be taken into account. We have demonstrated that: 1) the subcutaneous site is the best site for tumor take of the PCa cells to establish serially transplantable tumors; 2) using NSG mice undoubtedly increases tumor incidence; 3) 'helper' cells will improve PCa survival rate in vivo and boost the likelihood of successful tumor reconstitution (169); 4) the undifferentiated/poorly differentiated PCa cells may be THE cells to drive PCa reconstitution in immunodeficient mice. Among these variables, the most challenging is probably to find ways to select for undifferentiated PCa cells.

There are two potential approaches. *First,* it has been shown that benign prostate tissue can be selectively labeled and dissected out from the cancerous tissue in the same patient prostate tumor, and cells derived from this dissection can be considered as 'pure' benign prostatic cells (183). Our lab has been working on primary HPCa for more than 7 years with collaborations from highly experienced surgeons and pathologists (Dr. Fagin R, Dr. Giesler R, and Dr. Haas J) in TX, and our team is fully capable of performing similar experiments. To do so, once fresh PCa specimens are obtained, a senior pathology assistant from St David's Hospital will prepare several sections of ~4 mm each in thickness. Several frozen slides will be used to perform HE staining. The undifferentiated/poorly differentiated regions will be marked and mapped to the rest of the fresh tumor, which will later be dissociated into single cells as described in the Materials and Methods section. *Second,* we

can enrich the undifferentiated PCa cells using the PCSC markers, e.g., $PSA^{-/lo}$ (98) or HLA^{-} (105). After the undifferentiated PCa cells have been purified, we will coinject them with neonatal mouse mesenchyme (169) and inoculate the mixture to different sites in NSG mice, including s.c, DP, and KC. Tumor growth will be monitored at least twice a week, starting two weeks after injection. We will record tumor incidence, tumor weight, latency and weekly tumor volume. After the tissue harvest, the reconstituted tumors will be examined comprehensively by the following techniques: 1) HE and IHC staining using markers for PCa cells (e.g., AR, PSA, CK8, CK18, CK5, p63, and Racemase); 2) DNA finger printing to identify their origin (105); 3) an array-based genome-wide analysis (aCGH) to investigate if the reconstituted tumors maintains the same genetic background of their parental patient tumors; 4) Fluorescence *in Situ* Hybridization (FISH) break-apart assay to test if the PCa specific genetic abnormality, *TMPRESS2-ERG* gene fusion, exists in the regenerated tumor (167). Finally, we expect to see that, with this modified protocol, primary HPCa cells will re-initiate serially transplantable tumors in immunodeficient mice, providing us with a reliable in vivo model to study PCSCs in human patient samples.

Chapter 4

The study on the cell of origin for castration-resistant prostate cancer (CRPC)

4.1. Introduction

As mentioned in Chapter 1, many patients who have advanced PCa (GS 9/10) will initially remain as androgen-dependent PCa (ADPC) and respond well to the ADT, manifested by tumor regression. However, tumors will eventually recur and develop into CRPC, which is incurable, metastatic and lethal (also known as AIPC). The etiology of this process is not clearly understood, but many studies have implicated AR in CRPC development.

4.1.1. Natural process of androgen action

Both normal and cancerous prostatic cells need androgen to grow and survive. Testosterone is the most abundant circulating androgen, and it is secreted mainly from the testis, with a minor portion coming from the adrenal glands (2). Free testosterone circulates primarily in the blood, and when it enters the prostate, 5α-reductase converts the majority of free testosterone (>90%) into the more active dihydrotestosterone (DHT), which bears high affinity for AR binding.

AR, a nuclear hormone receptor, has several domains, including a NH2-terminal transcription activation domain, a DNA-binding domain, a hinge region, and a carboxy-terminal ligand binding domain (46). As shown in Figure 4-1, in the basal level, AR binds to heat-shock protein (HSP) to prevent its binding to target genes. Once AR binds to androgen, it will lead to a conformational change in the AR, resulting in the dissociation from HSP and AR phosphorylation. The phosphorylated AR dimerizes and binds to the androgen-response elements in the promoter regions of their target genes, forming an AR complex. The AR complex then recruits co-activators and co-repressors to further mediate AR complex

interaction with the general transcription apparatus to regulate target gene transcription (190, 191).

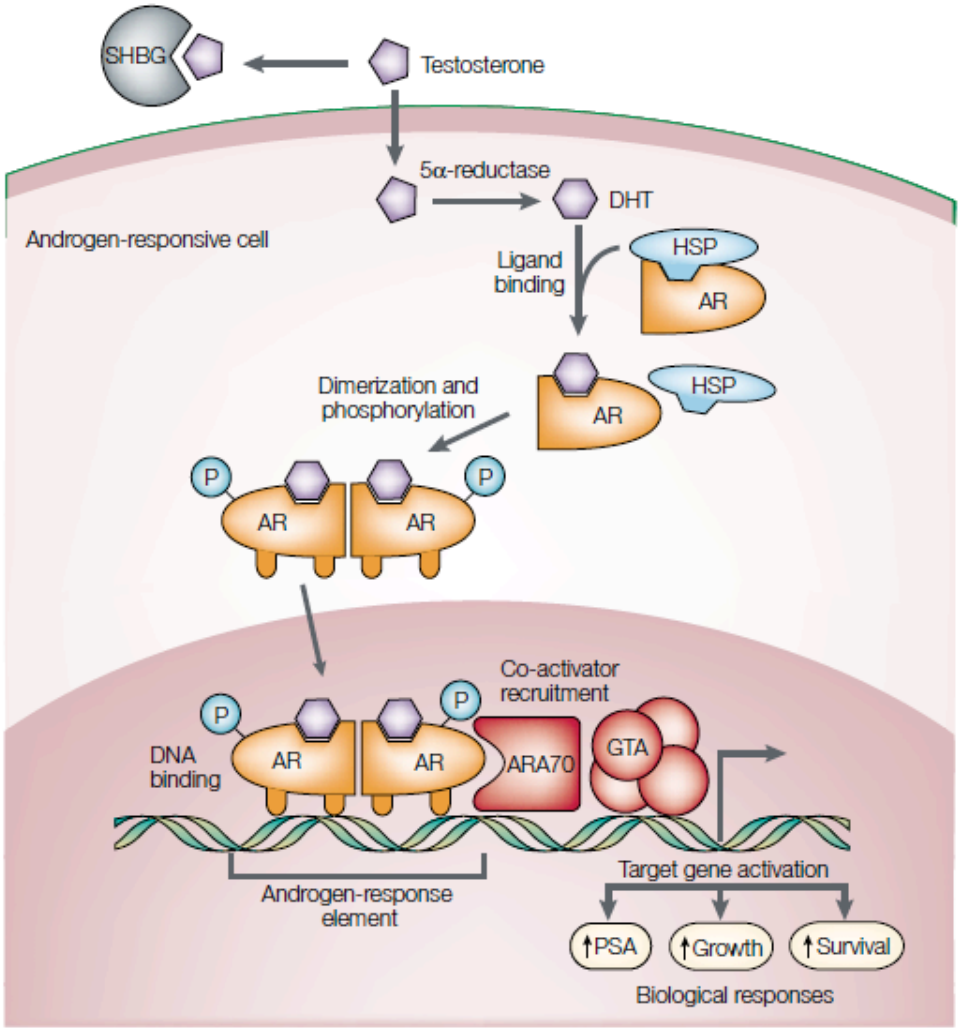

Figure 4-1. Androgen action. Taken from (46) with permission from Nature Publishing Group.

4.1.2. Mechanisms of CRPC development

Several mechanisms have been proposed to be responsible for CRPC development (46). *First,* AR may become highly sensitive to low levels of androgen via AR amplification, increased protein stability, or increased levels of circulating androgen. For example, it has been reported that ~30% of CRPC have an amplified AR gene copy number (192, 193), and another 10%-30% have mutations of AR resulting in increased AR protein stability and sensitivity (194). *Second*, AR mutation is common, and the resultant AR has decreased sensitivity and can be stimulated by non-androgen hormones and androgen antagonists (46). For instance, it has been shown that LNCaP cells have a missense mutation of the AR gene, leading to high levels of AR. Because of this, the androgen antagonist flutamide can activate AR in LNCaP cells to promote their proliferation (195). *Third,* like other steroid hormone receptors, AR can be activated via ligand-independent pathways. For example, a *PTEN* deletion in PCa may lead to upregulation of the PI3K/AKT pathway and the phosphorylation and activation of AR. In addition, growth factors (i.e., IGF-1, EGF and KGF) and receptor tyrosine kinases (i.e., HER-2/neu) can also activate the AR in different androgen independent mechanisms (46). *Fourth,* it is possible that other pathways independent of AR may be activated in CRPC. For example, AKT activated by loss of *PTEN* can bypass AR and further inactivate some pro-apoptotic proteins (i.e., BAD and procaspase-9) by phosphorylation (196). *Fifth,* pre-existing castration-resistant PCa cells may play a vital role for the development of CRPC, which bears SC properties. For example, as mentioned in Chapter 1, it has been shown that CARNs represent a cell of origin for PCa and it has been postulated that CARNs in prostate tumors may feature CSC characteristics (2, 21, 38).

Finally, there have been other proposed mechanisms, some of which include enhanced inflammatory reactions (197, 198), and increased expression levels of neuropeptides (199).

4.1.3. Current studies of castration-resistant prostate cancer stem cells (CaRP- CSCs)

Of all the proposed mechanisms discussed above, the concept of CaRP-CSCs is perhaps the most interesting although the identification of such cells has not been reported. The abundance of N-cadherin^{+} cells and the expression levels of N-cadherin are significantly higher in CRPC xenografts, compared to the levels in their isogenic ADPC xenografts (200). Also, N-cadherin is highly expressed in metastatic patient samples. In addition, ectopic expression of N-cadherin in ADPC cells (i.e., LNCaP, MDA-PCa-2b, and LAPC4) greatly increases their castration resistance and invasiveness as well as metastatic potentials, and specific monoclonal antibodies against N-cadherin can significantly delay CRPC progression (200). This data suggests that N-cadherin may play an intimate role in regulating CRPC development, and that N-cadherin^{+} CRPC cells may be enriched in CaRP-CSCs, although further study is needed to test this latter suggestion. A recent report has shown that the expression levels of the cell surface maker CD166 are highly upregulated in both WT mouse prostatic cells after castration and human CRPC samples. Moreover, LSC^{hi}CD166^{hi} cells from a *PTEN* null PCa model have significantly increased tumor sphere-forming abilities, compared to the other isogenic cells (201), indicating that CD166^{hi} cells may be enriched in PCSCs that are resistant to castration. In addition, our recent study has shown that PSA$^{-/lo}$ PCa cells are more clonal, clonogenic and tumorigenic than the isogenic PSA^{+} PCa cells (98) in androgen-deprived conditions, suggesting that PSA$^{-/lo}$ PCa cells likely represent a subpopulation of stem cell-like cells that are able to initiate CRPC.

To further enrich CaRP-CSCs in the $PSA^{-/lo}$ PCa cells, we performed a cDNA microarray analysis comparing $PSA^{-/lo}$ and isogenic PSA^{+} LAPC9 PCa cells, and observed that dozens of developmental and (cancer) stem cell markers are highly expressed in $PSA^{-/lo}$ cells, including *Nanog, Bcl-2, KIT, ALDH1A1, CD44, integrin α2, SOX12*, etc (98). Among these genes, we were particularly interested in *ALDH1A1, CD44* and *integrin α2,* each of which has been reported to be preferentially expressed in PCSCs (85, 87, 91, 93). Therefore, we used the combinatorial markers to purify $ALDH^{+}CD44^{+}\alpha2\beta1^{+}$ PCa cells from different models, and tested their castration-resistant properties *in vitro* and *in vivo*. We <u>*hypothesized*</u> that $ALDH^{+}CD44^{+}\alpha2\beta1^{+}$ PCa cells represent a population of CaRP-CSCs.

4.2. Materials and Methods

Basic procedures have been described in earlier reports (96, 98) and Chapter 3.

Establishment of androgen dependent (AD) and androgen independent (AI) tumor lines

As shown in Figure 4-2, the AD xenograft tumors (i.e., LAPC9 AD) were generated by injection of the original xenograft tumor cells or cultured cells into intact immunodeficient mice (i.e., NOD/SCID) supplemented with testosterone pellets (TP), in which the majority of AD PCa cells are PSA positive (>90% PSA^+). Simultaneously, the AI xenograft tumors (i.e., LAPC9 AI) were reconstituted by injection of the same original tumor cells into castrated immunodeficient mice supplemented with bicalutamide. This process was repeated at each generation.

FACS analysis/sorting and purification of $ALDH^+CD44^+\alpha2\beta1^+$ cells

Single PCa cells were obtained from xenograft tumors (AD and AI) and primary HPCa samples. These cells were then treated with FcR blocking agent for 10 min at 4°C, and stained with a primary mouse anti-human antibody against α2β1 (MAB1998Z, Millipore) for 30 min at 4°C followed by an APC conjugated goat anti-mouse IgG secondary antibody (550826, BD Bioscience) for 30 min at 4°C. Cells were then washed with PBS three times and incubated with a PE conjugated mouse anti-human CD44 antibody (555479, BD Pharmingen) and a biotinylated mouse H-2K[d] antibody for 30 min at 4°C. Cells were then washed with PBS and labeled with Alexa Fluor 405 conjugated streptavidin (Invitrogen, S-32351) for 10 min at 4°C. Subsequently, cells were washed three times and treated with the ALDEFLUOR assay kit (01700, Stem Cell Technology, Vancouver, Canada) according to

the manufacturers' protocol (68, 81, 98). In brief, PCa cells were suspended in ALDEFLUOR assay buffer containing ALDEFLUOR substrate with or without the ALDH specific inhibitor DEAB for 40 min at 37°C. As a result, the substrate is converted to a green fluorescent product by ALDH, and detected by FACS in the FITC channel. The stained PCa cells were then washed with PBS twice and re-suspended in cold ALDEFLUOR assay buffer. Finally, PCa cells were stained with propidium iodide (PI) to determine viability before FACS analysis.

Sphere-Formation Assays

Purified $ALDH^{+}CD44^{+}\alpha2\beta1^{+}$ PCa cells were plated in 6-well ULA plates containing CDSS medium at the density of 5,000–10,000 cells/well depending on cell type. Spheres were scored after ~2-4 weeks. For serial sphere-formation assays, the first-generation spheres were harvested with 0.025% trypsin/EDTA, triturated with a 27-G needle, filtered through a 40-μm strainer, and replated as above. This process was repeated for up to 3 generations.

Western blot

Whole cell lysates were prepared in complete RIPA buffer containing a protease inhibitor mixture. Protein concentrations were determined by MicroBCA kit (Pierce). Various amounts of proteins were loaded on a 15% SDS-PAGE gel. A standard western blot was performed using ECL Plus (PerkinElmer). Primary antibodies included: mouse mAb to AR (sc7305, Santa Cruz), mouse mAb to PSA (sc7316, Santa Cruz) and rabbit pAb β-actin (4967, Cell Signaling).

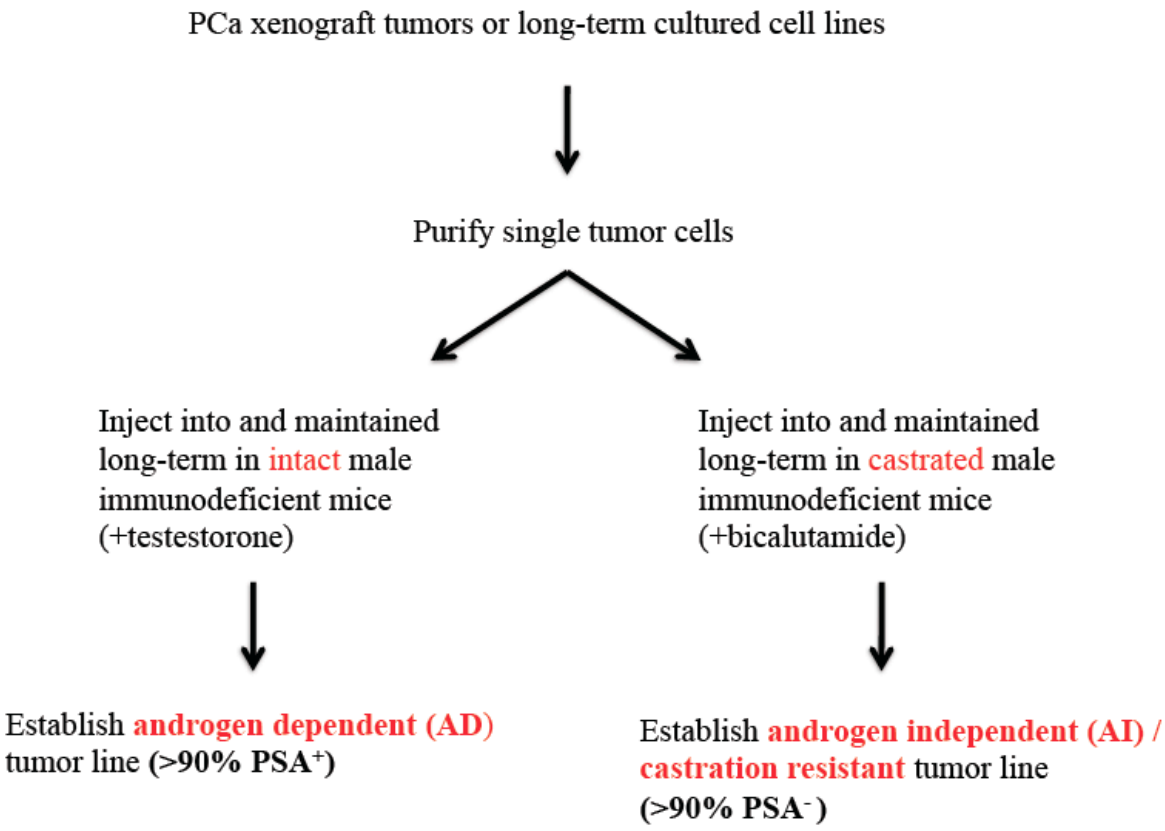

Figure 4-2. Experimental scheme for establishing AD and AI xenograft tumor lines.

4.3. Preliminary Results

The abundance of $ALDH^+CD44^+\alpha2\beta1^+$ PCa cells is significantly higher in androgen independent tumor lines

We have successfully established different pairs of AD and AI PCa xenograft tumor lines, including: LAPC9 AD and AI, LAPC4 AD and AI, LNCaP AD and AI, HPCa101 AD and AI, HPCa70 AD and AI, etc. To determine the expression levels of the triple markers ($ALDH^+CD44^+\alpha2\beta1^+$ or TM^+), we performed a FACS analysis on LAPC9 AD and AI tumor cells. We have reproducibly found that LAPC9 AI tumors contain significantly more TM^+ PCa cells (~18.5%) than the corresponding AD tumors (~2.2%), as shown in Figure 4-3. Similarly, ~0.02% LNCaP AI tumor cells are triple-marker positive, whereas only ~0.002% LNCaP AD tumor cells are positive for these markers. In addition, a similar pattern can be detected in HPCa101 tumor cells, i.e., ~0.003% AD tumor cells and ~0.2% AI tumor cells are triple-marker positive. Furthermore, we have consistently found that subsets of TM^+ PCa cells in two other well-known AI PCa lines, Du145 and PC3, in which TM^+ cells are ~8.8% and ~11.6%, respectively. Taken together, this data suggests that a subpopulation of PCa cells, manifested as $ALDH^+CD44^+\alpha2\beta1^+$ PCa cells, become enriched after androgen deprivation.

$ALDH^+CD44^+\alpha2\beta1^+$ LAPC9 PCa cells possess long-term tumor-initiating capacity in castrated male mice and have sphere-forming abilities in androgen-deprived conditions

To characterize whether $ALDH^+CD44^+\alpha2\beta1^+$ PCa cells are CaRP-CSCs, we purified $ALDH^+CD44^+\alpha2\beta1^+$ and isogenic $ALDH^-CD44^-\alpha2\beta1^-$ (TM^-) PCa cells from LAPC9 AI

tumors, and tested their tumor-initiating capacities in the fully castrated mice (castration + bicalutamide) using limiting-dilution assay (98). As shown in Figure 4-4, at the 1st generation, TM^+ LAPC9 AI cells were significantly more tumorigenic than TM^- LAPC9 AI cells. For example, TM^+ LAPC9 AI cells, in a cell dose dependent manner, could initiate tumor development with as few as 10 cells, whereas TM^- LAPC9 AI cells could only regenerate tumors at the injection of 10,000 cells. Furthermore, the TM^+ LAPC9 AI cells showed a TIF of ~1/448, while TM^- LAPC9 AI cells showed a TIF of ~1/21,298, suggesting that TM^+ have ~48-fold enrichment of tumor-initiating ability compared to TM^- cells in fully castrated hosts. Interestingly, a similar pattern could be observed in later generations of LAPC9 AI tumors, and the abundance of TM^+ cells was consistent during serial transplantations, suggesting that TM^+ cells can self-renew *in vivo*. To further examine if TM^+ cells are the most tumorigenic among all subpopulations, we sorted out TM^+ and TM^+-depleted LAPC9 AI cells and again determined their tumor-initiating capacities in castrated mice. Remarkably, the TM^+ LAPC9 AI cells were also more tumorigenic than the TM^+-depleted cells (Figure 4-5).

To test the clonogenicity of TM^+ cells, we used sphere formation assays. When purifying TM^+ and TM- LAPC9 AI cells, we plated them in 6-well ultra-low attachment plates. In ~2 weeks, we observed that TM^+ cells could form more and larger spheres than TM^- cells. Furthermore, a similar pattern could be detected in serially formed spheres (Figure 4-6).

Primary prostate tumors contain $ALDH^+CD44^+\alpha2\beta1^+$ PCa cells

To extend our work to primary PCa cells, we obtained ~10 patient samples, from GS6 to GS9 (2 GS6, 5 GS7 and 3 GS9) (Table 4-1). We consistently observed that each sample contains a subset of cells that are triple-marker positive. However, we have not yet found any correlation between the abundance of primary TM^+ PCa cells and tumor grade. Our functional characterizations are ongoing.

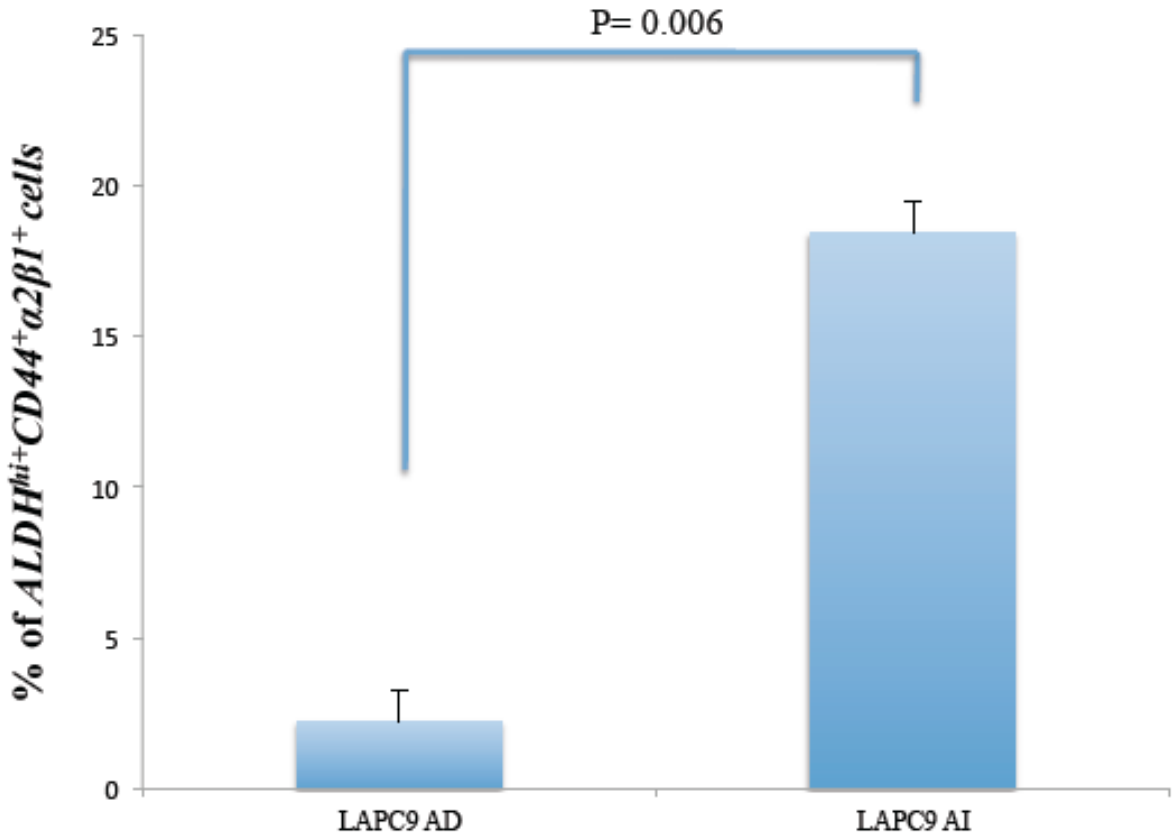

Figure 4-3. Abundance of ALDH$^+$CD44$^+$α2β1$^+$ cells in LAPC9 AD and AI tumors.

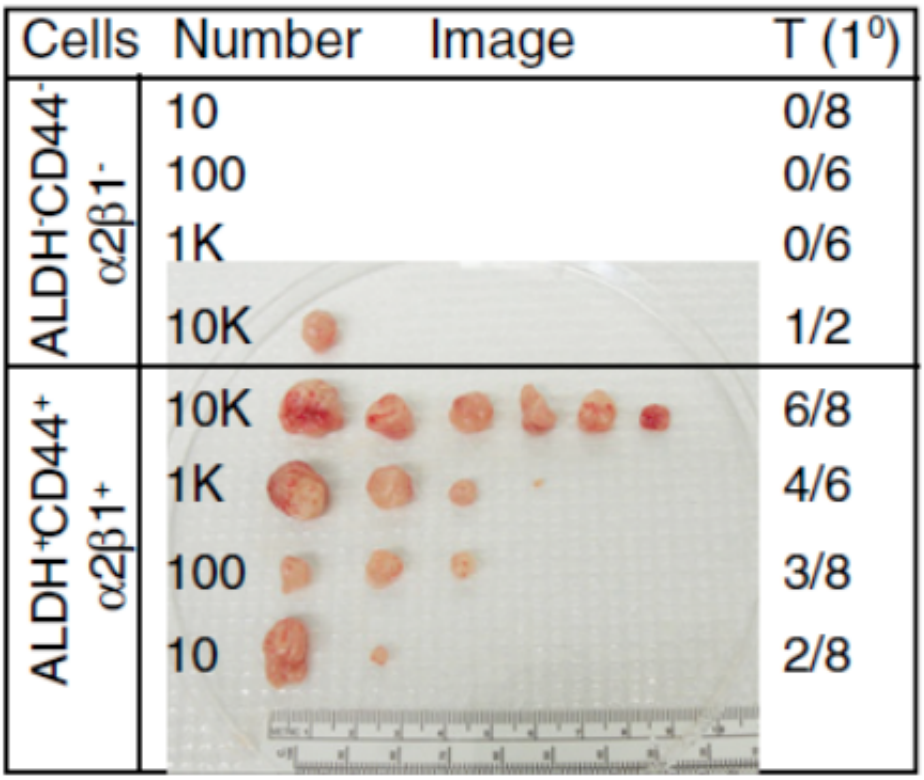

Figure 4-4. ALDH$^+$CD44$^+$α2β1$^+$ LAPC9 AI cells were significantly more tumorigenic than the isogenic ALDH$^-$CD44$^-$α2β1$^-$ cells. Triple marker-positive and -negative LAPC9 cells were purified from AI tumors and reimplanted at the indicated cell doses in fully castrated NOD/SCID mice. Adapted from (98) with permission from Elsevier.

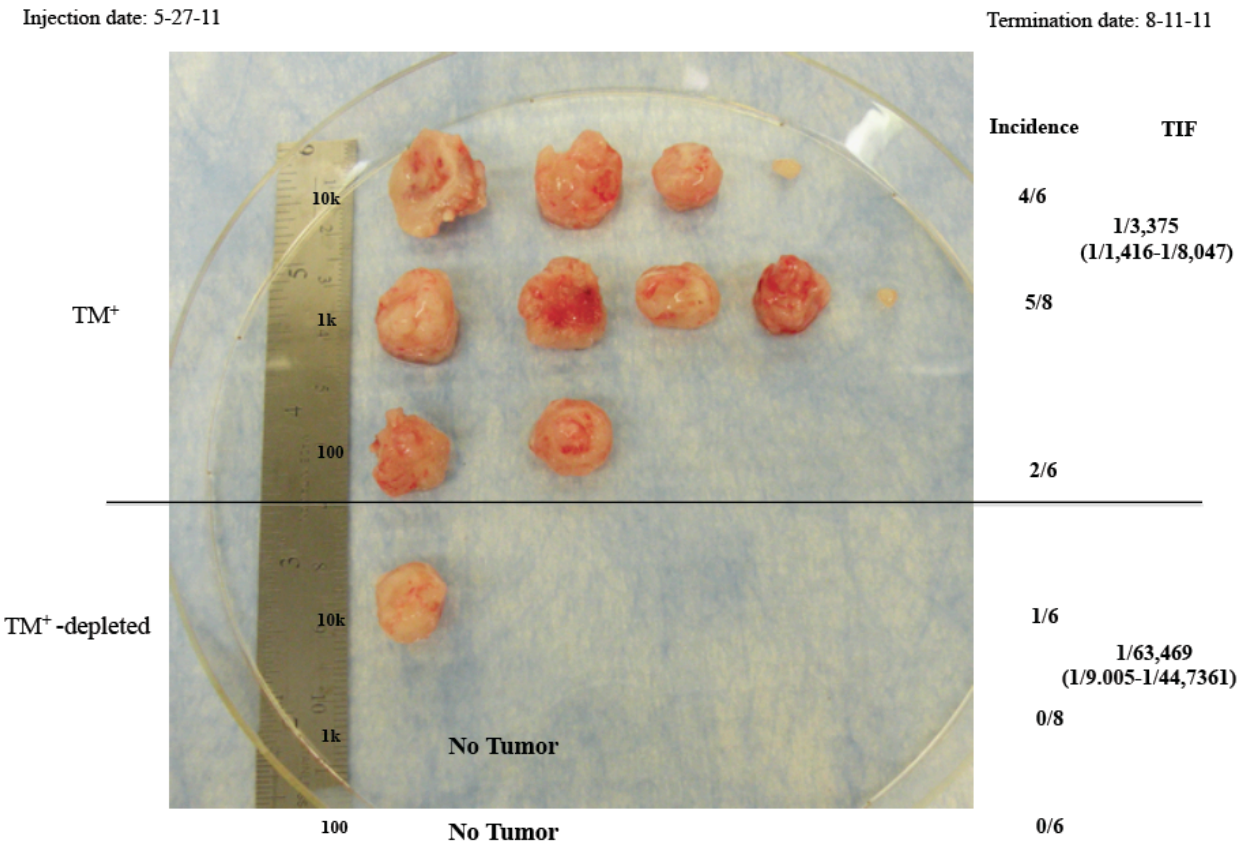

Figure 4-5. TM^+ LAPC9 AI cells were significantly more tumorigenic than the isogenic TM^+- depleted cells.

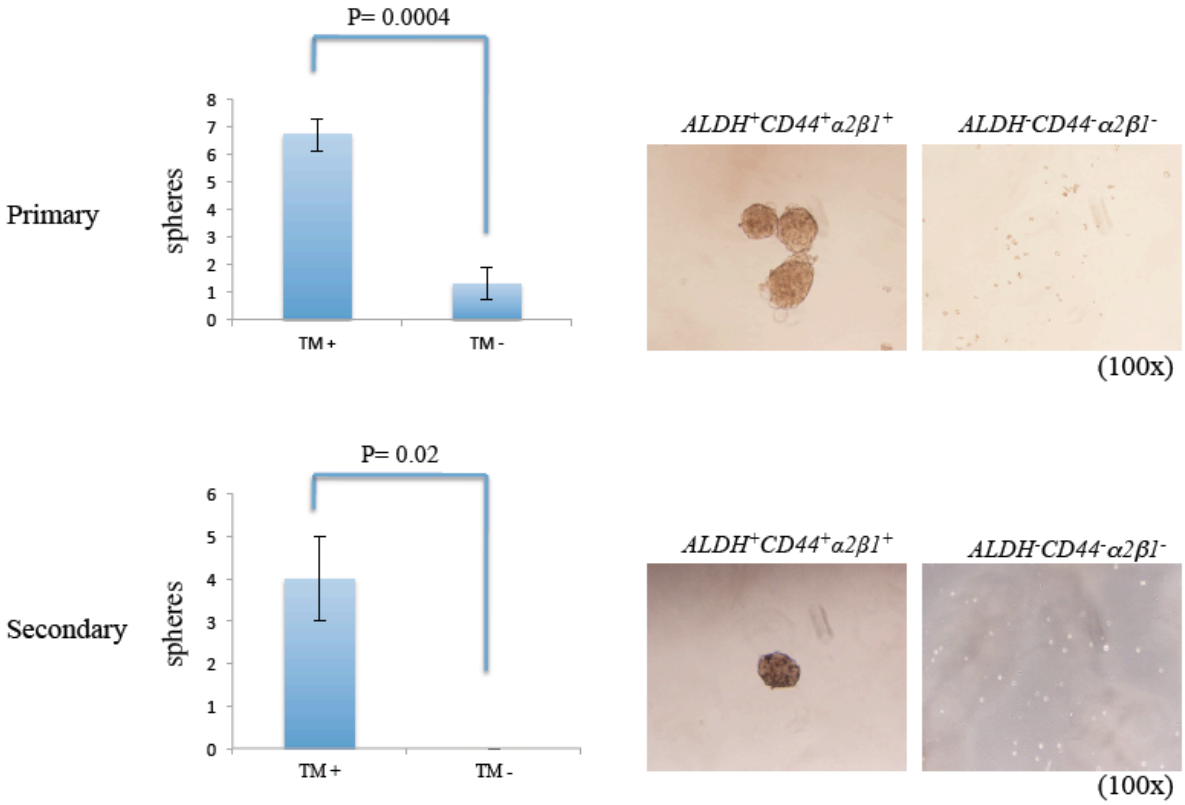

Figure 4-6. Characterization of clonogenicity of both TM^+ and TM^- LAPC9 AI cells using sphere formation assays.

HPCa sample	Age	Gleason	$ALDH^+$ (%)	$CD44^+\alpha2\beta1^+$ (%)	TM+ (%)
HPCa114	59	9 (5+4)	21.9	59.4	12.5
HPCa121	60	9 (5+4)	5.5	2.0	0.11
HPCa123	62	7 (3+4)	10.7	6.6	0.71
HPCa130	63	6 (3+3)	12.9	16.5	2.1
HPCa133	55	6 (3+3)	30.9	19.7	6.1
HPCa134	65	7 (4+3)	23.8	16.8	4.0
HPCa135	65	7 (3+4)	0.04	7.5	0.003
HPCa137	58	9 (5+4)	34.4	8.1	2.8
HPCa141	71	7 (3+4)	14.4	0.006	0.001
HPCa142	56	7 (3+4)	57	80.8	46.1

Table 4-1. Triple marker analysis in purified primary prostate cancer cells.

4.4. Future Studies

Our preliminary data has shown the presence of $ALDH^+CD44^+\alpha2\beta1^+$ (TM^+) PCa cells in long-term cultured cell lines, androgen-independent xenograft tumors, and untreated primary HPCa specimens. One of the most important facets of these TM^+ PCa cells is our finding that they are more clonogenic and tumorigenic than the other isogenic subpopulations of PCa cells in androgen deficient conditions. For our future studies, we plan to further phenotypically identify and functionally characterize CaRP-CSCs.

First, we will examine the expression levels of triple markers in primary CRPC patient samples. To achieve this, we will obtain paraffin-embedded tissue microarrays containing tissues of normal prostate (n=44), androgen-dependent PCa (n=98), and castration resistant PCa (n=230) from Dr. Arul Chinnaiyan (University of Michigan) (202). We will use these samples to perform multi-color immunofluorescent staining in tissue microarrays using primary antibodies against ALDH, CD44 and α2β1, followed by different fluorophore-conjugated secondary antibodies. Images will be captured by a Zeiss confocal microscope (81).

Second, we will further characterize stem cell-related properties of TM^+ PCa cells in CRPC xenograft models. Because fresh primary CRPC patient samples are very limited, we will use early-passage CRPC xenograft models to mimic clinical PCa progression and complete the assays listed below.

1) FACS analysis of the abundance of TM^+ PCa cells: Currently, our preliminary data has focused on the LAPC9 model, and we will now extend our functional studies to other CRPC xenografts. We will perform a FACS analysis on single PCa cells from pairs of AD and AI tumors as well as CRPC cell lines to determine the relative abundance of TM^+

PCa cells among all these models. The samples will additionally be screened by western blot to determine the expression levels of the various markers. We expect that AI PCa (CRPC/AIPC) will contain significantly more TM^+ PCa cells than AD PCa (ADPC) (as shown in LAPC9). After screening our samples, we believe that we will be able to identify other 1-2 AI PCa models (other than LAPC9 AI) for our *in vitro* and *in vivo* characterizations.

2) *In vitro* characterization of SC properties: We will purify TM^+ and TM^- cells from the above selected CRPC xenografts, and test their self-renewal capacity using a serial sphere-formation assays in androgen deficient conditions (CDSS medium plus bicalutamide). Furthermore, both TM^+ and TM^- AI cells will be tested for their clonal and proliferative capacity using clonal assays and BrdU incorporation assays (85, 96, 98) in CDSS medium plus bicalutamide. In addition, we will treat TM^+ and TM^- AI cells with commonly used therapeutic drugs for PCa (e.g., etoposide and paclitaxel) to examine their drug-tolerant potentials.

3) *In vivo* characterization of SC properties: Freshly purified TM^+ and TM^- cells of the selected CRPC xenografts will be tested for their tumor-initiating capacities via LDA and serial tumor transplantation assays in fully castrated mice. Tumor incidence, latency, tumor volume, and endpoint tumor weight will be monitored twice a week starting from the second week. In addition, we will perform LRC experiments using BrdU pulse-chase assays (98) to determine the quiescence of TM^+ and TM^- PCa AI cells. Based on our preliminary studies, we predict that TM^+ PCa AI cells are more quiescent, clonal, clonogenic, tumorigenic and drug-tolerant than isogenic TM^- PCa AI cells.

Third, we will study the underlying molecular mechanisms that regulate $ALDH^+CD44^+\alpha2\beta1^+$ HPCa cells in CRPC. Global transcriptional profiling using microarray analysis will be performed on TM^+ and TM^- CRPC cells. Gene Ontology (GO) analysis will be employed to assign differentially expressed genes into distinct functional categories, including developmental and (cancer) stem cell molecules/markers, cell cycle, transcription/nuclear factors, cell survival/death, etc. We will be particularly interested in (cancer) stem cell-related genes based on our preliminary data that TM^+ PCa AI cells have SC properties. We will select several genes that are significantly *upregulated* in TM^+ cells compared to TM^- cells, which have been identified in the literature as having potential roles in PCa progression. *Next*, qPCR will be used to validate microarray data of the selected SC-related molecules. *Subsequently*, to obtain a better understanding of how these molecules potentially regulate CRPC development, a lentiviral-mediated gene knockdown of these molecules will be performed in TM^+ cells. Serial sphere-formation and LDA assays will be employed to characterize their CSC properties in androgen deficient conditions. In a reciprocal experiment to further confirm the gene knockdown results, a lentiviral-mediated gene overexpression of these molecules will be conducted in TM^- cells, followed by characterization of their CSC functions *in vitro* and *in vivo* in androgen deficient conditions. We believe that these experiments will allow us to narrow our selection to 2-3 SC-related molecules, which have the most significant phenotype after knockdown and/or overexpression experiments. *Finally*, to uncover the involvement of our selected SC-related molecules in CRPC progression at a global molecular level, a chromatin immunoprecipitation sequencing (ChIP-Seq) analysis in both TM^+ and TM^- CRPC cells will be performed on 3 histone marks, i.e., H3K4me1, H3K4me3, and H3K27me3. By

combining the genome-wide protein-DNA binding profiles and IPA software (Ingenuity Systems), we will be able to analyze a group of genes or signaling pathways that are potentially regulated by our selected SC-related molecules. After we complete the proposed studies, we should have a better understanding of how the selected SC-related molecules regulate CRPC. Our lab is currently optimizing our ChIP-Seq protocols by using FACS sorted cells, which will facilitate this study in the future.

Chapter 5

Conclusion and Perspective

Ever since Dr. John Dick and his colleagues reported the first CSC population in AML, the concept of CSCs has flourished and been widely tested in different tumor systems (4, 6-8, 51). It has been demonstrated that PCa contains distinct subsets of PCSCs that may play a role in PCa initiation and progression. Understanding and molecularly dissecting the PCSCs may help us to elucidate the etiology of PCa and uncover the molecular mechanisms responsible for its androgen-independent progression.

Although we have made significant progress in the study of PCSCs, there are several critical issues to be resolved, some of which have been studied and presented in this dissertation. Firstly, it is not fully known whether PCSCs are therapy-resistant. In Chapter 2, we have shown that several cancer cell lines (i.e., Du145, DLD1 and UC14) chronically treated by anti-cancer drugs generate drug-tolerant cancer cells (DTCs). Surprisingly, these DTCs show greatly reduced tumor-initiating capacities and clonogenic abilities, which are contrary to the general assumption that CSCs are drug-resistant and, *vice versa*, DTCs possess CSC properties. In drug-tolerant Du145 cells, we have further demonstrated that the reduced CSC activity is associated with the depletion of cancer stem/progenitor cells (i.e., $CD44^+$ cells in our study) after chronic treatment of cells with chemotherapeutic drugs (e.g., etoposide and taxanes), which further substantiates the importance of CD44 in PCa. In addition, we have provided evidence that the drug-tolerant phenotype is reversible, indicating some epigenetic regulations may be involved. Secondly, it remains unanswered whether primary patient PCa samples also contain PCSCs because the relevant tumor experiments are lacking. It is well known that establishing HPCa development in immunodeficient mice using single patient cells is extremely challenging. In Chapter 3, we have employed three different stromal cells (rUGM, CAFs and Hs5) and two

immunodeficient mouse strains (NOD/SCID and NSG) in many of the 114 patient samples, to establish a reliable system that allows us to reproducibly reconstitute HPCa development in immunodeficient mice using single patient tumor cells. Our results have shown that coinjection of primary HPCa cells with immortalized Hs5 bone marrow derived stromal cells in NSG mice can generate undifferentiated tumors, providing indirect evidence that it is possible that undifferentiated PCa cells are responsible for tumor formation. Finally, most advanced PCa patients will progress from ADPC to CRPC even after tumor regression by ADT, and the exact mechanisms responsible are not completely understood. Herein, we have shown preliminary evidence that the $ALDH^{+}CD44^{+}\alpha2\beta1^{+}$ (TM^{+}) PCa cells possess CSC properties in androgen deficient conditions, and they may represent a cell-of-origin for CRPC.

Future studies will be needed to further characterize PCSCs in primary patient samples with improved techniques and optimized protocols in suitable systems, and it will also be meaningful to have a better understanding of the functional roles of PCSCs in PCa progression, therapy resistance and metastasis. The success of these projects will undoubtedly facilitate future drug development targeting PCSCs more efficiently and effectively, and ultimately benefiting PCa patients.

BIBLIOGRAPHY

1. Siegel, R., D. Naishadham, and A. Jemal. 2012. Cancer statistics, 2012. CA Cancer J Clin 62:10-29.
2. Shen, M. M., and C. Abate-Shen. 2010. Molecular genetics of prostate cancer: new prospects for old challenges. Genes Dev 24:1967-2000.
3. Clarke, M. F., J. E. Dick, P. B. Dirks, C. J. Eaves, C. H. Jamieson, D. L. Jones, J. Visvader, I. L. Weissman, and G. M. Wahl. 2006. Cancer stem cells--perspectives on current status and future directions: AACR Workshop on cancer stem cells. Cancer Res 66:9339-9344.
4. Clevers, H. 2011. The cancer stem cell: premises, promises and challenges. Nat Med 17:313-319.
5. Magee, J. A., E. Piskounova, and S. J. Morrison. 2012. Cancer stem cells: impact, heterogeneity, and uncertainty. Cancer Cell 21:283-296.
6. Reya, T., S. J. Morrison, M. F. Clarke, and I. L. Weissman. 2001. Stem cells, cancer, and cancer stem cells. Nature 414:105-111.
7. Tang, D. G. 2012. Understanding cancer stem cell heterogeneity and plasticity. Cell Res 22:457-472.
8. Visvader, J. E., and G. J. Lindeman. 2012. Cancer stem cells: current status and evolving complexities. Cell Stem Cell 10:717-728.
9. McNeal, J. E. 1969. Origin and development of carcinoma in the prostate. Cancer 23:24-34.
10. McNeal, J. E. 1981. The zonal anatomy of the prostate. Prostate 2:35-49.
11. McNeal, J. E. 1988. Normal histology of the prostate. Am J Surg Pathol 12:619-633.

12. Berquin, I. M., Y. Min, R. Wu, H. Wu, and Y. Q. Chen. 2005. Expression signature of the mouse prostate. J Biol Chem 280:36442-36451.

13. Abate-Shen, C., and M. M. Shen. 2000. Molecular genetics of prostate cancer. Genes Dev 14:2410-2434.

14. Li, H., and D. G. Tang. 2011. Prostate cancer stem cells and their potential roles in metastasis. J Surg Oncol 103:558-562.

15. Tang, D. G., L. Patrawala, T. Calhoun, B. Bhatia, G. Choy, R. Schneider-Broussard, and C. Jeter. 2007. Prostate cancer stem/progenitor cells: identification, characterization, and implications. Mol Carcinog 46:1-14.

16. Signoretti, S., D. Waltregny, J. Dilks, B. Isaac, D. Lin, L. Garraway, A. Yang, R. Montironi, F. McKeon, and M. Loda. 2000. p63 is a prostate basal cell marker and is required for prostate development. Am J Pathol 157:1769-1775.

17. Liu, A. Y., L. D. True, L. LaTray, P. S. Nelson, W. J. Ellis, R. L. Vessella, P. H. Lange, L. Hood, and G. van den Engh. 1997. Cell-cell interaction in prostate gene regulation and cytodifferentiation. Proc Natl Acad Sci USA 94:10705-10710.

18. Bhatia, B., S. Tang, P. Yang, A. Doll, G. Aumueller, R. A. Newman, and D. G. Tang. 2005. Cell-autonomous induction of functional tumor suppressor 15-lipoxygenase 2 (15-LOX2) contributes to replicative senescence of human prostate progenitor cells. Oncogene 24:3583-3595.

19. Fuchs, E., and V. Horsley. 2011. Ferreting out stem cells from their niches. Nat Cell Biol 13:513-518.

20. Li, L., and H. Clevers. 2010. Coexistence of quiescent and active adult stem cells in mammals. Science 327:542-545.

21. Wang, Z. A., and M. M. Shen. 2011. Revisiting the concept of cancer stem cells in prostate cancer. Oncogene 30:1261-1271.

22. Cotsarelis, G., S. Z. Cheng, G. Dong, T. T. Sun, and R. M. Lavker. 1989. Existence of slow-cycling limbal epithelial basal cells that can be preferentially stimulated to proliferate: implications on epithelial stem cells. Cell 57:201-209.

23. Zhou, S., J. D. Schuetz, K. D. Bunting, A. M. Colapietro, J. Sampath, J. J. Morris, I. Lagutina, G. C. Grosveld, M. Osawa, H. Nakauchi, and B. P. Sorrentino. 2001. The ABC transporter Bcrp1/ABCG2 is expressed in a wide variety of stem cells and is a molecular determinant of the side-population phenotype. Nat Med 7:1028-1034.

24. Goodell, M. A., K. Brose, G. Paradis, A. S. Conner, and R. C. Mulligan. 1996. Isolation and functional properties of murine hematopoietic stem cells that are replicating in vivo. J Exp Med 183:1797-1806.

25. Storms, R. W., A. P. Trujillo, J. B. Springer, L. Shah, O. M. Colvin, S. M. Ludeman, and C. Smith. 1999. Isolation of primitive human hematopoietic progenitors on the basis of aldehyde dehydrogenase activity. Proc Natl Acad Sci USA 96:9118-9123.

26. Kastan, M. B., E. Schlaffer, J. E. Russo, O. M. Colvin, C. I. Civin, and J. Hilton. 1990. Direct demonstration of elevated aldehyde dehydrogenase in human hematopoietic progenitor cells. Blood 75:1947-1950.

27. Pastrana, E., V. Silva-Vargas, and F. Doetsch. 2011. Eyes wide open: a critical review of sphere-formation as an assay for stem cells. Cell Stem Cell 8:486-498.

28. English, H. F., R. J. Santen, and J. T. Isaacs. 1987. Response of glandular versus basal rat ventral prostatic epithelial cells to androgen withdrawal and replacement. Prostate 11:229-242.

29. Lawson, D. A., and O. N. Witte. 2007. Stem cells in prostate cancer initiation and progression. J Clin Invest 117:2044-2050.

30. Tsujimura, A., Y. Koikawa, S. Salm, T. Takao, S. Coetzee, D. Moscatelli, E. Shapiro, H. Lepor, T. T. Sun, and E. L. Wilson. 2002. Proximal location of mouse prostate epithelial stem cells: a model of prostatic homeostasis. J Cell Biol 157:1257-1265.

31. Cunha, G. R., and B. Lung. 1978. The possible influence of temporal factors in androgenic responsiveness of urogenital tissue recombinants from wild-type and androgen-insensitive (Tfm) mice. J Exp Zool 205:181-193.

32. Burger, P. E., X. Xiong, S. Coetzee, S. N. Salm, D. Moscatelli, K. Goto, and E. L. Wilson. 2005. Sca-1 expression identifies stem cells in the proximal region of prostatic ducts with high capacity to reconstitute prostatic tissue. Proc Natl Acad Sci USA 102:7180-7185.

33. Xin, L., D. A. Lawson, and O. N. Witte. 2005. The Sca-1 cell surface marker enriches for a prostate-regenerating cell subpopulation that can initiate prostate tumorigenesis. Proc Natl Acad Sci USA 102:6942-6947.

34. Lawson, D. A., L. Xin, R. U. Lukacs, D. Cheng, and O. N. Witte. 2007. Isolation and functional characterization of murine prostate stem cells. Proc Natl Acad Sci USA 104:181-186.

35. Goldstein, A. S., D. A. Lawson, D. Cheng, W. Sun, I. P. Garraway, and O. N. Witte. 2008. Trop2 identifies a subpopulation of murine and human prostate basal cells with stem cell characteristics. Proc Natl Acad Sci USA 105:20882-20887.

36. Leong, K. G., B. E. Wang, L. Johnson, and W. Q. Gao. 2008. Generation of a prostate from a single adult stem cell. Nature 456:804-808.

37. Kurita, T., R. T. Medina, A. A. Mills, and G. R. Cunha. 2004. Role of p63 and basal cells in the prostate. Development 131:4955-4964.

38. Wang, X., M. Kruithof-de Julio, K. D. Economides, D. Walker, H. Yu, M. V. Halili, Y. P. Hu, S. M. Price, C. Abate-Shen, and M. M. Shen. 2009. A luminal epithelial stem cell that is a cell of origin for prostate cancer. Nature 461:495-500.

39. Choi, N., B. Zhang, L. Zhang, M. Ittmann, and L. Xin. 2012. Adult murine prostate basal and luminal cells are self-sustained lineages that can both serve as targets for prostate cancer initiation. Cancer Cell 21:253-265.

40. Liu, J., L. E. Pascal, S. Isharwal, D. Metzger, R. Ramos Garcia, J. Pilch, S. Kasper, K. Williams, P. H. Basse, J. B. Nelson, P. Chambon, and Z. Wang. 2011. Regenerated luminal epithelial cells are derived from preexisting luminal epithelial cells in adult mouse prostate. Mol Endocrinol 25:1849-1857.

41. Collins, A. T., F. K. Habib, N. J. Maitland, and D. E. Neal. 2001. Identification and isolation of human prostate epithelial stem cells based on alpha(2)beta(1)-integrin expression. J Cell Sci 114:3865-3872.

42. Richardson, G. D., C. N. Robson, S. H. Lang, D. E. Neal, N. J. Maitland, and A. T. Collins. 2004. CD133, a novel marker for human prostatic epithelial stem cells. J Cell Sci 117:3539-3545.

43. Huss, W. J., D. R. Gray, N. M. Greenberg, J. L. Mohler, and G. J. Smith. 2005. Breast cancer resistance protein-mediated efflux of androgen in putative benign and malignant prostate stem cells. Cancer Res 65:6640-6650.

44. Garraway, I. P., W. Sun, C. P. Tran, S. Perner, B. Zhang, A. S. Goldstein, S. A. Hahm, M. Haider, C. S. Head, R. E. Reiter, M. A. Rubin, and O. N. Witte. 2010. Human prostate sphere-forming cells represent a subset of basal epithelial cells capable of glandular regeneration in vivo. Prostate 70:491-501.

45. Cooperberg, M. R., J. W. Moul, and P. R. Carroll. 2005. The changing face of prostate cancer. J Clin Oncol 23:8146-8151.

46. Feldman, B. J., and D. Feldman. 2001. The development of androgen-independent prostate cancer. Nat Rev Cancer 1:34-45.

47. Kumar-Sinha, C., S. A. Tomlins, and A. M. Chinnaiyan. 2008. Recurrent gene fusions in prostate cancer. Nat Rev Cancer 8:497-511.

48. Tomlins, S. A., D. R. Rhodes, S. Perner, S. M. Dhanasekaran, R. Mehra, X. W. Sun, S. Varambally, X. Cao, J. Tchinda, R. Kuefer, C. Lee, J. E. Montie, R. B. Shah, K. J. Pienta, M. A. Rubin, and A. M. Chinnaiyan. 2005. Recurrent fusion of TMPRSS2 and ETS transcription factor genes in prostate cancer. Science 310:644-648.

49. Dick, J. E. 2008. Stem cell concepts renew cancer research. Blood 112:4793-4807.

50. Nguyen, L. V., R. Vanner, P. Dirks, and C. J. Eaves. 2012. Cancer stem cells: an evolving concept. Nat Rev Cancer 12:133-143.

51. Shackleton, M., E. Quintana, E. R. Fearon, and S. J. Morrison. 2009. Heterogeneity in cancer: cancer stem cells versus clonal evolution. Cell 138:822-829.

52. Nowell, P. C. 1976. The clonal evolution of tumor cell populations. Science 194:23-28.

53. Baylin, S. B., and P. A. Jones. 2011. A decade of exploring the cancer epigenome - biological and translational implications. Nat Rev Cancer 11:726-734.

54. Furth, J. a. K., M. 1937. The transmission of leukemia of mice with a single cell. Am J Cancer 31:276-282.

55. Bruce, W. R., and H. Van Der Gaag. 1963. A Quantitative Assay for the Number of Murine Lymphoma Cells Capable of Proliferation in Vivo. Nature 199:79-80.

56. Clarkson, B., J. Fried, A. Strife, Y. Sakai, K. Ota, and T. Okita. 1970. Studies of cellular proliferation in human leukemia. 3. Behavior of leukemic cells in three adults with acute leukemia given continuous infusions of 3H-thymidine for 8 or 10 days. Cancer 25:1237-1260.

57. Clarkson, B. D. 1969. Review of recent studies of cellular proliferation in acute leukemia. Natl Cancer Inst Monogr 30:81-120.

58. Killmann, S. A., E. P. Cronkite, J. S. Robertson, T. M. Fliedner, and V. P. Bond. 1963. Estimation of phases of the life cycle of leukemic cells from labeling in human beings in vivo with tritiated thymidine. Lab Invest 12:671-684.

59. Pierce, G. B., Jr., F. J. Dixon, Jr., and E. L. Verney. 1960. Teratocarcinogenic and tissue-forming potentials of the cell types comprising neoplastic embryoid bodies. Lab Invest 9:583-602.

60. Lapidot, T., C. Sirard, J. Vormoor, B. Murdoch, T. Hoang, J. Caceres-Cortes, M. Minden, B. Paterson, M. A. Caligiuri, and J. E. Dick. 1994. A cell initiating human acute myeloid leukaemia after transplantation into SCID mice. Nature 367:645-648.

61. Bonnet, D., and J. E. Dick. 1997. Human acute myeloid leukemia is organized as a hierarchy that originates from a primitive hematopoietic cell. Nat Med 3:730-737.

62. Al-Hajj, M., M. S. Wicha, A. Benito-Hernandez, S. J. Morrison, and M. F. Clarke. 2003. Prospective identification of tumorigenic breast cancer cells. Proc Natl Acad Sci USA 100:3983-3988.

63. Notta, F., C. G. Mullighan, J. C. Wang, A. Poeppl, S. Doulatov, L. A. Phillips, J. Ma, M. D. Minden, J. R. Downing, and J. E. Dick. 2011. Evolution of human BCR-ABL1 lymphoblastic leukaemia-initiating cells. Nature 469:362-367.

64. Naka, K., T. Hoshii, T. Muraguchi, Y. Tadokoro, T. Ooshio, Y. Kondo, S. Nakao, N. Motoyama, and A. Hirao. 2010. TGF-beta-FOXO signalling maintains leukaemia-initiating cells in chronic myeloid leukaemia. Nature 463:676-680.

65. Majeti, R., M. P. Chao, A. A. Alizadeh, W. W. Pang, S. Jaiswal, K. D. Gibbs, Jr., N. van Rooijen, and I. L. Weissman. 2009. CD47 is an adverse prognostic factor and therapeutic antibody target on human acute myeloid leukemia stem cells. Cell 138:286-299.

66. Wang, Y., A. V. Krivtsov, A. U. Sinha, T. E. North, W. Goessling, Z. Feng, L. I. Zon, and S. A. Armstrong. 2010. The Wnt/beta-catenin pathway is required for the development of leukemia stem cells in AML. Science 327:1650-1653.

67. Pece, S., D. Tosoni, S. Confalonieri, G. Mazzarol, M. Vecchi, S. Ronzoni, L. Bernard, G. Viale, P. G. Pelicci, and P. P. Di Fiore. 2010. Biological and molecular heterogeneity of breast cancers correlates with their cancer stem cell content. Cell 140:62-73.

68. Ginestier, C., M. H. Hur, E. Charafe-Jauffret, F. Monville, J. Dutcher, M. Brown, J. Jacquemier, P. Viens, C. G. Kleer, S. Liu, A. Schott, D. Hayes, D. Birnbaum, M. S. Wicha, and G. Dontu. 2007. ALDH1 is a marker of normal and malignant human

mammary stem cells and a predictor of poor clinical outcome. Cell Stem Cell 1:555-567.

69. Yu, F., H. Yao, P. Zhu, X. Zhang, Q. Pan, C. Gong, Y. Huang, X. Hu, F. Su, J. Lieberman, and E. Song. 2007. let-7 regulates self renewal and tumorigenicity of breast cancer cells. Cell 131:1109-1123.

70. Singh, S. K., C. Hawkins, I. D. Clarke, J. A. Squire, J. Bayani, T. Hide, R. M. Henkelman, M. D. Cusimano, and P. B. Dirks. 2004. Identification of human brain tumour initiating cells. Nature 432:396-401.

71. Anido, J., A. Saez-Borderias, A. Gonzalez-Junca, L. Rodon, G. Folch, M. A. Carmona, R. M. Prieto-Sanchez, I. Barba, E. Martinez-Saez, L. Prudkin, I. Cuartas, C. Raventos, F. Martinez-Ricarte, M. A. Poca, D. Garcia-Dorado, M. M. Lahn, J. M. Yingling, J. Rodon, J. Sahuquillo, J. Baselga, and J. Seoane. 2010. TGF-beta Receptor Inhibitors Target the CD44(high)/Id1(high) Glioma-Initiating Cell Population in Human Glioblastoma. Cancer Cell 18:655-668.

72. Eyler, C. E., Q. Wu, K. Yan, J. M. MacSwords, D. Chandler-Militello, K. L. Misuraca, J. D. Lathia, M. T. Forrester, J. Lee, J. S. Stamler, S. A. Goldman, M. Bredel, R. E. McLendon, A. E. Sloan, A. B. Hjelmeland, and J. N. Rich. 2011. Glioma stem cell proliferation and tumor growth are promoted by nitric oxide synthase-2. Cell 146:53-66.

73. Bao, S., Q. Wu, R. E. McLendon, Y. Hao, Q. Shi, A. B. Hjelmeland, M. W. Dewhirst, D. D. Bigner, and J. N. Rich. 2006. Glioma stem cells promote radioresistance by preferential activation of the DNA damage response. Nature 444:756-760.

74. O'Brien, C. A., A. Pollett, S. Gallinger, and J. E. Dick. 2007. A human colon cancer cell capable of initiating tumour growth in immunodeficient mice. Nature 445:106-110.

75. Ricci-Vitiani, L., D. G. Lombardi, E. Pilozzi, M. Biffoni, M. Todaro, C. Peschle, and R. De Maria. 2007. Identification and expansion of human colon-cancer-initiating cells. Nature 445:111-115.

76. Todaro, M., M. P. Alea, A. B. Di Stefano, P. Cammareri, L. Vermeulen, F. Iovino, C. Tripodo, A. Russo, G. Gulotta, J. P. Medema, and G. Stassi. 2007. Colon cancer stem cells dictate tumor growth and resist cell death by production of interleukin-4. Cell Stem Cell 1:389-402.

77. Shmelkov, S. V., J. M. Butler, A. T. Hooper, A. Hormigo, J. Kushner, T. Milde, R. St Clair, M. Baljevic, I. White, D. K. Jin, A. Chadburn, A. J. Murphy, D. M. Valenzuela, N. W. Gale, G. Thurston, G. D. Yancopoulos, M. D'Angelica, N. Kemeny, D. Lyden, and S. Rafii. 2008. CD133 expression is not restricted to stem cells, and both CD133+ and CD133- metastatic colon cancer cells initiate tumors. J Clin Invest 118:2111-2120.

78. Collins, A. T., P. A. Berry, C. Hyde, M. J. Stower, and N. J. Maitland. 2005. Prospective identification of tumorigenic prostate cancer stem cells. Cancer Res 65:10946-10951.

79. Gu, G., J. Yuan, M. Wills, and S. Kasper. 2007. Prostate cancer cells with stem cell characteristics reconstitute the original human tumor in vivo. Cancer Res 67:4807-4815.

80. Jeter, C. R., M. Badeaux, G. Choy, D. Chandra, L. Patrawala, C. Liu, T. Calhoun-Davis, H. Zaehres, G. Q. Daley, and D. G. Tang. 2009. Functional evidence that the self-renewal gene NANOG regulates human tumor development. Stem Cells 27:993-1005.

81. Jeter, C. R., B. Liu, X. Liu, X. Chen, C. Liu, T. Calhoun-Davis, J. Repass, H. Zaehres, J. J. Shen, and D. G. Tang. 2011. NANOG promotes cancer stem cell characteristics and prostate cancer resistance to androgen deprivation. Oncogene 30:3833-3845.

82. Li, H., X. Chen, T. Calhoun-Davis, K. Claypool, and D. G. Tang. 2008. PC3 human prostate carcinoma cell holoclones contain self-renewing tumor-initiating cells. Cancer Res 68:1820-1825.

83. Li, H., M. Jiang, S. Honorio, L. Patrawala, C. R. Jeter, T. Calhoun-Davis, S. W. Hayward, and D. G. Tang. 2009. Methodologies in assaying prostate cancer stem cells. Methods Mol Biol 568:85-138.

84. Miki, J., B. Furusato, H. Li, Y. Gu, H. Takahashi, S. Egawa, I. A. Sesterhenn, D. G. McLeod, S. Srivastava, and J. S. Rhim. 2007. Identification of putative stem cell markers, CD133 and CXCR4, in hTERT-immortalized primary nonmalignant and malignant tumor-derived human prostate epithelial cell lines and in prostate cancer specimens. Cancer Res 67:3153-3161.

85. Patrawala, L., T. Calhoun, R. Schneider-Broussard, H. Li, B. Bhatia, S. Tang, J. G. Reilly, D. Chandra, J. Zhou, K. Claypool, L. Coghlan, and D. G. Tang. 2006. Highly purified CD44+ prostate cancer cells from xenograft human tumors are enriched in tumorigenic and metastatic progenitor cells. Oncogene 25:1696-1708.

86. Patrawala, L., T. Calhoun, R. Schneider-Broussard, J. Zhou, K. Claypool, and D. G. Tang. 2005. Side population is enriched in tumorigenic, stem-like cancer cells, whereas ABCG2+ and ABCG2- cancer cells are similarly tumorigenic. Cancer Res 65:6207-6219.

87. Patrawala, L., T. Calhoun-Davis, R. Schneider-Broussard, and D. G. Tang. 2007. Hierarchical organization of prostate cancer cells in xenograft tumors: the CD44+alpha2beta1+ cell population is enriched in tumor-initiating cells. Cancer Res 67:6796-6805.

88. Hurt, E. M., B. T. Kawasaki, G. J. Klarmann, S. B. Thomas, and W. L. Farrar. 2008. CD44+ CD24(-) prostate cells are early cancer progenitor/stem cells that provide a model for patients with poor prognosis. Br J Cancer 98:756-765.

89. Dubrovska, A., S. Kim, R. J. Salamone, J. R. Walker, S. M. Maira, C. Garcia-Echeverria, P. G. Schultz, and V. A. Reddy. 2009. The role of PTEN/Akt/PI3K signaling in the maintenance and viability of prostate cancer stem-like cell populations. Proc Natl Acad Sci USA 106:268-273.

90. Guzman-Ramirez, N., M. Voller, A. Wetterwald, M. Germann, N. A. Cross, C. A. Rentsch, J. Schalken, G. N. Thalmann, and M. G. Cecchini. 2009. In vitro propagation and characterization of neoplastic stem/progenitor-like cells from human prostate cancer tissue. Prostate 69:1683-1693.

91. Li, T., Y. Su, Y. Mei, Q. Leng, B. Leng, Z. Liu, S. A. Stass, and F. Jiang. 2010. ALDH1A1 is a marker for malignant prostate stem cells and predictor of prostate cancer patients' outcome. Lab Invest 90:234-244.

92. Klarmann, G. J., E. M. Hurt, L. A. Mathews, X. Zhang, M. A. Duhagon, T. Mistree, S. B. Thomas, and W. L. Farrar. 2009. Invasive prostate cancer cells are tumor initiating cells that have a stem cell-like genomic signature. Clin Exp Metastasis 26:433-446.

93. van den Hoogen, C., G. van der Horst, H. Cheung, J. T. Buijs, J. M. Lippitt, N. Guzman-Ramirez, F. C. Hamdy, C. L. Eaton, G. N. Thalmann, M. G. Cecchini, R. C. Pelger, and G. van der Pluijm. 2010. High aldehyde dehydrogenase activity identifies tumor-initiating and metastasis-initiating cells in human prostate cancer. Cancer Res 70:5163-5173.

94. Rajasekhar, V. K., L. Studer, W. Gerald, N. D. Socci, and H. I. Scher. 2011. Tumour-initiating stem-like cells in human prostate cancer exhibit increased NF-kappaB signalling. Nat Commun 2:162.

95. Kobayashi, A., H. Okuda, F. Xing, P. R. Pandey, M. Watabe, S. Hirota, S. K. Pai, W. Liu, K. Fukuda, C. Chambers, A. Wilber, and K. Watabe. 2011. Bone morphogenetic protein 7 in dormancy and metastasis of prostate cancer stem-like cells in bone. J Exp Med 208:2641-2655.

96. Liu, C., K. Kelnar, B. Liu, X. Chen, T. Calhoun-Davis, H. Li, L. Patrawala, H. Yan, C. Jeter, S. Honorio, J. F. Wiggins, A. G. Bader, R. Fagin, D. Brown, and D. G. Tang. 2011. The microRNA miR-34a inhibits prostate cancer stem cells and metastasis by directly repressing CD44. Nat Med 17:211-215.

97. Mulholland, D. J., N. Kobayashi, M. Ruscetti, A. Zhi, L. M. Tran, J. Huang, M. Gleave, and H. Wu. 2012. Pten loss and RAS/MAPK activation cooperate to

promote EMT and metastasis initiated from prostate cancer stem/progenitor cells. Cancer Res 72:1878-1889.

98. Qin, J., X. Liu, B. Laffin, X. Chen, G. Choy, C. R. Jeter, T. Calhoun-Davis, H. Li, G. S. Palapattu, S. Pang, K. Lin, J. Huang, I. Ivanov, W. Li, M. V. Suraneni, and D. G. Tang. 2012. The PSA(-/lo) prostate cancer cell population harbors self-renewing long-term tumor-propagating cells that resist castration. Cell Stem Cell 10:556-569.

99. Nishida, S., Y. Hirohashi, T. Torigoe, H. Kitamura, A. Takahashi, N. Masumori, T. Tsukamoto, and N. Sato. 2012. Gene expression profiles of prostate cancer stem cells isolated by aldehyde dehydrogenase activity assay. J Urol 188:294-299.

100. Germann, M., A. Wetterwald, N. Guzman-Ramirez, G. van der Pluijm, Z. Culig, M. G. Cecchini, E. D. Williams, and G. N. Thalmann. 2012. Stem-like cells with luminal progenitor phenotype survive castration in human prostate cancer. Stem Cells 30:1076-1086.

101. Colombel, M., C. L. Eaton, F. Hamdy, E. Ricci, G. van der Pluijm, M. Cecchini, F. Mege-Lechevallier, P. Clezardin, and G. Thalmann. 2012. Increased expression of putative cancer stem cell markers in primary prostate cancer is associated with progression of bone metastases. Prostate 72:713-720.

102. Dubrovska, A., J. Elliott, R. J. Salamone, G. D. Telegeev, A. E. Stakhovsky, I. B. Schepotin, F. Yan, Y. Wang, L. C. Bouchez, S. A. Kularatne, J. Watson, C. Trussell, V. A. Reddy, C. Y. Cho, and P. G. Schultz. 2012. CXCR4 expression in prostate cancer progenitor cells. PLoS One 7:e31226.

103. Mimeault, M., S. L. Johansson, and S. K. Batra. 2012. Pathobiological implications of the expression of EGFR, pAkt, NF-kappaB and MIC-1 in prostate cancer stem cells and their progenies. PLoS One 7:e31919.

104. Liu, C., K. Kelnar, A. V. Vlassov, D. Brown, J. Wang, and D. G. Tang. 2012. Distinct microRNA expression profiles in prostate cancer stem/progenitor cells and tumor-suppressive functions of let-7. Cancer Res 72:3393-3404.

105. Domingo-Domenech, J., S. J. Vidal, V. Rodriguez-Bravo, M. Castillo-Martin, S. A. Quinn, R. Rodriguez-Barrueco, D. M. Bonal, E. Charytonowicz, N. Gladoun, J. de la Iglesia-Vicente, D. P. Petrylak, M. C. Benson, J. M. Silva, and C. Cordon-Cardo. 2012. Suppression of Acquired Docetaxel Resistance in Prostate Cancer through Depletion of Notch- and Hedgehog-Dependent Tumor-Initiating Cells. Cancer Cell 22:373-388.

106. Curtis, S. J., K. W. Sinkevicius, D. Li, A. N. Lau, R. R. Roach, R. Zamponi, A. E. Woolfenden, D. G. Kirsch, K. K. Wong, and C. F. Kim. 2010. Primary tumor genotype is an important determinant in identification of lung cancer propagating cells. Cell Stem Cell 7:127-133.

107. Eramo, A., F. Lotti, G. Sette, E. Pilozzi, M. Biffoni, A. Di Virgilio, C. Conticello, L. Ruco, C. Peschle, and R. De Maria. 2008. Identification and expansion of the tumorigenic lung cancer stem cell population. Cell Death Differ 15:504-514.

108. Damelin, M., K. G. Geles, M. T. Follettie, P. Yuan, M. Baxter, J. Golas, J. F. DiJoseph, M. Karnoub, S. Huang, V. Diesl, C. Behrens, S. E. Choe, C. Rios, J. Gruzas, L. Sridharan, M. Dougher, A. Kunz, P. R. Hamann, D. Evans, D. Armellino, K. Khandke, K. Marquette, L. Tchistiakova, E. R. Boghaert, R. T. Abraham,

Wistuba, II, and B. B. Zhou. 2011. Delineation of a cellular hierarchy in lung cancer reveals an oncofetal antigen expressed on tumor-initiating cells. Cancer Res 71:4236-4246.

109. Yang, Z. F., D. W. Ho, M. N. Ng, C. K. Lau, W. C. Yu, P. Ngai, P. W. Chu, C. T. Lam, R. T. Poon, and S. T. Fan. 2008. Significance of CD90+ cancer stem cells in human liver cancer. Cancer Cell 13:153-166.

110. Cairo, S., C. Armengol, A. De Reynies, Y. Wei, E. Thomas, C. A. Renard, A. Goga, A. Balakrishnan, M. Semeraro, L. Gresh, M. Pontoglio, H. Strick-Marchand, F. Levillayer, Y. Nouet, D. Rickman, F. Gauthier, S. Branchereau, L. Brugieres, V. Laithier, R. Bouvier, F. Boman, G. Basso, J. F. Michiels, P. Hofman, F. Arbez-Gindre, H. Jouan, M. C. Rousselet-Chapeau, D. Berrebi, L. Marcellin, F. Plenat, D. Zachar, M. Joubert, J. Selves, D. Pasquier, P. Bioulac-Sage, M. Grotzer, M. Childs, M. Fabre, and M. A. Buendia. 2008. Hepatic stem-like phenotype and interplay of Wnt/beta-catenin and Myc signaling in aggressive childhood liver cancer. Cancer Cell 14:471-484.

111. Lee, T. K., A. Castilho, V. C. Cheung, K. H. Tang, S. Ma, and I. O. Ng. 2011. CD24(+) liver tumor-initiating cells drive self-renewal and tumor initiation through STAT3-mediated NANOG regulation. Cell Stem Cell 9:50-63.

112. Li, C., D. G. Heidt, P. Dalerba, C. F. Burant, L. Zhang, V. Adsay, M. Wicha, M. F. Clarke, and D. M. Simeone. 2007. Identification of pancreatic cancer stem cells. Cancer Res 67:1030-1037.

113. Lonardo, E., P. C. Hermann, M. T. Mueller, S. Huber, A. Balic, I. Miranda-Lorenzo, S. Zagorac, S. Alcala, I. Rodriguez-Arabaolaza, J. C. Ramirez, R. Torres-Ruiz, E.

Garcia, M. Hidalgo, D. A. Cebrian, R. Heuchel, M. Lohr, F. Berger, P. Bartenstein, A. Aicher, and C. Heeschen. 2011. Nodal/Activin signaling drives self-renewal and tumorigenicity of pancreatic cancer stem cells and provides a target for combined drug therapy. Cell Stem Cell 9:433-446.

114. Nishizawa, S., Y. Hirohashi, T. Torigoe, A. Takahashi, Y. Tamura, T. Mori, T. Kanaseki, K. Kamiguchi, H. Asanuma, R. Morita, A. Sokolovskaya, J. Matsuzaki, R. Yamada, R. Fujii, H. H. Kampinga, T. Kondo, T. Hasegawa, I. Hara, and N. Sato. 2012. HSP DNAJB8 controls tumor-initiating ability in renal cancer stem-like cells. Cancer Res 72:2844-2854.

115. Grange, C., M. Tapparo, F. Collino, L. Vitillo, C. Damasco, M. C. Deregibus, C. Tetta, B. Bussolati, and G. Camussi. 2011. Microvesicles released from human renal cancer stem cells stimulate angiogenesis and formation of lung premetastatic niche. Cancer Res 71:5346-5356.

116. Ho, P. L., E. J. Lay, W. Jian, D. Parra, and K. S. Chan. 2012. Stat3 activation in urothelial stem cells leads to direct progression to invasive bladder cancer. Cancer Res 72:3135-3142.

117. Chan, K. S., I. Espinosa, M. Chao, D. Wong, L. Ailles, M. Diehn, H. Gill, J. Presti, Jr., H. Y. Chang, M. van de Rijn, L. Shortliffe, and I. L. Weissman. 2009. Identification, molecular characterization, clinical prognosis, and therapeutic targeting of human bladder tumor-initiating cells. Proc Natl Acad Sci USA 106:14016-14021.

118. Silva, I. A., S. Bai, K. McLean, K. Yang, K. Griffith, D. Thomas, C. Ginestier, C. Johnston, A. Kueck, R. K. Reynolds, M. S. Wicha, and R. J. Buckanovich. 2011.

Aldehyde dehydrogenase in combination with CD133 defines angiogenic ovarian cancer stem cells that portend poor patient survival. Cancer Res 71:3991-4001.

119. Meirelles, K., L. A. Benedict, D. Dombkowski, D. Pepin, F. I. Preffer, J. Teixeira, P. S. Tanwar, R. H. Young, D. T. MacLaughlin, P. K. Donahoe, and X. Wei. 2012. Human ovarian cancer stem/progenitor cells are stimulated by doxorubicin but inhibited by Mullerian inhibiting substance. Proc Natl Acad Sci USA 109:2358-2363.

120. Prince, M. E., R. Sivanandan, A. Kaczorowski, G. T. Wolf, M. J. Kaplan, P. Dalerba, I. L. Weissman, M. F. Clarke, and L. E. Ailles. 2007. Identification of a subpopulation of cells with cancer stem cell properties in head and neck squamous cell carcinoma. Proc Natl Acad Sci USA 104:973-978.

121. Schatton, T., G. F. Murphy, N. Y. Frank, K. Yamaura, A. M. Waaga-Gasser, M. Gasser, Q. Zhan, S. Jordan, L. M. Duncan, C. Weishaupt, R. C. Fuhlbrigge, T. S. Kupper, M. H. Sayegh, and M. H. Frank. 2008. Identification of cells initiating human melanomas. Nature 451:345-349.

122. Quintana, E., M. Shackleton, M. S. Sabel, D. R. Fullen, T. M. Johnson, and S. J. Morrison. 2008. Efficient tumour formation by single human melanoma cells. Nature 456:593-598.

123. Boiko, A. D., O. V. Razorenova, M. van de Rijn, S. M. Swetter, D. L. Johnson, D. P. Ly, P. D. Butler, G. P. Yang, B. Joshua, M. J. Kaplan, M. T. Longaker, and I. L. Weissman. 2010. Human melanoma-initiating cells express neural crest nerve growth factor receptor CD271. Nature 466:133-137.

124. Driessens, G., B. Beck, A. Caauwe, B. D. Simons, and C. Blanpain. 2012. Defining the mode of tumour growth by clonal analysis. Nature 488:527-530.

125. Schepers, A. G., H. J. Snippert, D. E. Stange, M. van den Born, J. H. van Es, M. van de Wetering, and H. Clevers. 2012. Lineage tracing reveals Lgr5+ stem cell activity in mouse intestinal adenomas. Science 337:730-735.

126. Chen, J., Y. Li, T. S. Yu, R. M. McKay, D. K. Burns, S. G. Kernie, and L. F. Parada. 2012. A restricted cell population propagates glioblastoma growth after chemotherapy. Nature 488:522-526.

127. Son, M. J., K. Woolard, D. H. Nam, J. Lee, and H. A. Fine. 2009. SSEA-1 is an enrichment marker for tumor-initiating cells in human glioblastoma. Cell Stem Cell 4:440-452.

128. Lim, E., F. Vaillant, D. Wu, N. C. Forrest, B. Pal, A. H. Hart, M. L. Asselin-Labat, D. E. Gyorki, T. Ward, A. Partanen, F. Feleppa, L. I. Huschtscha, H. J. Thorne, S. B. Fox, M. Yan, J. D. French, M. A. Brown, G. K. Smyth, J. E. Visvader, and G. J. Lindeman. 2009. Aberrant luminal progenitors as the candidate target population for basal tumor development in BRCA1 mutation carriers. Nat Med 15:907-913.

129. Yang, Z. J., T. Ellis, S. L. Markant, T. A. Read, J. D. Kessler, M. Bourboulas, U. Schuller, R. Machold, G. Fishell, D. H. Rowitch, B. J. Wainwright, and R. J. Wechsler-Reya. 2008. Medulloblastoma can be initiated by deletion of Patched in lineage-restricted progenitors or stem cells. Cancer Cell 14:135-145.

130. Wei, C., W. Guomin, L. Yujun, and Q. Ruizhe. 2007. Cancer stem-like cells in human prostate carcinoma cells DU145: the seeds of the cell line? Cancer Biol Ther 6:763-768.

131. Pienta, K. J., C. Abate-Shen, D. B. Agus, R. M. Attar, L. W. Chung, N. M. Greenberg, W. C. Hahn, J. T. Isaacs, N. M. Navone, D. M. Peehl, J. W. Simons, D. B. Solit, H. R. Soule, T. A. VanDyke, M. J. Weber, L. Wu, and R. L. Vessella. 2008. The current state of preclinical prostate cancer animal models. Prostate 68:629-639.

132. Knoblich, J. A. 2008. Mechanisms of asymmetric stem cell division. Cell 132:583-597.

133. Chambers, I., D. Colby, M. Robertson, J. Nichols, S. Lee, S. Tweedie, and A. Smith. 2003. Functional expression cloning of Nanog, a pluripotency sustaining factor in embryonic stem cells. Cell 113:643-655.

134. Mulholland, D. J., L. Xin, A. Morim, D. Lawson, O. Witte, and H. Wu. 2009. Lin-Sca-1+CD49fhigh stem/progenitors are tumor-initiating cells in the Pten-null prostate cancer model. Cancer Res 69:8555-8562.

135. Abou-Kheir, W. G., P. G. Hynes, P. L. Martin, R. Pierce, and K. Kelly. 2010. Characterizing the contribution of stem/progenitor cells to tumorigenesis in the Pten-/-TP53-/- prostate cancer model. Stem Cells 28:2129-2140.

136. Zhou, B. B., H. Zhang, M. Damelin, K. G. Geles, J. C. Grindley, and P. B. Dirks. 2009. Tumour-initiating cells: challenges and opportunities for anticancer drug discovery. Nat Rev Drug Discov 8:806-823.

137. Singh, S. K., I. D. Clarke, T. Hide, and P. B. Dirks. 2004. Cancer stem cells in nervous system tumors. Oncogene 23:7267-7273.

138. Al-Hajj, M., M. W. Becker, M. Wicha, I. Weissman, and M. F. Clarke. 2004. Therapeutic implications of cancer stem cells. Curr Opin Genet Dev 14:43-47.

139. Clarke, M. F., and M. W. Becker. 2006. Stem cells: the real culprits in cancer? Sci Am 295:52-59.

140. Al-Hajj, M. 2007. Cancer stem cells and oncology therapeutics. Curr Opin Oncol 19:61-64.

141. Li, L., and R. Bhatia. 2011. Stem cell quiescence. Clin Cancer Res 17:4936-4941.

142. Goodell, M. A., M. Rosenzweig, H. Kim, D. F. Marks, M. DeMaria, G. Paradis, S. A. Grupp, C. A. Sieff, R. C. Mulligan, and R. P. Johnson. 1997. Dye efflux studies suggest that hematopoietic stem cells expressing low or undetectable levels of CD34 antigen exist in multiple species. Nat Med 3:1337-1345.

143. Doyle, L. A., and D. D. Ross. 2003. Multidrug resistance mediated by the breast cancer resistance protein BCRP (ABCG2). Oncogene 22:7340-7358.

144. Yajima, T., H. Ochiai, T. Uchiyama, N. Takano, T. Shibahara, and T. Azuma. 2009. Resistance to cytotoxic chemotherapy-induced apoptosis in side population cells of human oral squamous cell carcinoma cell line Ho-1-N-1. Int J Oncol 35:273-280.

145. Diehn, M., R. W. Cho, N. A. Lobo, T. Kalisky, M. J. Dorie, A. N. Kulp, D. Qian, J. S. Lam, L. E. Ailles, M. Wong, B. Joshua, M. J. Kaplan, I. Wapnir, F. M. Dirbas, G. Somlo, C. Garberoglio, B. Paz, J. Shen, S. K. Lau, S. R. Quake, J. M. Brown, I. L. Weissman, and M. F. Clarke. 2009. Association of reactive oxygen species levels and radioresistance in cancer stem cells. Nature 458:780-783.

146. Wicha, M. S., S. Liu, and G. Dontu. 2006. Cancer stem cells: an old idea--a paradigm shift. Cancer Res 66:1883-1890; discussion 1895-1886.

147. Bhatia, B., M. Jiang, M. Suraneni, L. Patrawala, M. Badeaux, R. Schneider-Broussard, A. S. Multani, C. R. Jeter, T. Calhoun-Davis, L. Hu, J. Hu, S.

Tsavachidis, W. Zhang, S. Chang, S. W. Hayward, and D. G. Tang. 2008. Critical and distinct roles of p16 and telomerase in regulating the proliferative life span of normal human prostate epithelial progenitor cells. J Biol Chem 283:27957-27972.

148. Yan, H., X. Chen, Q. Zhang, J. Qin, H. Li, C. Liu, T. Calhoun-Davis, L. D. Coletta, J. Klostergaard, I. Fokt, S. Skora, W. Priebe, Y. Bi, and D. G. Tang. 2011. Drug-tolerant cancer cells show reduced tumor-initiating capacity: depletion of CD44 cells and evidence for epigenetic mechanisms. PLoS One 6:e24397.

149. Thompson, C. B. 2009. Attacking cancer at its root. Cell 138:1051-1054.

150. Pasquier, E., M. Kavallaris, and N. Andre. 2010. Metronomic chemotherapy: new rationale for new directions. Nat Rev Clin Oncol 7:455-465.

151. Auzenne, E., S. C. Ghosh, M. Khodadadian, B. Rivera, D. Farquhar, R. E. Price, M. Ravoori, V. Kundra, R. S. Freedman, and J. Klostergaard. 2007. Hyaluronic acid-paclitaxel: antitumor efficacy against CD44(+) human ovarian carcinoma xenografts. Neoplasia 9:479-486.

152. Sharma, S. V., D. Y. Lee, B. Li, M. P. Quinlan, F. Takahashi, S. Maheswaran, U. McDermott, N. Azizian, L. Zou, M. A. Fischbach, K. K. Wong, K. Brandstetter, B. Wittner, S. Ramaswamy, M. Classon, and J. Settleman. 2010. A chromatin-mediated reversible drug-tolerant state in cancer cell subpopulations. Cell 141:69-80.

153. Gupta, P. B., T. T. Onder, G. Jiang, K. Tao, C. Kuperwasser, R. A. Weinberg, and E. S. Lander. 2009. Identification of selective inhibitors of cancer stem cells by high-throughput screening. Cell 138:645-659.

154. Beier, D., S. Rohrl, D. R. Pillai, S. Schwarz, L. A. Kunz-Schughart, P. Leukel, M. Proescholdt, A. Brawanski, U. Bogdahn, A. Trampe-Kieslich, B. Giebel, J.

Wischhusen, G. Reifenberger, P. Hau, and C. P. Beier. 2008. Temozolomide preferentially depletes cancer stem cells in glioblastoma. Cancer Res 68:5706-5715.

155. Bao, S., Q. Wu, Z. Li, S. Sathornsumetee, H. Wang, R. E. McLendon, A. B. Hjelmeland, and J. N. Rich. 2008. Targeting cancer stem cells through L1CAM suppresses glioma growth. Cancer Res 68:6043-6048.

156. Todaro, M., M. D'Asaro, N. Caccamo, F. Iovino, M. G. Francipane, S. Meraviglia, V. Orlando, C. La Mendola, G. Gulotta, A. Salerno, F. Dieli, and G. Stassi. 2009. Efficient killing of human colon cancer stem cells by gammadelta T lymphocytes. J Immunol 182:7287-7296.

157. Aulmann, S., N. Waldburger, R. Penzel, M. Andrulis, P. Schirmacher, and H. P. Sinn. 2010. Reduction of CD44(+)/CD24(-) breast cancer cells by conventional cytotoxic chemotherapy. Hum Pathol 41:574-581.

158. Hirsch, H. A., D. Iliopoulos, P. N. Tsichlis, and K. Struhl. 2009. Metformin selectively targets cancer stem cells, and acts together with chemotherapy to block tumor growth and prolong remission. Cancer Res 69:7507-7511.

159. Perl, A. K., P. Wilgenbus, U. Dahl, H. Semb, and G. Christofori. 1998. A causal role for E-cadherin in the transition from adenoma to carcinoma. Nature 392:190-193.

160. Grady, W. M., J. Willis, P. J. Guilford, A. K. Dunbier, T. T. Toro, H. Lynch, G. Wiesner, K. Ferguson, C. Eng, J. G. Park, S. J. Kim, and S. Markowitz. 2000. Methylation of the CDH1 promoter as the second genetic hit in hereditary diffuse gastric cancer. Nat Genet 26:16-17.

161. Graff, J. R., J. G. Herman, R. G. Lapidus, H. Chopra, R. Xu, D. F. Jarrard, W. B. Isaacs, P. M. Pitha, N. E. Davidson, and S. B. Baylin. 1995. E-cadherin expression is

silenced by DNA hypermethylation in human breast and prostate carcinomas. Cancer Res 55:5195-5199.

162. Aghdassi, A., M. Sendler, A. Guenther, J. Mayerle, C. O. Behn, C. D. Heidecke, H. Friess, M. Buchler, M. Evert, M. M. Lerch, and F. U. Weiss. 2012. Recruitment of histone deacetylases HDAC1 and HDAC2 by the transcriptional repressor ZEB1 downregulates E-cadherin expression in pancreatic cancer. Gut 61:439-448.

163. Cespedes, M. V., I. Casanova, M. Parreno, and R. Mangues. 2006. Mouse models in oncogenesis and cancer therapy. Clin Transl Oncol 8:318-329.

164. Ellis, W. J., R. L. Vessella, K. R. Buhler, F. Bladou, L. D. True, S. A. Bigler, D. Curtis, and P. H. Lange. 1996. Characterization of a novel androgen-sensitive, prostate-specific antigen-producing prostatic carcinoma xenograft: LuCaP 23. Clin Cancer Res 2:1039-1048.

165. Klein, K. A., R. E. Reiter, J. Redula, H. Moradi, X. L. Zhu, A. R. Brothman, D. J. Lamb, M. Marcelli, A. Belldegrun, O. N. Witte, and C. L. Sawyers. 1997. Progression of metastatic human prostate cancer to androgen independence in immunodeficient SCID mice. Nat Med 3:402-408.

166. Corey, E., J. E. Quinn, K. R. Buhler, P. S. Nelson, J. A. Macoska, L. D. True, and R. L. Vessella. 2003. LuCaP 35: a new model of prostate cancer progression to androgen independence. Prostate 55:239-246.

167. Priolo, C., M. Agostini, N. Vena, A. H. Ligon, M. Fiorentino, E. Shin, A. Farsetti, A. Pontecorvi, E. Sicinska, and M. Loda. 2010. Establishment and genomic characterization of mouse xenografts of human primary prostate tumors. Am J Pathol 176:1901-1913.

168. Zhao, H., R. Nolley, Z. Chen, and D. M. Peehl. 2010. Tissue slice grafts: an in vivo model of human prostate androgen signaling. Am J Pathol 177:229-239.

169. Toivanen, R., D. M. Berman, H. Wang, J. Pedersen, M. Frydenberg, A. K. Meeker, S. J. Ellem, G. P. Risbridger, and R. A. Taylor. 2011. Brief report: a bioassay to identify primary human prostate cancer repopulating cells. Stem Cells 29:1310-1314.

170. Olumi, A. F., G. D. Grossfeld, S. W. Hayward, P. R. Carroll, T. D. Tlsty, and G. R. Cunha. 1999. Carcinoma-associated fibroblasts direct tumor progression of initiated human prostatic epithelium. Cancer Res 59:5002-5011.

171. Silvers, C. R., K. Williams, L. Salamone, J. Huang, C. T. Jordan, H. Zhou, and G. S. Palapattu. 2010. A novel in vitro assay of tumor-initiating cells in xenograft prostate tumors. Prostate 70:1379-1387.

172. Hayward, S. W., Y. Wang, M. Cao, Y. K. Hom, B. Zhang, G. D. Grossfeld, D. Sudilovsky, and G. R. Cunha. 2001. Malignant transformation in a nontumorigenic human prostatic epithelial cell line. Cancer Res 61:8135-8142.

173. Karnoub, A. E., A. B. Dash, A. P. Vo, A. Sullivan, M. W. Brooks, G. W. Bell, A. L. Richardson, K. Polyak, R. Tubo, and R. A. Weinberg. 2007. Mesenchymal stem cells within tumour stroma promote breast cancer metastasis. Nature 449:557-563.

174. Roecklein, B. A., and B. Torok-Storb. 1995. Functionally distinct human marrow stromal cell lines immortalized by transduction with the human papilloma virus E6/E7 genes. Blood 85:997-1005.

175. O'Connor, J. C., M. C. Farach-Carson, C. J. Schneider, and D. D. Carson. 2007. Coculture with prostate cancer cells alters endoglin expression and attenuates

transforming growth factor-beta signaling in reactive bone marrow stromal cells. Mol Cancer Res 5:585-603.

176. Delk, N. A., and M. C. Farach-Carson. 2012. Interleukin-6: a bone marrow stromal cell paracrine signal that induces neuroendocrine differentiation and modulates autophagy in bone metastatic PCa cells. Autophagy 8:650-663.

177. Lacombe, L., I. Orlow, V. E. Reuter, W. R. Fair, G. Dalbagni, Z. F. Zhang, and C. Cordon-Cardo. 1996. Microsatellite instability and deletion analysis of chromosome 10 in human prostate cancer. Int J Cancer 69:110-113.

178. Li, J., C. Yen, D. Liaw, K. Podsypanina, S. Bose, S. I. Wang, J. Puc, C. Miliaresis, L. Rodgers, R. McCombie, S. H. Bigner, B. C. Giovanella, M. Ittmann, B. Tycko, H. Hibshoosh, M. H. Wigler, and R. Parsons. 1997. PTEN, a putative protein tyrosine phosphatase gene mutated in human brain, breast, and prostate cancer. Science 275:1943-1947.

179. Steck, P. A., M. A. Pershouse, S. A. Jasser, W. K. Yung, H. Lin, A. H. Ligon, L. A. Langford, M. L. Baumgard, T. Hattier, T. Davis, C. Frye, R. Hu, B. Swedlund, D. H. Teng, and S. V. Tavtigian. 1997. Identification of a candidate tumour suppressor gene, MMAC1, at chromosome 10q23.3 that is mutated in multiple advanced cancers. Nat Genet 15:356-362.

180. Garber, K. 2009. From human to mouse and back: 'tumorgraft' models surge in popularity. J Natl Cancer Inst 101:6-8.

181. Wang, Y., M. P. Revelo, D. Sudilovsky, M. Cao, W. G. Chen, L. Goetz, H. Xue, M. Sadar, S. B. Shappell, G. R. Cunha, and S. W. Hayward. 2005. Development and

characterization of efficient xenograft models for benign and malignant human prostate tissue. Prostate 64:149-159.

182. van Bokhoven, A., M. Varella-Garcia, C. Korch, W. U. Johannes, E. E. Smith, H. L. Miller, S. K. Nordeen, G. J. Miller, and M. S. Lucia. 2003. Molecular characterization of human prostate carcinoma cell lines. Prostate 57:205-225.

183. Goldstein, A. S., J. Huang, C. Guo, I. P. Garraway, and O. N. Witte. 2010. Identification of a cell of origin for human prostate cancer. Science 329:568-571.

184. DeRose, Y. S., G. Wang, Y. C. Lin, P. S. Bernard, S. S. Buys, M. T. Ebbert, R. Factor, C. Matsen, B. A. Milash, E. Nelson, L. Neumayer, R. L. Randall, I. J. Stijleman, B. E. Welm, and A. L. Welm. 2011. Tumor grafts derived from women with breast cancer authentically reflect tumor pathology, growth, metastasis and disease outcomes. Nat Med 17:1514-1520.

185. Pretlow, T. G., C. M. Delmoro, G. G. Dilley, C. G. Spadafora, and T. P. Pretlow. 1991. Transplantation of human prostatic carcinoma into nude mice in Matrigel. Cancer Res 51:3814-3817.

186. Bhatia, B., A. S. Multani, L. Patrawala, X. Chen, T. Calhoun-Davis, J. Zhou, L. Schroeder, R. Schneider-Broussard, J. Shen, S. Pathak, S. Chang, and D. G. Tang. 2008. Evidence that senescent human prostate epithelial cells enhance tumorigenicity: cell fusion as a potential mechanism and inhibition by p16INK4a and hTERT. Int J Cancer 122:1483-1495.

187. Placencio, V. R., X. Li, T. P. Sherrill, G. Fritz, and N. A. Bhowmick. 2010. Bone marrow derived mesenchymal stem cells incorporate into the prostate during regrowth. PLoS One 5:e12920.

188. Wang, R., X. Sun, C. Y. Wang, P. Hu, C. Y. Chu, S. Liu, H. E. Zhau, and L. W. Chung. 2012. Spontaneous cancer-stromal cell fusion as a mechanism of prostate cancer androgen-independent progression. PLoS One 7:e42653.

189. Chung, L. W., S. M. Chang, C. Bell, H. E. Zhau, J. Y. Ro, and A. C. von Eschenbach. 1989. Co-inoculation of tumorigenic rat prostate mesenchymal cells with non-tumorigenic epithelial cells results in the development of carcinosarcoma in syngeneic and athymic animals. Int J Cancer 43:1179-1187.

190. Brinkmann, A. O., L. J. Blok, P. E. de Ruiter, P. Doesburg, K. Steketee, C. A. Berrevoets, and J. Trapman. 1999. Mechanisms of androgen receptor activation and function. J Steroid Biochem Mol Biol 69:307-313.

191. McKenna, N. J., R. B. Lanz, and B. W. O'Malley. 1999. Nuclear receptor coregulators: cellular and molecular biology. Endocr Rev 20:321-344.

192. Visakorpi, T., E. Hyytinen, P. Koivisto, M. Tanner, R. Keinanen, C. Palmberg, A. Palotie, T. Tammela, J. Isola, and O. P. Kallioniemi. 1995. In vivo amplification of the androgen receptor gene and progression of human prostate cancer. Nat Genet 9:401-406.

193. Linja, M. J., K. J. Savinainen, O. R. Saramaki, T. L. Tammela, R. L. Vessella, and T. Visakorpi. 2001. Amplification and overexpression of androgen receptor gene in hormone-refractory prostate cancer. Cancer Res 61:3550-3555.

194. Taplin, M. E., G. J. Bubley, T. D. Shuster, M. E. Frantz, A. E. Spooner, G. K. Ogata, H. N. Keer, and S. P. Balk. 1995. Mutation of the androgen-receptor gene in metastatic androgen-independent prostate cancer. N Engl J Med 332:1393-1398.

195. Veldscholte, J., C. A. Berrevoets, C. Ris-Stalpers, G. G. Kuiper, G. Jenster, J. Trapman, A. O. Brinkmann, and E. Mulder. 1992. The androgen receptor in LNCaP cells contains a mutation in the ligand binding domain which affects steroid binding characteristics and response to antiandrogens. J Steroid Biochem Mol Biol 41:665-669.

196. Zhou, H., X. M. Li, J. Meinkoth, and R. N. Pittman. 2000. Akt regulates cell survival and apoptosis at a postmitochondrial level. J Cell Biol 151:483-494.

197. Luo, J. L., W. Tan, J. M. Ricono, O. Korchynskyi, M. Zhang, S. L. Gonias, D. A. Cheresh, and M. Karin. 2007. Nuclear cytokine-activated IKKalpha controls prostate cancer metastasis by repressing Maspin. Nature 446:690-694.

198. Zhu, P., S. H. Baek, E. M. Bourk, K. A. Ohgi, I. Garcia-Bassets, H. Sanjo, S. Akira, P. F. Kotol, C. K. Glass, M. G. Rosenfeld, and D. W. Rose. 2006. Macrophage/cancer cell interactions mediate hormone resistance by a nuclear receptor derepression pathway. Cell 124:615-629.

199. Debes, J. D., and D. J. Tindall. 2004. Mechanisms of androgen-refractory prostate cancer. N Engl J Med 351:1488-1490.

200. Tanaka, H., E. Kono, C. P. Tran, H. Miyazaki, J. Yamashiro, T. Shimomura, L. Fazli, R. Wada, J. Huang, R. L. Vessella, J. An, S. Horvath, M. Gleave, M. B. Rettig, Z. A. Wainberg, and R. E. Reiter. 2010. Monoclonal antibody targeting of N-cadherin inhibits prostate cancer growth, metastasis and castration resistance. Nat Med 16:1414-1420.

201. Jiao, J., A. Hindoyan, S. Wang, L. M. Tran, A. S. Goldstein, D. Lawson, D. Chen, Y. Li, C. Guo, B. Zhang, L. Fazli, M. Gleave, O. N. Witte, I. P. Garraway, and H. Wu.

2012. Identification of CD166 as a Surface Marker for Enriching Prostate Stem/Progenitor and Cancer Initiating Cells. PLoS One 7:e42564.

202. Wang, Q., W. Li, Y. Zhang, X. Yuan, K. Xu, J. Yu, Z. Chen, R. Beroukhim, H. Wang, M. Lupien, T. Wu, M. M. Regan, C. A. Meyer, J. S. Carroll, A. K. Manrai, O. A. Janne, S. P. Balk, R. Mehra, B. Han, A. M. Chinnaiyan, M. A. Rubin, L. True, M. Fiorentino, C. Fiore, M. Loda, P. W. Kantoff, X. S. Liu, and M. Brown. 2009. Androgen receptor regulates a distinct transcription program in androgen-independent prostate cancer. Cell 138:245-256.

VITA

Xin Chen was born in Wuhan, Hubei, P.R.China on April, 10 1982, the son of Weimin Chen and Guimei Peng. After completing his work at Wuhan No. 11 High School, Wuhan, Hubei, P.R.China in 2000, he entered Tongji Medical College of Huazhong University of Science and Technology. Xin received the degree of Bachelor of Medicine in July, 2005. In August of the same year, Xin entered The University of Texas Health Science Center at Houston Graduate School of Biomedical Sciences (GSBS) to pursue his Master's degree under the guidance of Dr. Dean G Tang. Xin received his Master's degree majoring in Cancer Biology in December, 2007. In January of 2008, Xin entered GSBS to pursue his Ph.D. degree in Dr. Dean G Tang's laboratory at the University of Texas M.D. Anderson Cancer Center, Department of Molecular Carcinogenesis, Science Park, Smithville, Texas.

Permanent address:

Tongxin Garden, Phase 2 Project, Group 2, Building 2, Unit 4, Apt 1601

586 Jie Fang Avenue, Qiaokou

Wuhan, Hubei, 430030

P.R.China